



**Calhoun: The NPS Institutional Archive**

---

Theses and Dissertations

Thesis Collection

---

1990-09

# F-18 robust control design using H2 and H-infinity methods

Hartley, Gerald A.

Monterey, California: Naval Postgraduate School

---

<http://hdl.handle.net/10945/34898>



Calhoun is a project of the Dudley Knox Library at NPS, furthering the precepts and goals of open government and government transparency. All information contained herein has been approved for release by the NPS Public Affairs Officer.

**Dudley Knox Library / Naval Postgraduate School**  
**411 Dyer Road / 1 University Circle**  
**Monterey, California USA 93943**

<http://www.nps.edu/library>

AD-A242 562



va  
(2)

# NAVAL POSTGRADUATE SCHOOL

## Monterey, California



DTIC  
ELECTE  
NOV 18 1991  
S B D

### THESIS

F-18 ROBUST CONTROL DESIGN  
USING H2 AND H-INFINITY  
METHODS

by

Gerald A. Hartley

September 1990

Thesis Advisor:

Prof. D. J. Collins

Approved for public release; distribution is unlimited.

91-15831



91 1118 061

UNCLASSIFIED

SECURITY CLASSIFICATION OF THIS PAGE

REPORT DOCUMENTATION PAGE				Form Approved OMB No 0704-0188	
1a REPORT SECURITY CLASSIFICATION Unclassified			1b RESTRICTIVE MARKINGS		
2a SECURITY CLASSIFICATION AUTHORITY			3 DISTRIBUTION/AVAILABILITY OF REPORT Approved for public release; distribution is unlimited.		
2b DECLASSIFICATION/DOWNGRADING SCHEDULE					
4 PERFORMING ORGANIZATION REPORT NUMBER(S)			5 MONITORING ORGANIZATION REPORT NUMBER(S)		
6a NAME OF PERFORMING ORGANIZATION Naval Postgraduate School		6b OFFICE SYMBOL (If applicable) 31	7a. NAME OF MONITORING ORGANIZATION Naval Postgraduate School		
6c. ADDRESS (City, State, and ZIP Code) Monterey, CA 93943-5000			7b ADDRESS (City, State, and ZIP Code) Monterey, CA 93943-5000		
8a. NAME OF FUNDING / SPONSORING ORGANIZATION		8b OFFICE SYMBOL (If applicable)	9 PROCUREMENT INSTRUMENT IDENTIFICATION NUMBER		
8c. ADDRESS (City, State, and ZIP Code)			10 SOURCE OF FUNDING NUMBERS		
			PROGRAM ELEMENT NO	PROJECT NO	TASK NO
					WORK UNIT ACCESSION NO
11. TITLE (Include Security Classification) F-18 Robust Control Design Using H2 and H-infinity Methods					
12. PERSONAL AUTHOR(S) Hartley, Gerald A.					
13a TYPE OF REPORT Master's Thesis		13b TIME COVERED FROM _____ TO _____		14. DATE OF REPORT (Year, Month, Day) 1990, September	
				15 PAGE COUNT 120	
16 SUPPLEMENTARY NOTATION The views expressed in this thesis are those of the author and do not reflect the official policy or position of the Department of Defense or the U.S. Government.					
17 COSATI CODES			18 SUBJECT TERMS (Continue on reverse if necessary and identify by block number)		
FIELD	GROUP	SUB-GROUP			
			Modern Control Theory, H infinity Control Theory, H2 Control Theory, Multivariable Robustness, F-18 Control Design or Synthesis, Super-Augmented Aircraft		
19 ABSTRACT (Continue on reverse if necessary and identify by block number) The open loop F-18 longitudinal control system is stabilized using H2 and H-infinity singular value loop shaping for a multivariable feedback control system. The H2 and H-infinity control theories involve suppressing the sensitivity matrix transfer function at the lower frequencies for high gain performance and suppressing the transmissivity at higher frequencies, i.e. loop shaping. The singular value Bode plot is used for MIMO systems in analogy with the classical Bode frequency analysis for SISO systems. There are two control inputs with input 1 controlling the stabilator and input 2 controlling the leading edge flap and trailing edge flap in tandem. There are two outputs: angle of attack and pitch rate. The H-infinity design achieved a separation in that input 1 controlled angle of attack and input 2 controlled pitch rate. The first design is an optimum design which imposed no limitations on control input. A cost penalty associated with control actuator limitations is imposed to achieve a limited performance design.					
20 DISTRIBUTION/AVAILABILITY OF ABSTRACT <input checked="" type="checkbox"/> UNCLASSIFIED/UNLIMITED <input type="checkbox"/> SAME AS RPT <input type="checkbox"/> DTIC USERS			21 ABSTRACT SECURITY CLASSIFICATION Unclassified		
22a NAME OF RESPONSIBLE INDIVIDUAL Dr. D. J. Collins			22b TELEPHONE (Include Area Code) (408) 646-2628		22c OFFICE SYMBOL 67Co

DD Form 1473, JUN 86

Previous editions are obsolete

S/N 0102-LF-014-6603

SECURITY CLASSIFICATION OF THIS PAGE

UNCLASSIFIED

UNCLASSIFIED

SECURITY CLASSIFICATION OF THIS PAGE

BLOCK #18 (CONTD)

Feedback Properties of a Multivariable Feedback Controller, H infinity Small Gain Problem

Accession For	
NTIS GRA&I	<input checked="checked" type="checkbox"/>
DTIC TAB	<input type="checkbox"/>
Unannounced	<input type="checkbox"/>
Justification	
By	
Distribution/	
Availability Codes	
Dist	Avail and/or Special
A-1	



Approved for public release; distribution is unlimited.

F-18 Robust Control Design  
Using  $H_2$  and  $H_\infty$  Methods

by

Gerald A. Hartley  
Aerospace Engineer, Naval Weapons Center  
B.A.A.E., Ohio State University, 1964  
M.S. (Physics), University of Denver, 1971

Submitted in partial fulfillment  
of the requirements for the degree of

MASTER OF SCIENCE IN AERONAUTICAL ENGINEERING

from the

NAVAL POSTGRADUATE SCHOOL  
September, 1990

Author:

Gerald A. Hartley

Approved by:

Daniel J. Collins, Thesis Advisor

Louis V. Schmidt, Second Reader

E. Roberts Wood, Chairman  
Department of Aeronautics and Astronautics

## ABSTRACT

The open loop F-18 longitudinal control system is stabilized using  $H_2$  and  $H_\infty$  singular value loop shaping for a multivariable feedback control system. The  $H_2$  and  $H_\infty$  control theories involve suppressing the sensitivity matrix transfer function at the lower frequencies for high gain performance and suppressing the transmissivity at higher frequencies, i.e. loop shaping. The singular value Bode plot is used for MIMO systems in analogy with the classical Bode frequency analysis for SISO systems. There are two control inputs with input 1 controlling the stabilator and input 2 controlling the leading edge flap and trailing edge flap in tandem. There are two outputs: angle of attack and pitch rate. The  $H_\infty$  design achieved a separation in that input 1 controlled angle of attack and input 2 controlled pitch rate. The first design is an optimum design which imposed no limitations on control input. A cost penalty associated with control actuator limitations is imposed to achieve a limited performance design.

## TABLE OF CONTENTS

I. INTRODUCTION .....	1
II. PROPERTIES OF MULTIPLE-INPUT MULTIPLE-OUTPUT (MIMO) FEEDBACK CONTROL SYSTEMS .....	3
A. MATRIX NORMS, SINGULAR VALUES AND THEIR APPLICATION TO FEEDBACK PROPERTIES OF MIMO SYSTEMS .....	3
B. SINGULAR VALUE LOOP SHAPING FOR MIMO ROBUSTNESS ....	6
III. $H_{\infty}$ CONTROL DESIGN .....	11
A. THEORETICAL APPROACH .....	11
B. DETERMINATION OF WEIGHTING CONSTRAINTS .....	13
C. DISCUSSION OF $H_2$ AND $H_{\infty}$ DESIGN ITERATION .....	16
IV. F-18 CONTROL DESIGN .....	18
A. F-18 OPEN LOOP STATE SPACE MODEL .....	18
B. DESIGN APPROACH .....	23
C. DESIGN RESULTS OF THE OPTIMUM $H_{\infty}$ CONTROLLER.....	25
1. $H_{\infty}$ INPUT RETURN DIFFERENCE ANALYSIS .....	36
2. PRECISION LONGITUDINAL CONTROL MODES .....	38
D. DESIGN RESULTS OF LIMITED PERFORMANCE CONTROLLER ...	47
1. LIMITED PERFORMANCE $H_{\infty}$ PLANT INPUT PROBLEM .....	52
2. LIMITED PERFORMANCE PRECISION LONGITUDINAL MODES	53
V. CONCLUSIONS AND RECOMMENDATIONS .....	66
APPENDIX A: F-18 MATLAB SCRIPT FILES .....	68
APPENDIX B: F-18 STATE SPACE MODEL MATRICES .....	95

TABLE OF CONTENTS (CONTINUED)

LIST OF REFERENCES .....	110
INITIAL DISTRIBUTION LIST .....	111



## ACKNOWLEDGMENTS

One feels a lot of satisfaction and relief when a thesis project is completed since it required such a concentrated effort and dedication of time. It is only then that one can truly appreciate the efforts of others who made it possible.

I am especially grateful to Professor Dan Collins who suggested the topic and gave me guidance when I needed guidance. I appreciated the fact that he made himself readily available for me to ask questions and was very helpful in resolving them.

I also would like to thank Professor Lou Schmidt who served as second reader and even though I never had him for a class he was very encouraging to me during my stay at the Naval Postgraduate School. As far as receiving advice and encouragement I also wish to thank Professor Jerry Lindsey who went beyond his role as academic advisor.

Finally, I wish to thank my wife Charlotte and my two sons Alan and Daniel who have had to sacrifice greatly to allow me to have the opportunity to attend Naval Postgraduate School. Without her support and love this thesis would not have been possible.

## I. INTRODUCTION

Classical control analysis for single-input single-output (SISO) systems have the use of Bode plots, root locus techniques, Nyquist diagrams and simple time response analysis to judge system performance and stability margins. Stability margin rates the system's ability to withstand disturbances and/or modeling error of a given magnitude and still remain stable. The bandwidth in a Bode plot, defined as the maximum frequency at which the system response does not fall more than 3 db from steady state gain, is easily shown for SISO systems. Classical techniques usually aren't applicable to determining the stability margins and performance characteristics of MIMO systems.

The stability margin and system performance of MIMO systems have been successfully evaluated using the techniques of singular value Bode plots of return difference matrices and loop gain matrices in frequency domain analysis by Doyle, Stein and Safonov [Refs. 1, 2]. A MIMO system is said to have good robustness if the system has a large stability margin, good disturbance attenuation and low sensitivity [Ref. 2].

H-infinity ( $H_\infty$ ) and frequency-weighted linear quadratic gaussian ( $H_2$  LQG) apply singular value loop shaping to MIMO systems. Singular value loop shaping involves shaping the system feedback gains over a specified frequency range in order to meet system gain requirements at the lower frequencies and disturbance

attenuation specifications at the higher frequencies. Gordon [Ref.3] developed numerical optimization techniques for singular value loop shaping which manipulates the system feedback gains as design parameters.

Textbook examples of  $H_2$  and  $H_\infty$  theories have been shown by Postlethwaite [Ref. 4] and Chiang [Ref. 5]. Chiang discusses the design of a hypothetical fighter design at Mach 0.9 and 25,000 feet altitude. Rogers and Hsu [Refs. 6 and 7] developed  $H_\infty$  compensated designs for the X-29 for a two- and three- input longitudinal control system.

The purpose of this thesis was to develop a  $H_\infty$  longitudinal controller for the F-18 for one flight condition at Mach 0.6 at 10,000 feet altitude. The open-loop F-18 longitudinal model was developed by Rojek [Ref. 8] and simplified by the author. Chapter II discusses the properties of MIMO feedback control systems, use of the return difference matrix, and the basic concepts of singular value loop shaping. Chapter III presents the background and concepts of the  $H_2$  and  $H_\infty$  theories. Chapter IV describes the F-18 controller design beginning with the open loop F-18 uncompensated model, the design specifications, the design approach and the design results. The conclusions are given in Chapter V. The appendices contain the MATLAB computer code and F-18 state space models.

## II. PROPERTIES OF MULTIPLE-INPUT MULTIPLE-OUTPUT

### (MIMO) FEEDBACK CONTROL SYSTEMS

The robustness of a MIMO system includes good stability margin, low sensitivity to plant and controller variations, and good disturbance rejection to high frequency disturbance inputs. The above robustness properties can only be modified by altering the feedback paths and the associated gains. The following chapter will illustrate the concepts of feedback manipulation to achieve a good robust design upon which the  $H_2$  and  $H_\infty$  methods in Chapter III are based. Rogers [Ref. 6] and Hsu [Ref. 7] describe in detail the feedback properties of multivariate systems so the current chapter will not attempt to examine this subject in great depth. Matrices will be denoted by bold upper-case letters and vectors by bold lower-case letters in this text.

#### A. MATRIX NORMS, SINGULAR VALUES AND THEIR APPLICATION TO FEEDBACK PROPERTIES OF MIMO SYSTEMS.

Singular values of matrices have been found in the last decade to be extremely useful in extending the frequency domain Bode analysis of classical SISO theory to singular value Bode plots for MIMO systems [Refs. 1,2 and 5]. The singular values of a matrix  $\mathbf{A}$  of rank  $r$  where  $\mathbf{A} \in \mathbb{C}^{m \times n}$  are denoted by  $\sigma_i$  and are defined as the non-negative eigenvalues of  $\mathbf{A}^H \mathbf{A}$  where  $^H$  denotes the complex conjugate transpose of  $\mathbf{A}$ . The singular values are ordered such that  $\sigma_1 \geq \sigma_2 \geq \dots \geq \sigma_n$ . The maximum singular value  $\sigma_1$  can be expressed in terms of the spectral norm:

$$\|A\|_2 = \max_i \lambda_i^{1/2}(A^H A) = \sigma_{\max}(A) = \bar{\sigma}_1 \quad (2-1)$$

where  $\lambda_i$  is the  $i$ th eigenvalue of  $A^H A$ . The singular values of a complex  $n \times n$  matrix  $A$ ,  $\sigma_i$ , are the non-negative square roots of the eigenvalues of  $A^H A$ :

$$\sigma_i(A) = \lambda_i^{1/2}(A^H A) \quad (2-2)$$

The maximum singular value  $\sigma_{\max}$  is given by  $\sigma_1$  and the minimum singular value  $\sigma_{\min}$  is equal to  $\sigma_n$  since the  $\sigma$ 's are ordered from  $\sigma_1$  in monotonically descending order down to  $\sigma_n$ .

There are 12 useful properties of singular values listed by Chiang [Ref. 5] but the three most important for the purposes of this paper are:

$$1. \bar{\sigma}(A) = \max_{x \in \mathbb{C}^n} \frac{\|Ax\|_2}{\|x\|_2} = \sigma_{\max}$$

$$2. \underline{\sigma}(A) = \min_{x \in \mathbb{C}^n} \frac{\|Ax\|_2}{\|x\|_2} = \sigma_{\min}$$

$$3. \underline{\sigma}(A) \leq |\lambda_i(A)| \leq \bar{\sigma}(A)$$

Property 1 is important because it establishes the greatest singular value of a matrix  $A$  as the maximum gain of the matrix over all possible directions of  $x$ . Property 2 is important because the least singular value of a matrix  $A$  is the minimum gain of a matrix  $A$  over all possible values of  $x$ . Property 3 simply states that the absolute value of all eigenvalues are bounded by the maximum and minimum singular values.

Singular values are useful to define the maximum and minimum gains of the return difference matrix (to be discussed in the next section). For a given plant  $G(s)$  the  $H_2$ -norm and the  $H_\infty$ -norm are defined in terms of singular values by:

$$\|G\|_2 = \sqrt{\int_{-\infty}^{\infty} \sum_{i=1}^n (\sigma_i(j\omega))^2 d\omega} \quad (2-3)$$

$$\|G\|_\infty = \sup_{\omega} \bar{\sigma}(G(j\omega)) \quad (2-4)$$

The supremum stands for least upper bound. Minimizing these norms form the basis of  $H_2$  and  $H_\infty$  theory. The band of maximum and minimum singular values plotted as a function of the frequency in a singular value Bode plot shows the degree of disturbance rejection, stability, and performance or system gain as reflected in the system bandwidth. The need to suppress high frequency plant disturbances suggests shaping the loop singular value so as to have low system gain at high frequency. The need to have a small sensitivity to measurement noise requires suppressing the response at the lower frequencies. Kwaakernak (Ref. 9) discusses for SISO

systems the shaping of the feedback response by reducing the scalar sensitivity  $S(s)$  at the lower frequencies and the transmissivity  $T(s)$  at the higher frequencies. Note that the transmissivity is also called the complementary sensitivity.

#### B. SINGULAR VALUE LOOP SHAPING FOR MIMO ROBUSTNESS.

Consideration of Figure 2.1 will assist in developing the concept of singular value loop shaping. There are two sources of disturbances: plant disturbance and reference noise. The controller is  $F(s)$ , the plant is  $G(s)$ , the input is  $r$ , the control output from  $F(s)$  is  $u$ , and the output of the system is  $y$ . The output return difference matrix is  $I + G(s)F(s)$  while the input return difference matrix is  $I + F(s)G(s)$ . The quantities  $F(s)G(s)$  and  $G(s)F(s)$  are the input and output loop gain matrices,

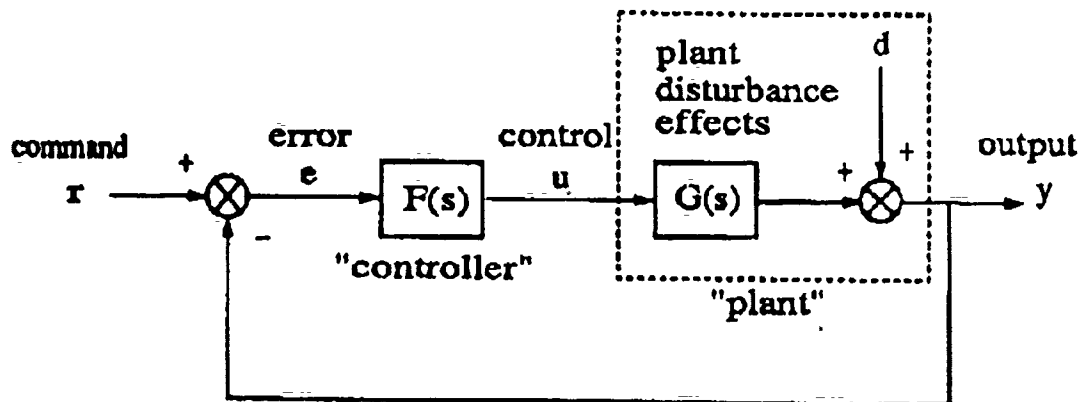


Figure 2-1 MIMO Feedback Control System

respectively. A large loop gain,  $L(s)=G(s)F(s)$ , will suppress the

plant disturbance but will tend to amplify measurement noise. The transfer matrix from  $d$  to the output  $y$  is denoted by  $S(s)$ , the transfer matrix from  $r$  to  $y$  is called  $T(s)$  and the transfer matrix from  $r$  to  $u$  is denoted by  $R(s)$ . The sensitivity matrix  $S(s)$  is given by

$$S(s) \triangleq [I + L(s)]^{-1} \quad (2-5)$$

The complementary sensitivity matrix  $T(s)$  is found by

$$T(s) \triangleq L(s) [I + L(s)]^{-1} = [I - S(s)] \quad (2-6)$$

There is no common name for  $R(s)$  which plays a part in penalizing the control deflections and is given as follows:

$$R(s) \triangleq F(s) [I + L(s)]^{-1} \quad (2-7)$$

The concept of singular value loop shaping requires high loop gain at low frequency to drive the sensitivity matrix  $S(s)$  to small values thereby suppressing plant disturbances. The sensitivity matrix will approach  $I$  at the higher frequencies. The complementary sensitivity matrix  $T(s)$  will go towards zero at higher frequencies.

Since  $S(s)$  is the closed-loop transfer matrix from the plant disturbance  $d$  to the plant output  $y$ , the singular values of  $S(s)$  determine the degree of plant disturbance attenuation of the system. The disturbance rejection specification is usually written as:



$$\bar{\sigma}(S(j\omega)) \leq W_1^{-1}(j\omega) \quad (2-8)$$

where  $|W_1^{-1}(j\omega)|$  is the disturbance attenuation factor. The disturbance attenuation factor is made a function of frequency so that a different attenuation factor can be specified for each frequency.

Consideration of figure 2.2 will lead to development of the stability criteria as applied to MIMO systems. The effect of

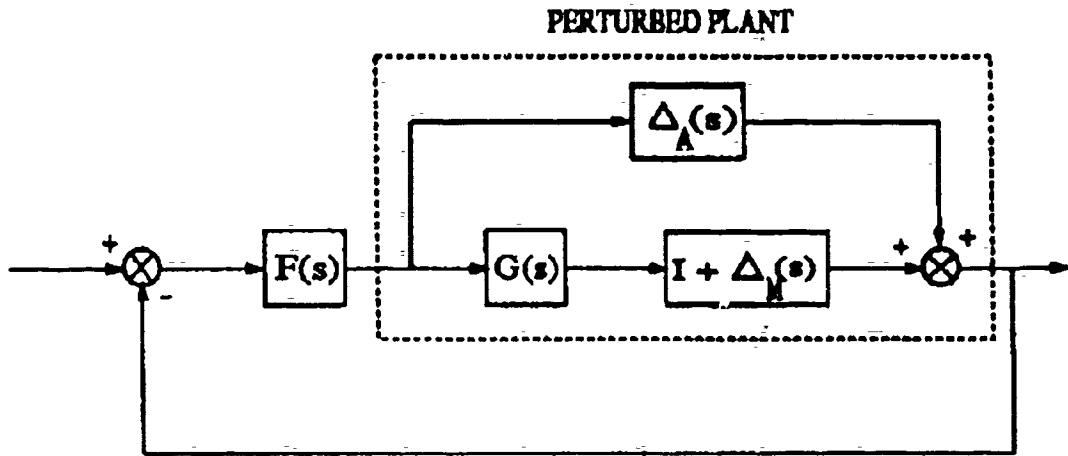


Figure 2-2 Additive/Multiplicative Perturbations

additive and multiplicative perturbations can be determined by the use of singular value plots of  $R(s)$  and  $T(s)$ . The following discussion assumes that the system without the perturbations is stable.

If  $\Delta_A$  is set to zero and  $\sigma_{\max}(\Delta_M(j\omega))$  is taken to be the definition of the size of  $\Delta_M(j\omega)$  then the smallest  $\Delta_M(s)$  for which the system is unstable is [Ref. 5]

$$\bar{\sigma}(\Delta_M(j\omega)) = \frac{1}{\bar{\sigma}(T(j\omega))} \quad (2-9)$$

multiplicative perturbation that the system can stand without going unstable. Hence the stability margin will be greater. If  $\Delta_M=0$  then the smallest  $\Delta_A(j\omega)$  that makes the system unstable is

$$\bar{\sigma}(\Delta_A(j\omega)) = \frac{1}{\bar{\sigma}(R(j\omega))} \quad (2-10)$$

The last two equations express Robustness Theorems 1 and 2 respectively [Ref. 5]. As a consequence of these two theorems, specifications can be made on the maximum allowable singular values of  $R$  and  $T$  matrices in terms of the weighting matrices  $W_2(j\omega)$  and  $W_3(j\omega)$  as follows:

$$\bar{\sigma}(R(j\omega)) \leq |W_2^{-1}(j\omega)| \quad (2-11)$$

$$\bar{\sigma}(T(j\omega)) \leq |W_3^{-1}(j\omega)| \quad (2-12)$$

Figure 2-3 shows the performance boundary on a singular value Bode plot as determined by  $|W_1(j\omega)|$  and the robustness boundary as determined by  $|W_3(j\omega)|$ . The two dashed lines represent the minimum and maximum singular values of the loop gain  $L(s)$  which is the product  $F(s)G(s)$ . The plot of the reciprocal of the maximum singular value of  $S(s)$  is seen to follow the minimum singular value of  $L(s)$  above the 0 db line then approaches the 0 db line at the higher frequencies where  $S(s)$  approaches the  $I$  matrix. The maximum singular value of  $T(s)$  approaches the maximum singular value of the loop gain  $L(s)$  below the 0 db line while approaching the 0 db line at the lower frequencies where  $T(s)$  approaches  $I$ .

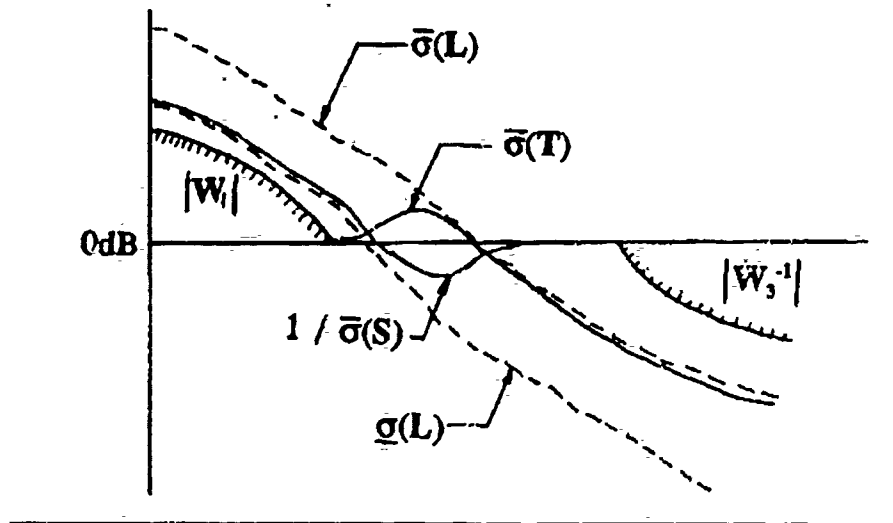


Figure 2-3 Singular Value Specifications on  $S(s)$  and  $T(s)$

### III. $H_\infty$ CONTROL DESIGN

#### A. THEORETICAL APPROACH.

The  $H_\infty$  control problem consists of solving the small gain problem for the controller  $F(s)$  such that the infinity norm of the closed loop transfer matrix  $T_{y_1 u_1}$  is less than or equal to 1 and is stable, see figure 3-1. The closed loop transfer

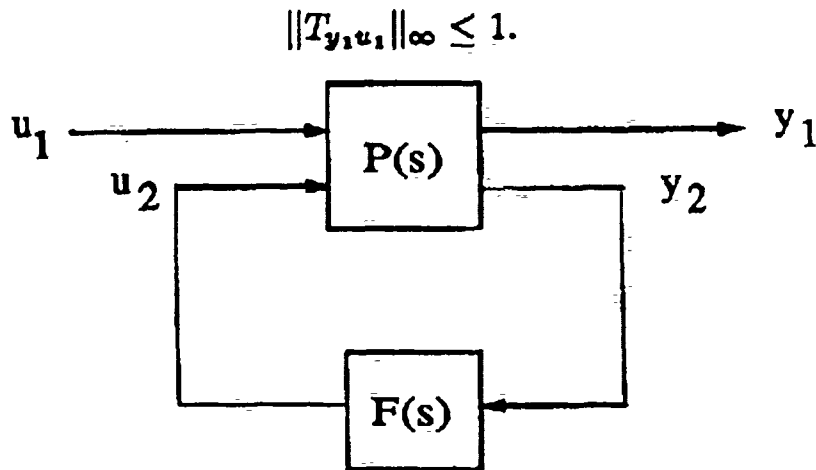


Figure 3-1 The Small Gain Problem

matrix  $T_{y_1 u_1}$  for the plant  $P(s)$  is modified by the feedback of output  $y_2$  to the controller  $F(s)$  and returning a control  $u_2$  to the plant to achieve robust stability. The transfer matrix  $T_{y_1 u_1}$  is defined in terms of the weighting matrices  $W_1$ ,  $W_3$ ,  $S(s)$ , and  $T(s)$  as defined by:

$$T_{y_1 u_1} \triangleq \begin{bmatrix} W_1 S \\ W_3 T \end{bmatrix} \quad (3-1)$$

If one includes the weighting matrix  $W_2$  to penalize the control then equation (3-1) becomes:

$$T_{y_1 u_1} \triangleq \begin{bmatrix} W_1 S \\ W_2 R \\ W_3 T \end{bmatrix} \quad (3-2)$$

The open loop plant  $G(s)$  must be augmented with the weighting matrices to form the augmented plant  $P(s)$  as shown in figure 3-2.

The relation between the input and the output is given by equation (3-3).

$$\begin{pmatrix} Y_1 \\ Y_2 \end{pmatrix} = \begin{pmatrix} Y_{1a} \\ Y_{1b} \\ Y_{1c} \\ Y_2 \end{pmatrix} = \left( \begin{array}{c|c} W_1 & -W_1 G \\ 0 & W_2 \\ 0 & W_3 G \\ \hline I & -G \end{array} \right) \begin{pmatrix} u_1 \\ u_2 \end{pmatrix} \quad (3-3)$$

The matrices in the brackets which contain the weighting matrices is the augmented plant  $P(s)$ . The state space representation of the augmented plant is

$$P(s) = \left( \begin{array}{c|cc} A & B_1 & B_2 \\ \hline C_1 & D_{11} & D_{12} \\ C_2 & D_{21} & D_{22} \end{array} \right) = \left( \begin{array}{c|c} P_{11} & P_{12} \\ \hline P_{21} & P_{22} \end{array} \right) \quad (3-4)$$

In the  $H_2$  analysis which precedes the  $H_\infty$  final design the  $D_{11}$  matrix must be a null matrix and the  $D_{12}$  matrix must be full rank.

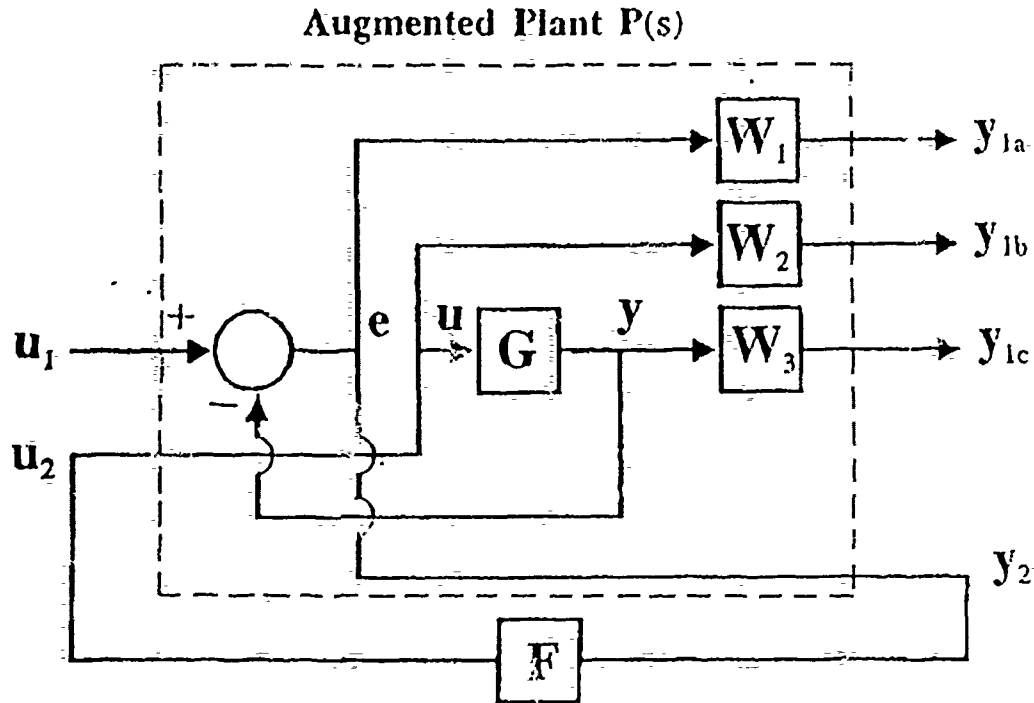


Figure 3-2 Compensated System with Augmented Plant  $P(s)$

The small gain problem is to find a stabilizing controller  $F(s)$  for the augmented plant  $P(s)$  so that the control  $u_2(s) = F(s)y_2(s)$  will minimize the norm of the closed loop transfer matrix:

$$T_{y1u1} = P_{11}(s) + P_{12}(s)(I - F(s)P_{22}(s))^{-1}F(s)P_{21}(s) \quad (3-5)$$

where the closed loop transfer matrix (equation 3-1) is represented in terms of the partitioned matrices given in equation 3-4.

#### B. DETERMINATION OF WEIGHTING CONSTRAINTS.

The weighting constraints chosen were the same as used in the X-29  $H_\infty$  design [Ref. 6]. The first objective is to suppress the sensitivity matrix singular values as much as possible for the largest possible bandwidth by large loop gains. Secondly, the

complementary sensitivity matrix singular values must be suppressed by 20 db at a frequency of 100 rad/sec with a second order fall off of -40 db/decade for frequencies above 100 rad/sec. The resultant weighting constraints are:

$$(\gamma * W_1)^{-1}(s) = \gamma^{-1} * .01 * \frac{(100s+1)}{.01s+1} * I_{2 \times 2} \quad (3-6)$$

$$W_2(s) = -.001 * I_{2 \times 2} \quad (3-7)$$

$$W_3^{-1}(s) = \frac{1000}{s^2} * I_{2 \times 2} \quad (3-8)$$

The parameter  $\gamma$  in equation (3-6) is used in an iteration scheme discussed in the next section which allows us to approach the maximum design limits of the H2 and  $H_\infty$  approaches.

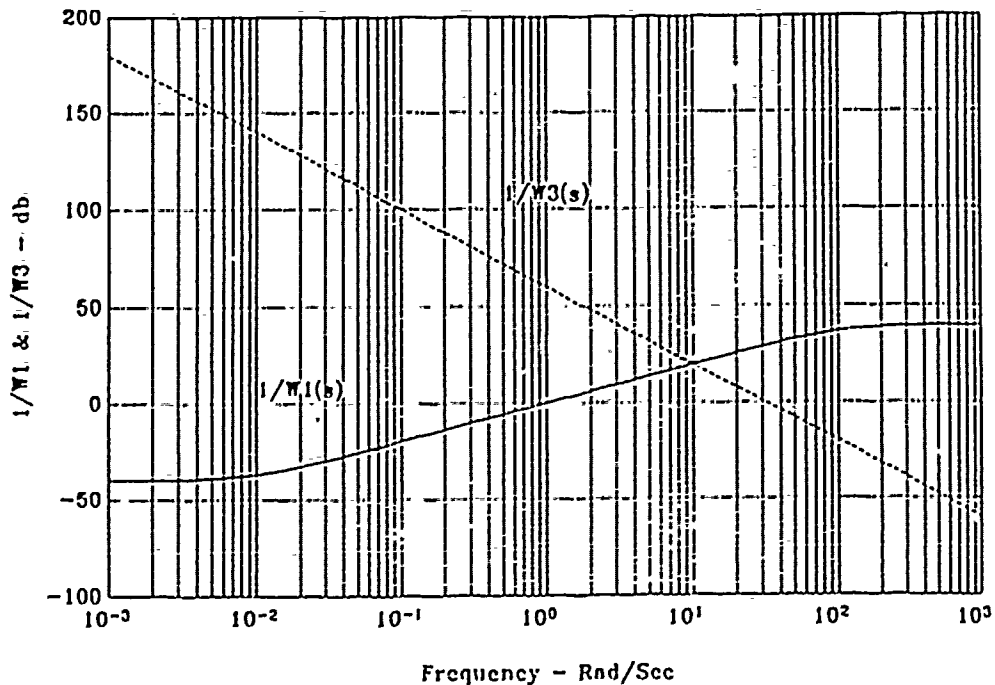


Figure 3-3  $H_\infty$  Design Specifications

The 0 db crossover frequency of the  $W_1$  plot must be sufficiently below the 0 db crossover frequency of the  $W_3$  plot or conditions (2-10) through (2-12) won't be satisfied. The  $W_3(s)$  weighting matrix can be seen to not have a proper state space representation as there are two zeros and no poles. However,  $W_3(s)G(s)$  equation (3-3) for  $P(s)$  has a proper state space representation. The  $W_2(s)$  weighting matrix ensures that the  $D_{12}$  submatrix has the full column rank required by  $H_\infty$  theory. The  $W_1^{-1}$  weighting matrix was modified for the H2 design by eliminating the 100 rad/sec corner frequency and making the denominator equal to 1. The plot of the F-18  $H_\infty$  design specifications can be seen in figure 3-3. The F-18 H2 design specifications is shown in figure 3-4.

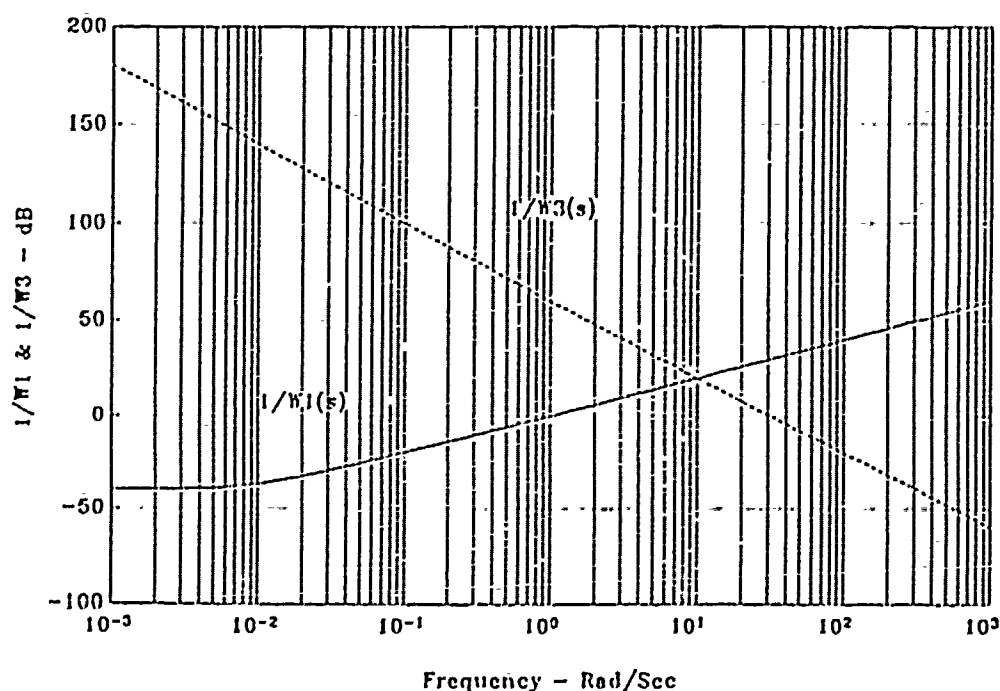


Figure 3-4 H2 Design Specifications



### C. DISCUSSION OF H2 AND $H_\infty$ DESIGN ITERATION.

A thorough discussion of the  $H_\infty$  and H2 theory can be found in references 6 and 7. The H2 and  $H_\infty$  techniques are usually used together with the H2 theory used as a first approximation with  $\gamma=1$ . The  $\gamma$  parameter in the performance weighting matrix  $\gamma W_1^{-1}(s)$  is iteratively increased until the H2 design reaches the design specification limit. The final  $\gamma$  for the H2 design is used as the starting point for the  $H_\infty$  design whereupon the parameter  $\gamma$  can be further increased before exceeding the design constraints. This iterative procedure is shown in figure 3-5.

The fact that a higher  $\gamma$  is realizable with the  $H_\infty$  design is an indication of the larger bandwidth, greater disturbance and uncertainty attenuation within the design constraints of the  $H_\infty$  design over the H2 design.

$H_2/H_\infty$   $\gamma$ -Iteration

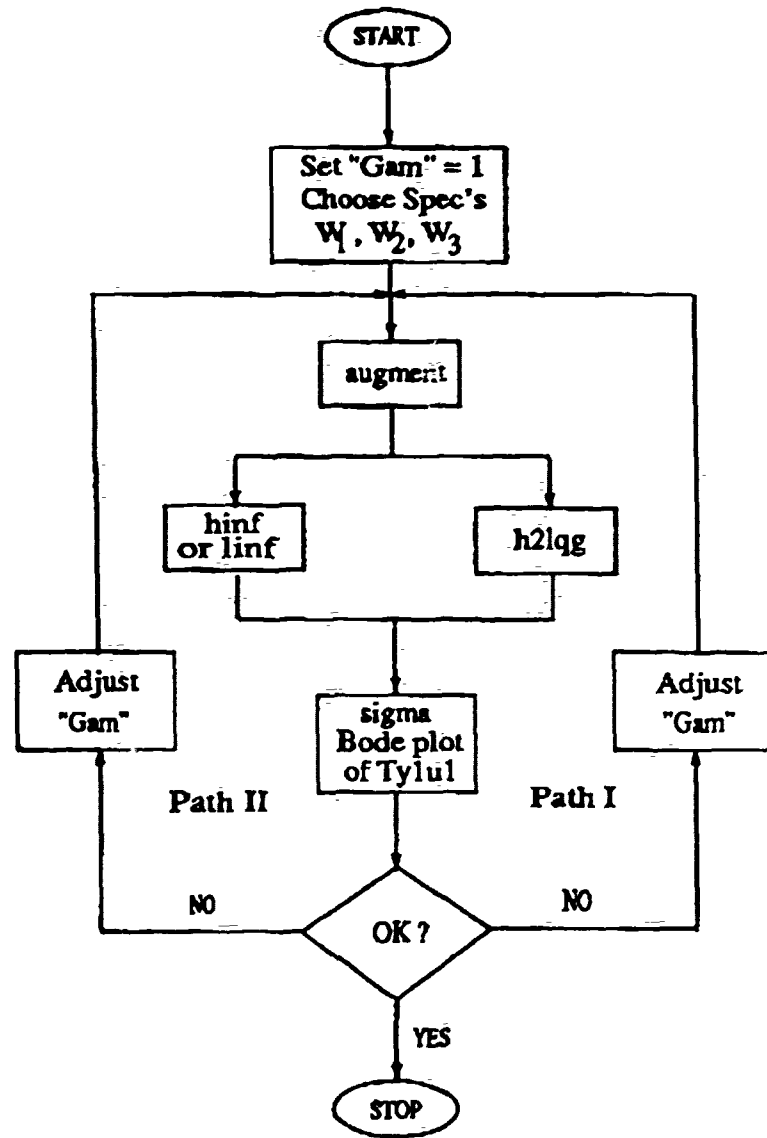


Figure 3-5  $H_2/H_\infty$  Design With  $\gamma$ -Iteration

#### IV. F-18 CONTROL DESIGN

##### A. F-18 OPEN LOOP PITCH AXIS STATE SPACE MODEL

The F-18 state space model is based on the model by Rojek [Ref. 8] for a flight condition of 0.6 Mach number at 10000 feet altitude. Figure 4-1 shows the F-18 with the control surfaces and

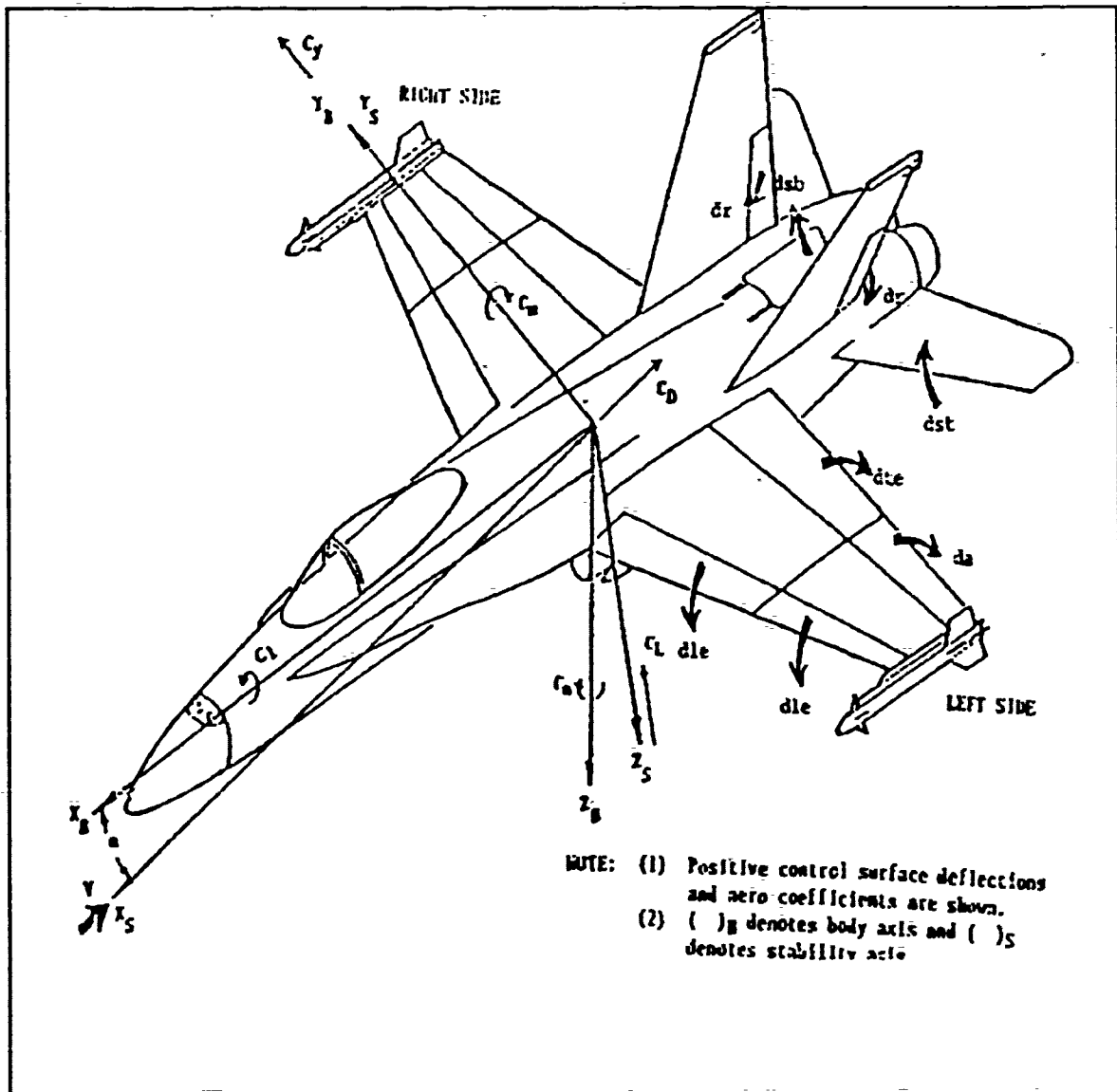


Figure 4-1 F-18 Control Surfaces and Sign Conventions

the positive sign conventions for the deflections. The pitch control surface deflections are denoted  $d_{le}$ ,  $d_{te}$ , and  $d_{st}$  for wing leading edge, wing trailing edge, and stabilator deflections, respectively. In the discussion of the state space representation to follow, the deflections will be referred to as  $\delta_{le}$ ,  $\delta_{te}$ , and  $\delta_{st}$  for the leading edge, trailing edge, and stabilator, respectively. The multiple control inputs make the F-18 an ideal candidate for the robust control theory. Control input 1 controlled the stabilator while control input 2 controlled the leading and trailing flaps together. The pitch rate and angle of attack were chosen as the two outputs of interest so that the control system is a two input-two output system similar to the example of an advanced fighter  $H_\infty$  controller treated by Chiang [Ref. 5].

The airframe equations of motion consists of two states: the downwash velocity  $w$  and the pitch rate  $q$ . Only the short period aircraft modes were considered neglecting the phugoid modes similar to Rogers [Ref. 6]. The equations of motion are linearized about a trim condition resulting in a set of first order differential equations of the general form:

$$\dot{\mathbf{x}} = \mathbf{Ax} + \mathbf{B}\delta \quad (4-1)$$

Expanding the above equation in terms of the stability derivatives similar to that shown in McRuer [Ref. 9] gives:

$$\begin{bmatrix} \dot{w} \\ \dot{q} \end{bmatrix} = \begin{bmatrix} Z_w / (1-Z_w) & (Z_q + U_b) / (1-Z_w) \\ M_w + \frac{M_w \cdot Z_w}{1-Z_w} & M_q + \frac{M_q \cdot (Z_q + U_b)}{1-Z_w} \end{bmatrix} \begin{bmatrix} w \\ q \end{bmatrix} + \begin{bmatrix} \frac{Z_{\delta_s}}{1-Z_w} & \frac{Z_{\delta_{lf}}}{1-Z_w} & \frac{Z_{\delta_{tf}}}{1-Z_w} \\ M_{\delta_s} + \frac{M_w \cdot Z_{\delta_s}}{1-Z_w} & M_{\delta_{lf}} + \frac{M_w \cdot Z_{\delta_{lf}}}{1-Z_w} & M_{\delta_{tf}} + \frac{M_w \cdot Z_{\delta_{tf}}}{1-Z_w} \end{bmatrix} \begin{bmatrix} \delta_{st} \\ \delta_{lf} \\ \delta_{tf} \end{bmatrix} \quad (4-2)$$

At 10000 feet altitude and Mach 0.6 the trim angle of attack and corresponding pitch angle is 2.6184 degrees for level flight.  $U_b$  is the body longitudinal component of flight velocity which is computed knowing the true velocity of 646.42 ft/sec and the pitch angle.

Figure 4-2 presents the two-input open loop actuator/ aircraft interface. There are two inputs  $u_1$  and  $u_2$  with  $u_1$  being the input to the stabilator and  $u_2$  the input to both the leading and trailing flaps. The stabilator is a fourth order actuator while the two flaps have second order actuators giving a total of eight actuator states. Scaling of the system matrix by transforming downwash velocity  $w$  to the angle of attack by the relation  $w=V*\alpha$  and transforming the units of the stabilator third derivative from  $\text{rad/sec}^3$  to  $10^4 \text{ rad/sec}^3$  reduced the condition number of the system matrix from  $10^7$  to  $10^4$ .

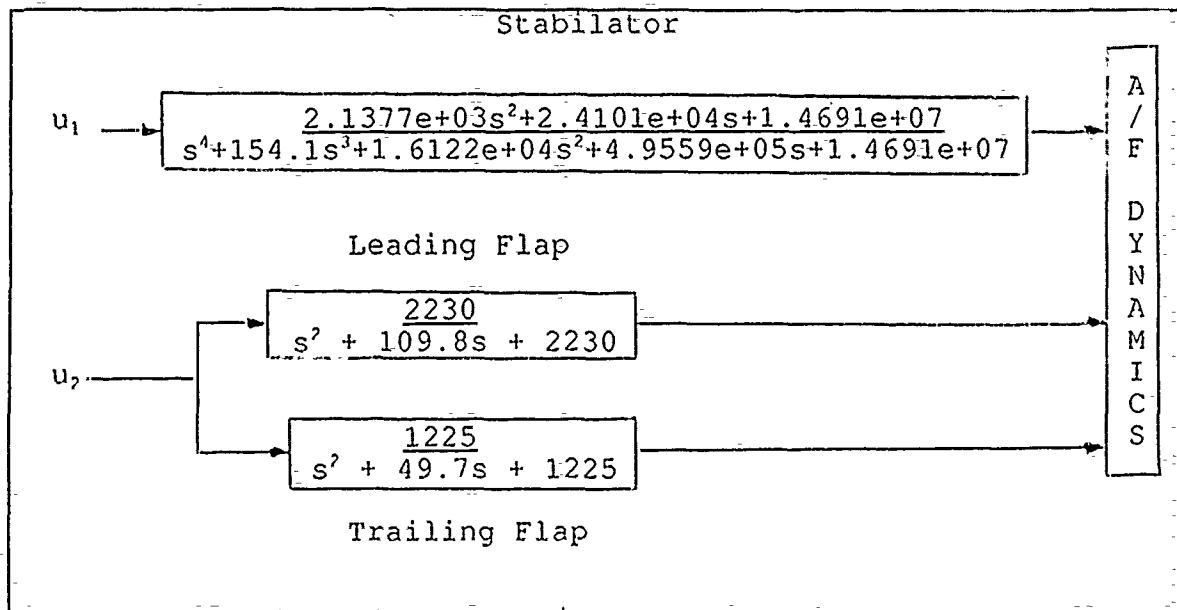


Figure 4-2 Uncompensated F-18 Open Loop Configuration

The F-18 open loop state space model is a 10 state model consisting of the two airframe states and eight states for the three actuators. The resultant 10 state linear model of  $G(s) = C(sI - A)^{-1}B + D$  is presented in Appendix B. The order of the state variables with description and units is shown in Table 4-1 and the open loop poles in Table 4-2. Note there are no unstable poles in the F-18 open loop system matrix. The example aircraft by Chiang [Ref. 5] had a complex pair of unstable poles and the X-29 design by Rogers and Hsu [Ref. 6 and 7] had a single real unstable pole. The first pair of complex poles is the short period airframe poles with a frequency of 2.80 rad/sec. The other eight poles are the higher frequency actuator states.

---

Table 4-1 The Ordered Uncompensated F-18 Model States

State	Description	Units
$\alpha$	angle-of-attack	radians
$q$	pitch rate	rad/sec
$\delta_s$	stabilator deflection	rad
$\dot{\delta}_s$	stabilator rate	rad/sec
$\ddot{\delta}_s$	stabilator accel.	rad/sec <sup>2</sup>
$\dots \delta_s$	stabilator jerk	1e+04 rad/sec <sup>3</sup>
$\delta_{lf}$	leading flap defl.	rad
$\dot{\delta}_{lf}$	leading flap rate	rad/sec
$\delta_{tf}$	trailing flap defl.	rad
$\dot{\delta}_{tf}$	trailing flap rate	rad/sec

---



---

Table 4-2

Uncompensated F-18 Open Loop Poles

$-.975 \pm j 2.627$   
 $-62.126 \pm j85.022$   
 $-14.924 \pm j33.199$   
 $-26.902$   
 $-82.898$   
 $-24.850 \pm j24.647$

---

## B. DESIGN APPROACH

The singular values of the uncompensated F-18 open loop plant are plotted in figure 4-3, the upper curve is  $\sigma_{\max}(G(j\omega))$  and the

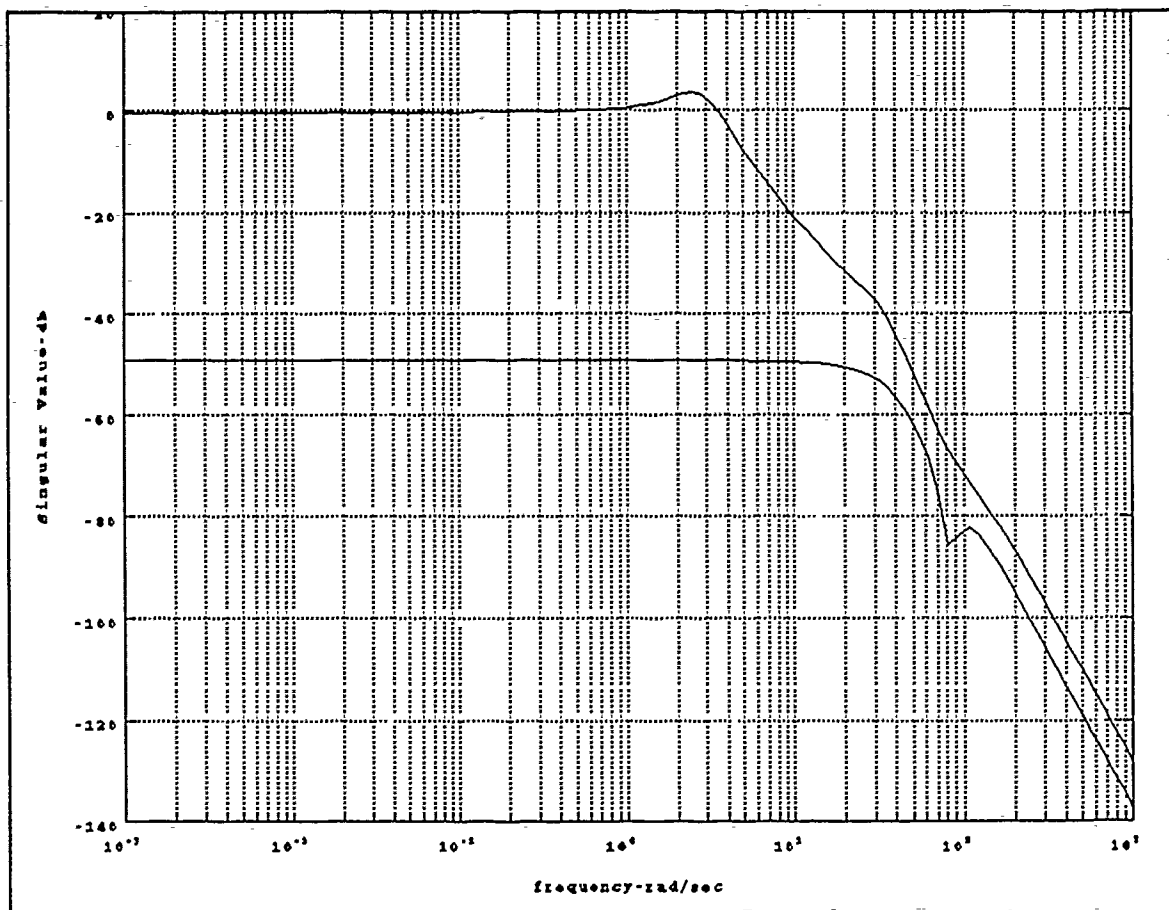


Figure 4-3 Uncompensated F-18 Open Loop Singular Value Plot

lower curve is  $\sigma_{\min}(G(j\omega))$ . The bandwidth of 3.7 rad/sec is narrow. The small loop gains for  $\sigma_{\min}(G(j\omega))$  at the lower frequencies show that the F-18 open loop plant has poor disturbance rejection and is highly sensitive to modeling errors and system variations. From the  $H_2$  and  $H_\infty$  control design methodologies presented, the sensitivity function singular values must be suppressed to the maximum extent possible by increasing the loop gains to as high a



value for the maximum possible bandwidth without conflicting with the system's stability constraints. The maximum singular value must show an attenuation of 20 db at a frequency of 100 rad/sec with a second order falloff of 40 db/decade. The above stability constraint has the purpose of attenuating the control effort at the higher frequencies so that the flexible structural modes are not excited.

The weighting constraints selected for the problem are given in equations (3-6) through (3-8). Figures 3-3 and 3-4 showed the specifications for the  $H_\infty$  and  $H_2$  controllers, respectively.

The open loop plant has 10 states but the augmented plant has a 14th order state space representation as  $W_1(s)$  and  $W_2(s)$  each add two states to the F-18 plant  $G(s)$ . The  $W_3(s)$  weighting function, having no state space representation, adds no states to the augmented plant. The  $H_2$  and  $H_\infty$  controllers will also be 14th order, the same as the augmented plant.

### C. DESIGN RESULTS OF THE H<sub>2</sub> AND OPTIMUM H<sub>∞</sub> CONTROLLER

The H<sub>2</sub> design was undertaken first per the approach shown in figure 3-5 with the assumed value of 1 for  $\gamma$ . The Matlab fl812.m script file listed in Appendix A was used. The value of  $\gamma$  was increased until the cost function  $\|T_{y1u1}\|_2$  reached the all pass limit or 0 db for the H<sub>2</sub> controller. The H<sub>∞</sub> solution was then performed using the fl8inf.m script file with  $\gamma$  being increased until a  $\gamma$  is reached in which any further increase will not result in a stabilized controller. Figures 4-4 and 4-5 show plots of the cost function  $\|T_{y1u1}\|_2$  for the H<sub>2</sub> solution with  $\gamma=1$  and  $\gamma=5.3$ . At  $\gamma=1$ , the  $\sigma_{\max}$  singular value indicated by the solid line is about 8 db below the all pass 0 db line. Increasing  $\gamma$  to 5.3 pushes the

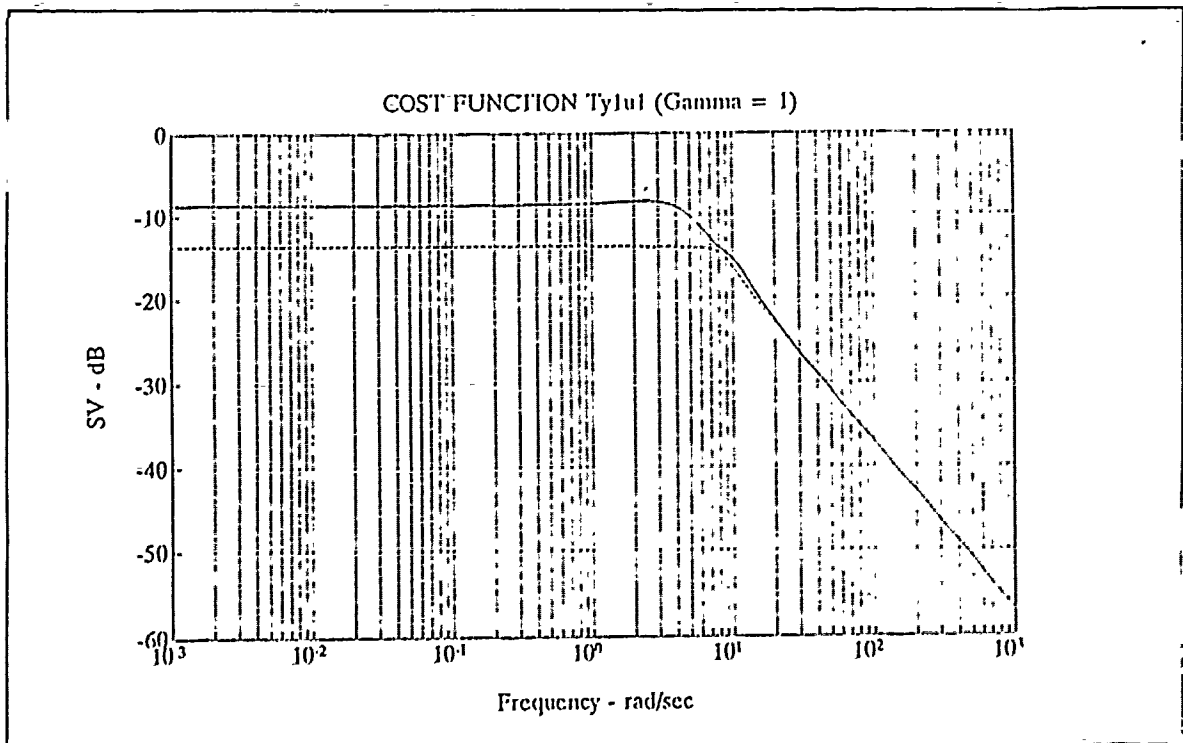


Figure 4-4 H<sub>2</sub> Cost Function  $\|T_{y1u1}\|_2$  for  $\gamma=1$

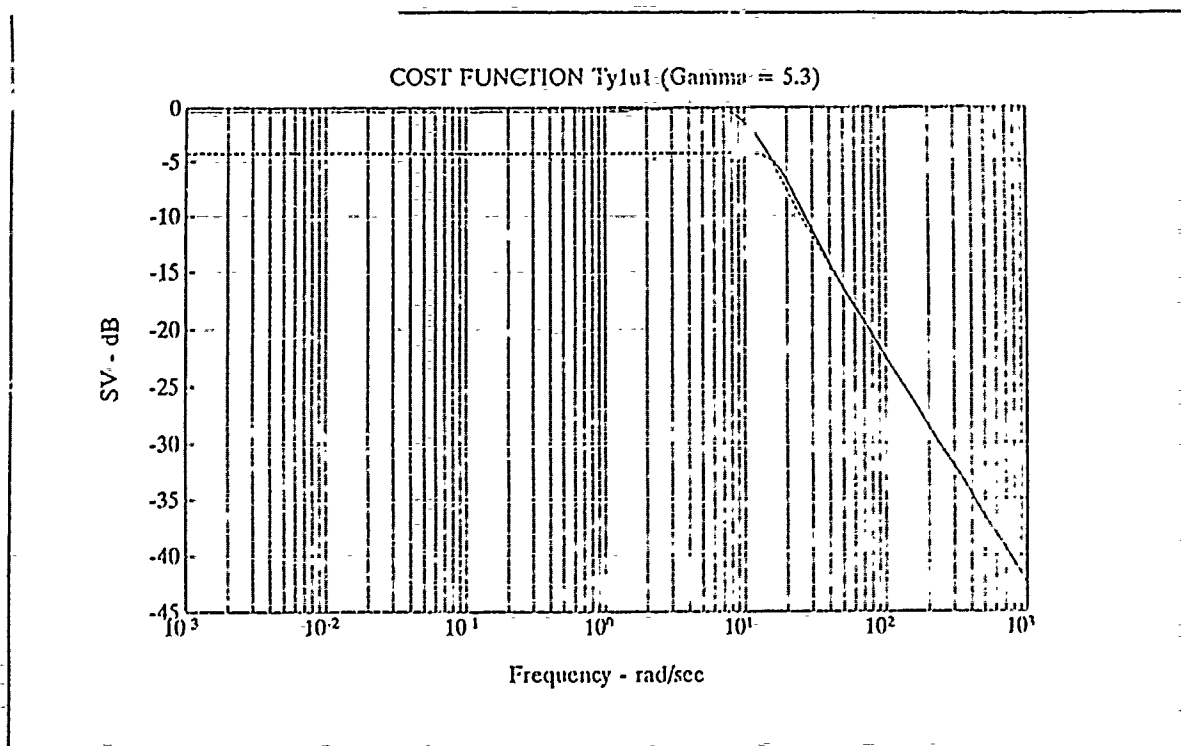


Figure 4-5 H2 Cost Function  $\|T_{y1u1}\|_2$  for  $\gamma=5.3$

H2 cost function  $\|T_{y1u1}\|_2$  to the 0 db line near a frequency of 5 rad/sec with the  $\sigma_{\min}$  singular value (dotted line) pushed to within 4 db of the 0 db line.

In figure 4-6 the  $H_\infty$  solution with a  $\gamma=13.5$  pushes the cost function  $\|T_{y1u1}\|_\infty$  minimum singular value to within .6 db of the 0 db line. The significantly higher value of  $\gamma$  possible with the  $H_\infty$  design shows that it is clearly superior to the H2 design in performance.

A comparison of the singular value plots of the sensitivity function  $S(s)$  and  $(\gamma W_1)^{-1}(s)$  weighting function can be seen in figures 4-7 through 4-9 for the H2 design with  $\gamma=1$  and 5.3 and the  $H_\infty$  design with  $\gamma=13.5$ , respectively. The  $\sigma_{\max}$  singular value is the

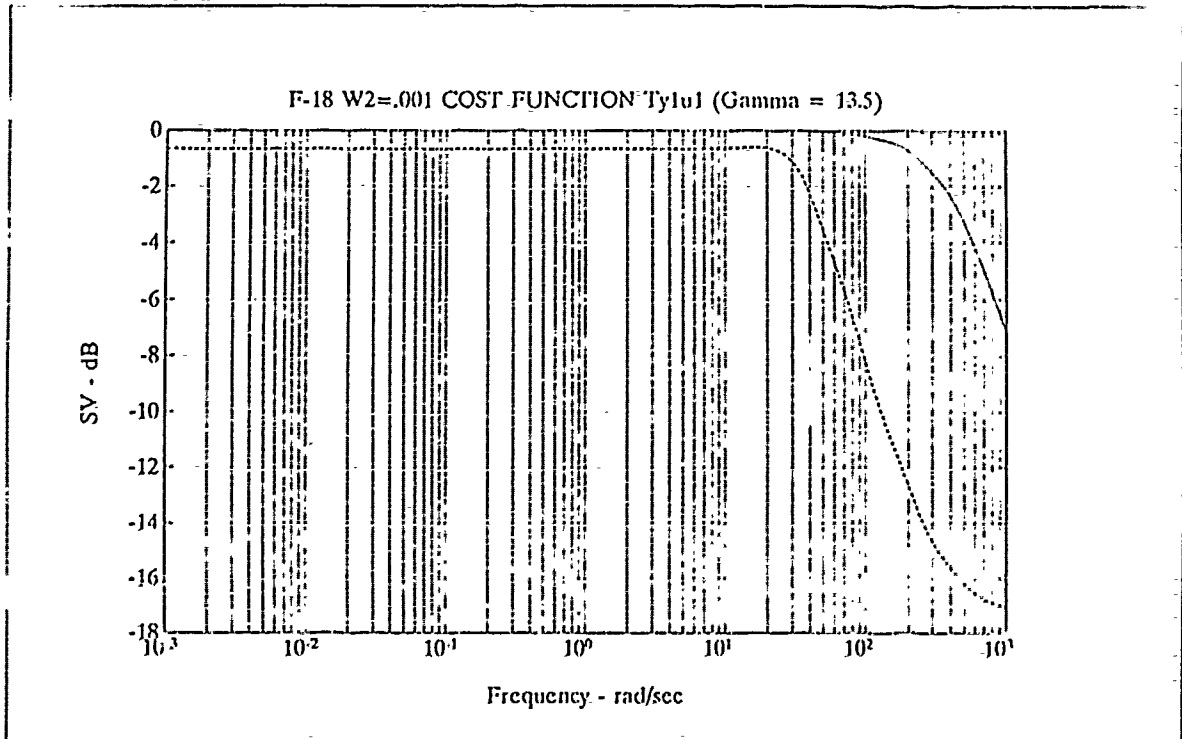


Figure 4-6  $H_\infty$  Cost Function  $\|T_{y1u1}\|_\infty$  for  $\gamma=13.5$

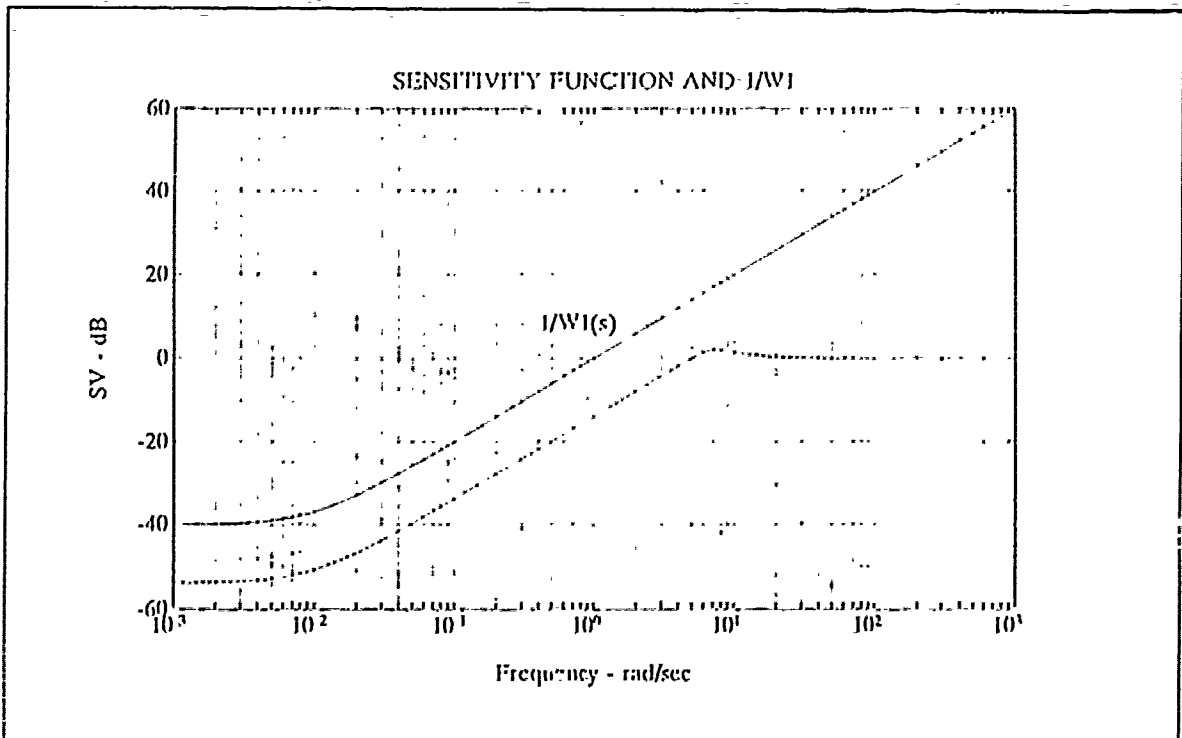


Figure 4-7 Sensitivity Function  $S(s)$  for  $H_2$  Solution,  $\gamma=1$

top dotted curve in each of the figures and the  $\sigma_{\min}$  singular value curve is represented by the dashed lower curve. In figure 4-7 the performance boundary levels out at -40 db below .01 rad/sec and the minimum singular value is 14 db below the  $W_1^{-1}$  boundary. Increasing  $\gamma$  to 5.3 in figure 4-8, the  $W_1^{-1}$  boundary dips to -54 db and the minimum singular value of the sensitivity function is 5 db below the performance boundary. The  $H_\infty$  solution at  $\Delta=13.5$  in figure 4-9 is now suppressed to -63 db and the sensitivity function's minimum singular value is now within 1 db of the performance boundary  $W_1^{-1}$ . As  $\gamma$  is increased the weighting constraint  $(\gamma W_1)^{-1}(s)$  is suppressed to lower magnitudes and the singular values of the sensitivity function  $S(s)$  are pressed closer to the weighting function. The lower sensitivity curve  $S(s)$  achieved by the  $H_\infty$  design shows that

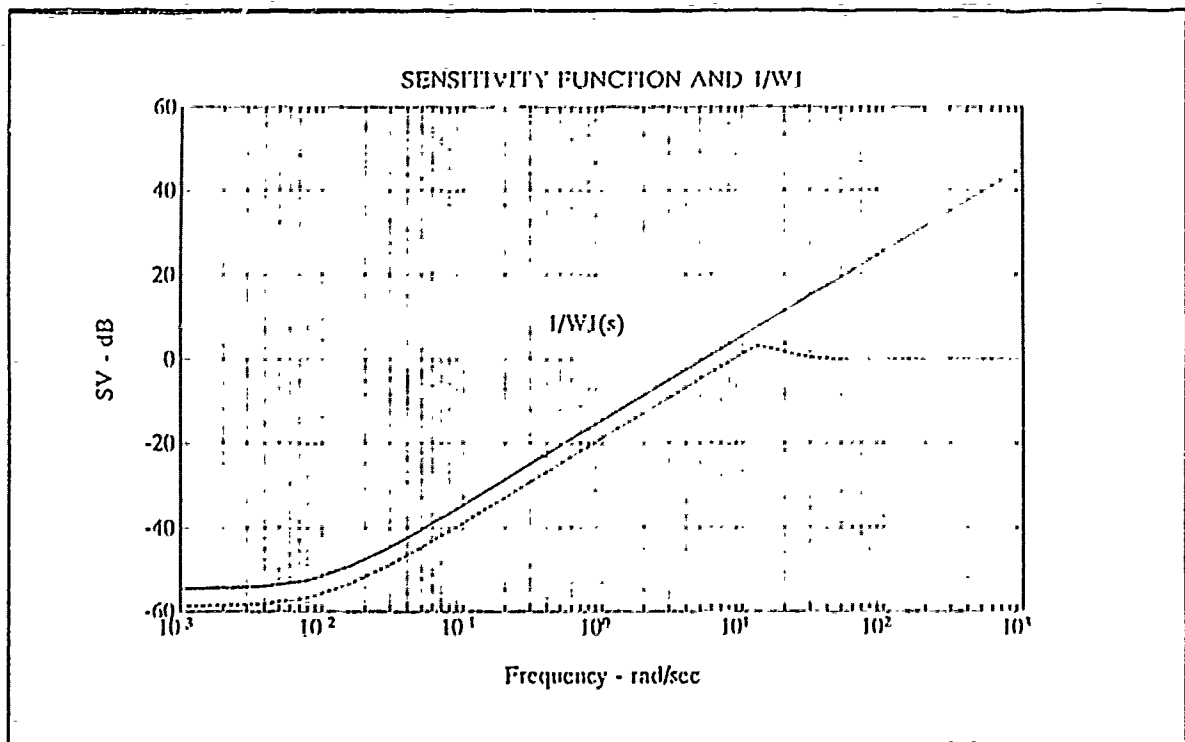


Figure 4-8 Sensitivity Function  $S(s)$  for  $H_2$  Solution,  $\gamma=5.3$

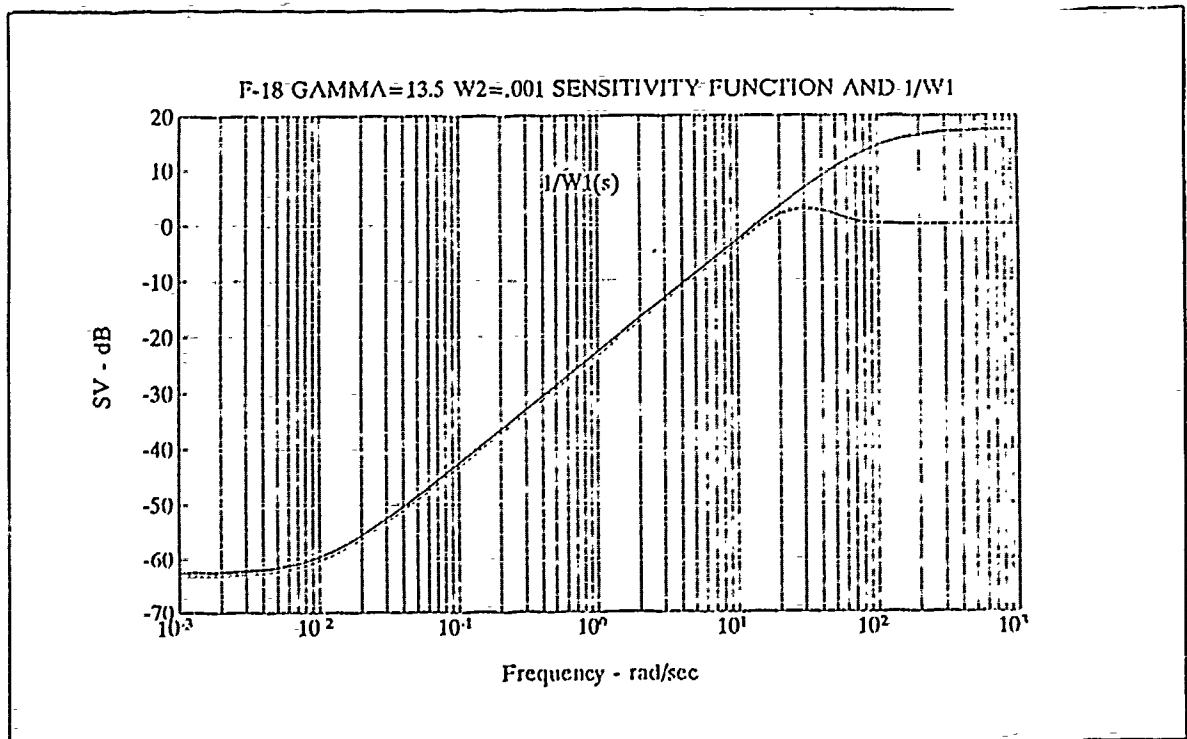


Figure 4-9 Sensitivity Function  $S(s)$  for  $H_\infty$  Solution,  $\gamma=13.5$

it has superior disturbance attenuation, lower sensitivity to plant variations and modeling errors, and a wider control bandwidth.

The complementary sensitivity function  $T(s)$  is plotted in figures 4-10 through 4-12 for the  $H_2$  case with  $\gamma=1$  and 5.3 and the  $H_\infty$  design with  $\gamma=13.5$ . The dashed curves here represent the  $\sigma_{\max}$  singular values and the dotted curves represent the  $\sigma_{\min}$  singular values. In figure 4-10 at  $\gamma=1$ , the complementary sensitivity function,  $T(s)$ , has a corner frequency of 10 rad/sec and at 100 rad/sec the maximum singular value is at -60 db compared to the -20 db robustness boundary. At  $\gamma=5.3$ , the  $H_2$  solution for  $T(s)$  in figure 4-11 shows a corner frequency of 18 rad/sec and a gain of -45 db at 100 rad/sec. At  $\gamma=13.5$  in figure 4-12, the  $H_\infty$  solution yields a corner frequency of 22 db and a maximum singular value of

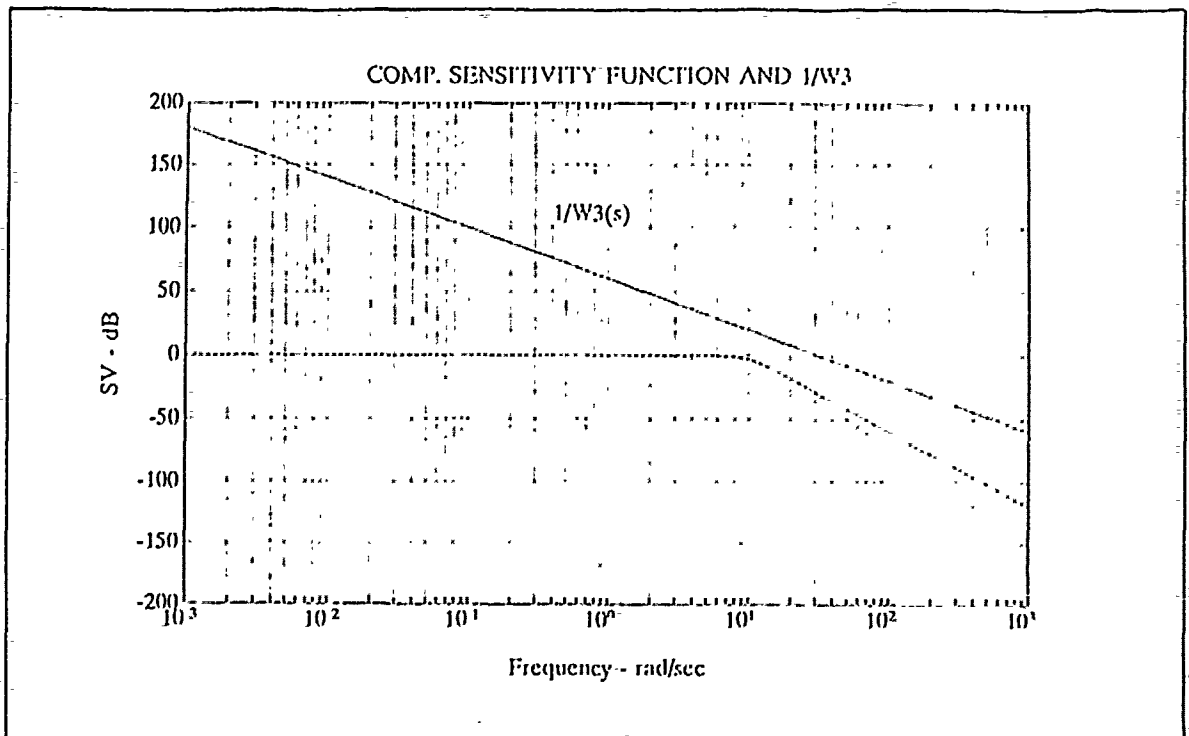


Figure 4-10 H2 Complementary Sensitivity Function  $T(s)$ ,  $\gamma=1$

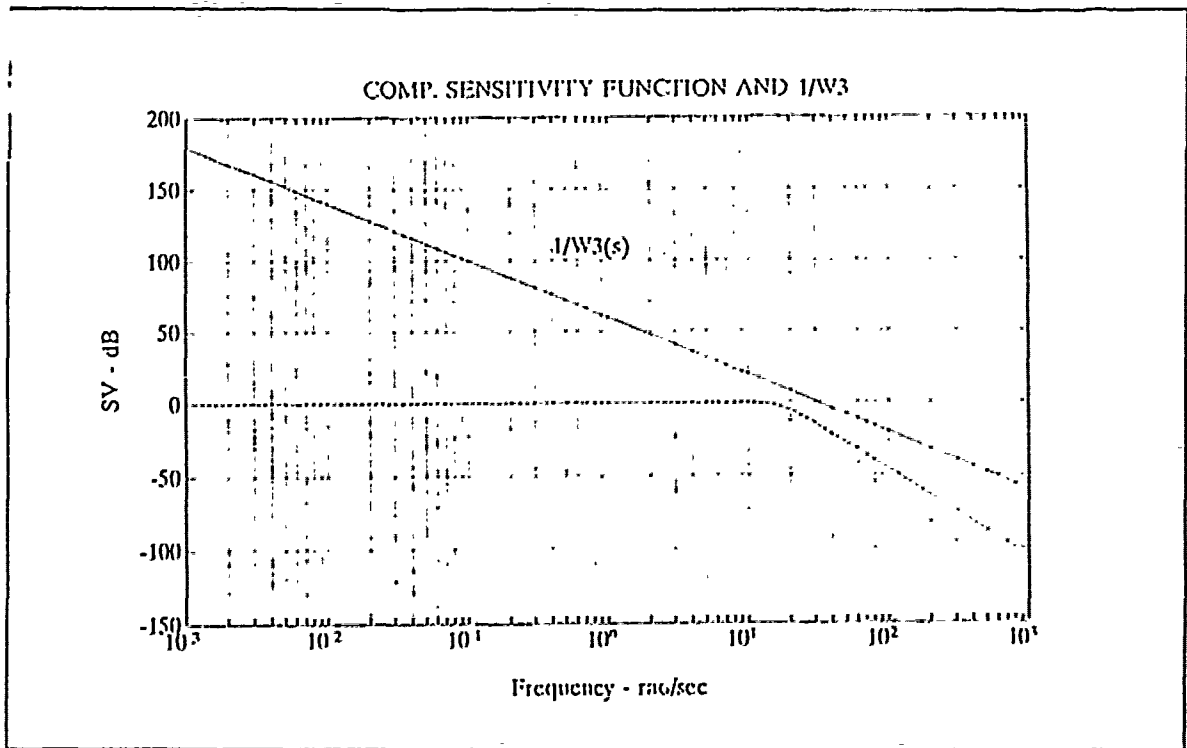


Figure 4-11 H2 Complementary Sensitivity Function  $T(s)$ ,  $\gamma=5.3$

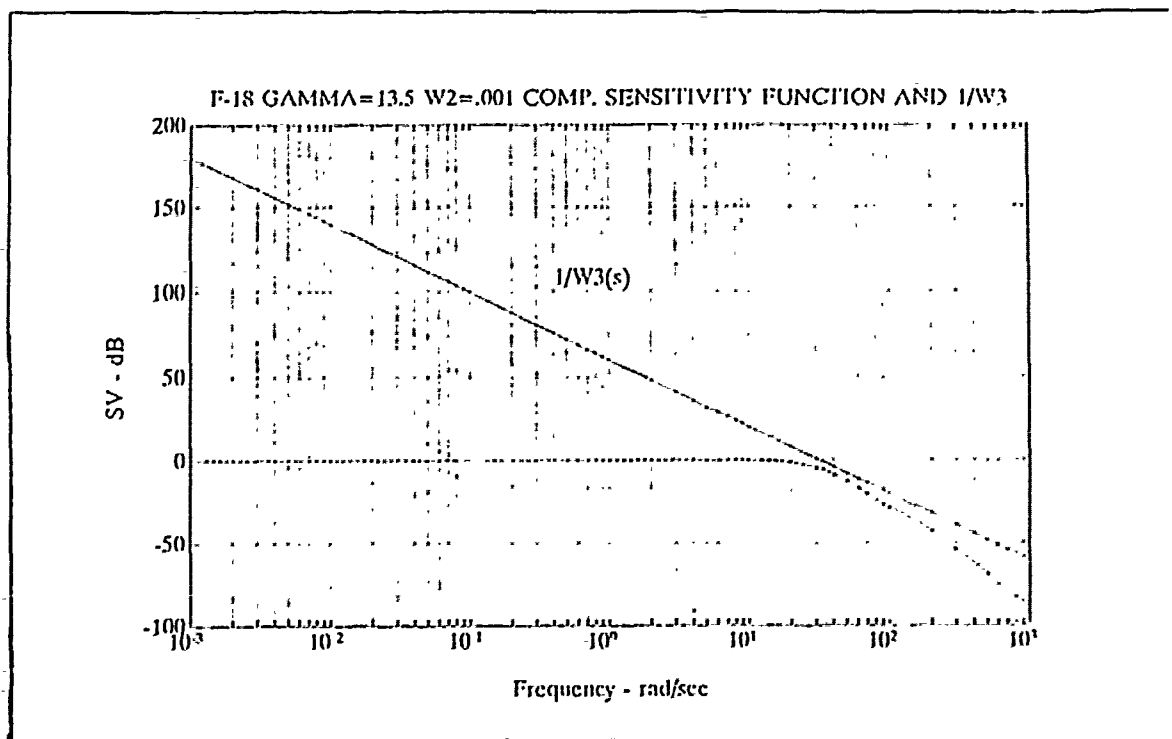


Figure 4-12  $H_\infty$  Complementary Sensitivity Function,  $\gamma=13.5$

-28 db at 100 rad/sec. From these results, the higher  $\gamma$  that the  $H_\infty$  controller is able to achieve resulted in pushing  $T(s)$  as close to the robustness boundary as possible.

The effect on control bandwidth of increasing  $\gamma$  can be quantified from figures 4-10 through 4-12. At  $\gamma=1$ , the  $H_2$  bandwidth determined by the frequency at the -3 db maximum singular value is about 10 rad/sec while the  $\gamma=5.3$   $H_2$  solution achieves about a 16 rad/sec bandwidth. The  $H_\infty$  solution at  $\gamma=13.5$  has a higher bandwidth of 20 rad/sec. Rogers [Ref. 6] found for the X-29 that the best  $H_2$  and  $H_\infty$  solutions gave 20 and 30 rad/sec, respectively. Both sets of results indicate that the  $H_\infty$  compensated aircraft is a more responsive aircraft.



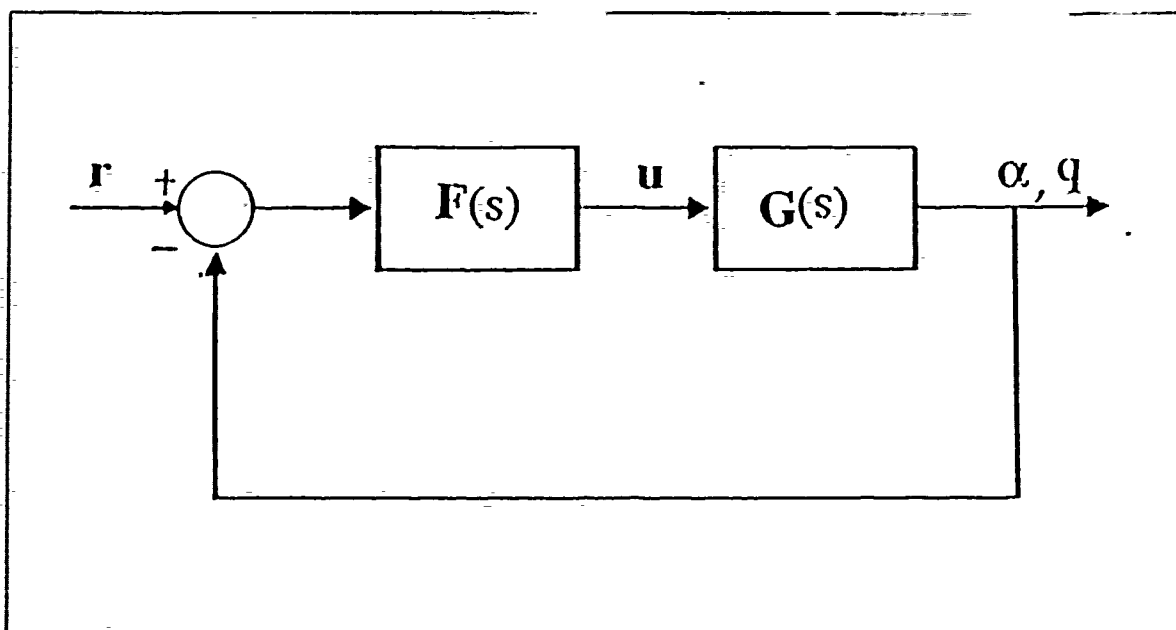


Figure 4-13 Feedback Configuration

The controller is a 14-state controller as was expected. The closed loop controller as shown in figure 4-13 is a 24-state configuration. The output vector  $y$  consists of the output states  $\alpha$  and  $q$ . The control input vector  $r$  contains the control inputs  $u_1$  and  $u_2$ . Since the controller is placed in series with the F-18 plant the commands  $u_1$  and  $u_2$  are reference commands to the outputs  $\alpha$  and  $q$ . The closed loop model has 2 inputs, 2 outputs and 24 states.

The state space model of the 24th order closed loop  $H_\infty$  compensated model is presented in Appendix B. The poles of the  $H_\infty$  compensated closed loop system are shown in Table 4-3. The poles of the open loop plant  $G(s)$  can be seen to also exist in the closed loop  $H_\infty$  compensated plant. The low condition number of the open loop plant  $G(s)$  means that the augmented plant  $P(s)$  and the controller  $F(s)$  are well-conditioned. The well-conditioned

---

Table 4-3  $H_{\infty}$  Compensated Closed Loop Poles

-1.7985e+04  
-4.6415e+02  
-6.2126e+01  $\pm$  j8.5022e+01  
-1.4533e+01  $\pm$  j8.1275e+01  
-1.0183e+02  
-8.1898e+01  
-1.4924e+01  $\pm$  j3.3199e+01  
-1.9460e+01  $\pm$  j2.2795e+01  
-2.6990e+01  $\pm$  j2.3233e+01  
-2.4850e+01  $\pm$  j2.4647e+01  
-2.5633e+01  $\pm$  j1.3283e+01  
-2.6902e+01  
-3.9708e+01  
-9.7451e-01  $\pm$  j2.6269e+00  
-1.0000e-03  
-1.0000e-03

---

numerical properties of these matrices required no minimum realization nor balancing to be performed which is desirable as the meaning of the state variables becomes obscure if the matrices undergo balancing. The open loop 10 state matrix can be seen, in Appendix B, to occupy rows 15 through 24 and columns 15 through 24. The open loop states 1 through 10 correspond to states 15 through 24 of the  $H_{\infty}$  closed loop controller.

The output return difference matrix  $[I+G(s)F(s)]$  is the inverse of the sensitivity matrix and as such the minimum singular value approximates the loop gains if the loop gains are large. The plot of the output return difference matrix  $I+G(s)$  of the uncompensated closed loop plant, figure 4-14, show that with the minimum singular value well below the 0 db line that the loop gain is low. The low loop gain of the uncompensated plant means that it has low disturbance rejection and high sensitivity to plant

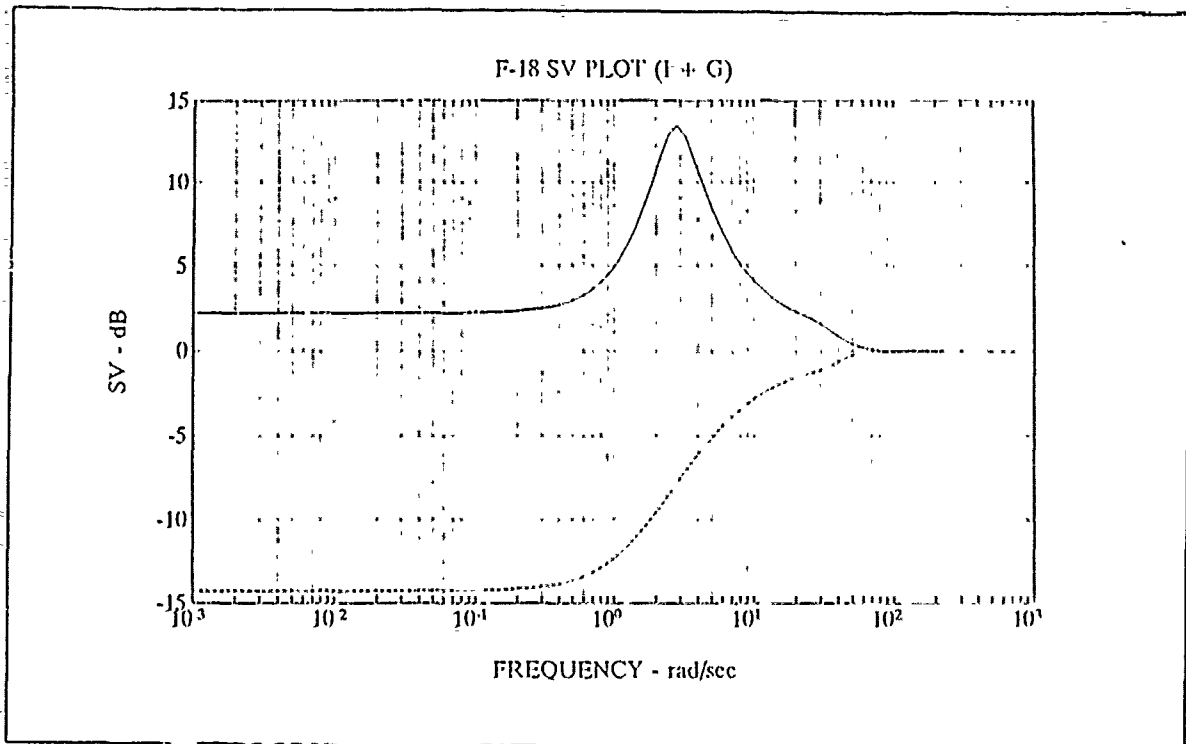


Figure 4-14 Singular Value Plot  $I+G(s)$ , Uncompensated F-18

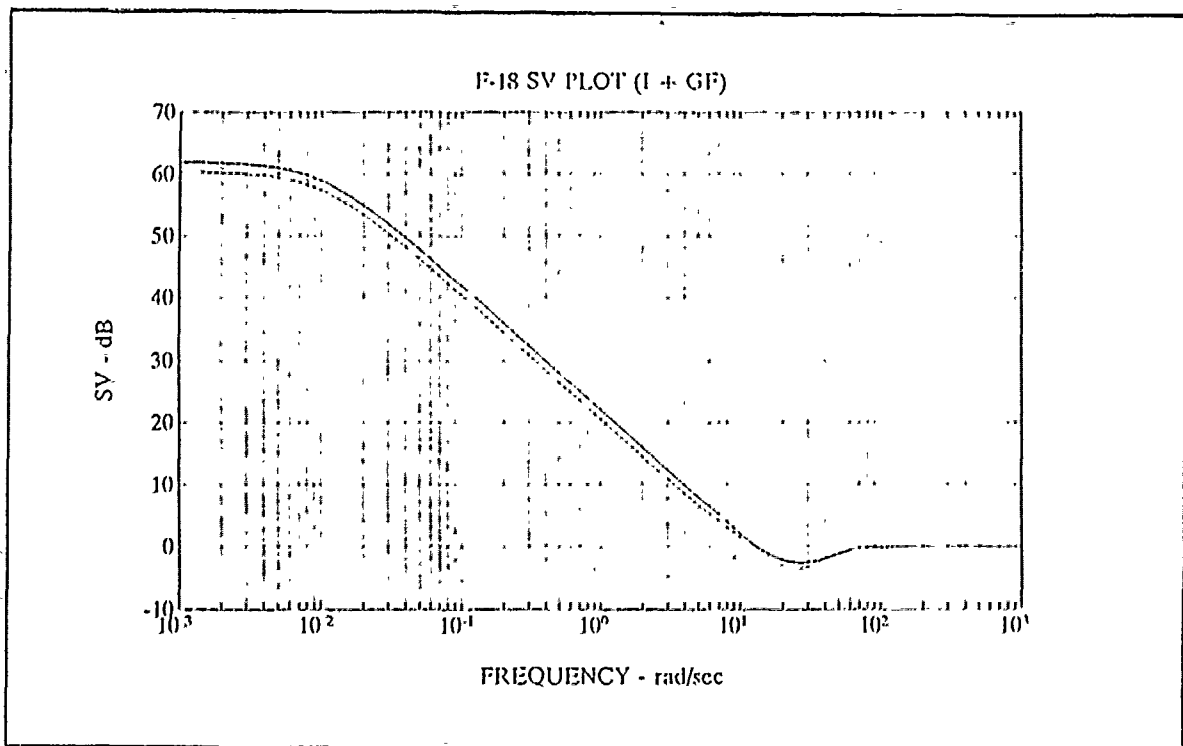


Figure 4-15 Singular Value Plot  $I+G(s)F(s)$ ,  $H_\infty$  Compensated F-18

variations and modeling errors as was surmised from the singular value plot of the open loop plant earlier in the chapter. The plot of the singular values of the compensated return difference matrix  $I + F(s)G(s)$  in figure 4-15 show that the loop gains at the lower frequencies are much improved over the uncompensated plant. Thus the  $H_\infty$  compensated plant has good disturbance rejection and low sensitivity to plant variations and modeling errors. The steep second order roll-off designed into the complementary sensitivity function  $T(s)$  probably caused the dip of the singular values below 0 db between 14 and 80 rad/sec indicates a lower level of performance near the 0 db crossover frequency. The crossover point of 13 rad/sec is below the 30 rad/sec crossover of the  $W_3$  weighting matrix which is one of the requirements for stability.

The inverse-return matrix  $I + (G(s)F(s))^{-1}$  is plotted in figure 4-16 for the  $H_\infty$  design. The stability margins were determined by examining the universal gain and phase margin curve [Ref. 6, pg.68] and are the same as those guaranteed by the linear quadratic regulator problem. The minimum singular value of 0 db or 1 shown for the  $H_\infty$  design in figure 4-16 guarantees gain margins of -6 db to infinity and phase margins of  $\pm 60^\circ$ .

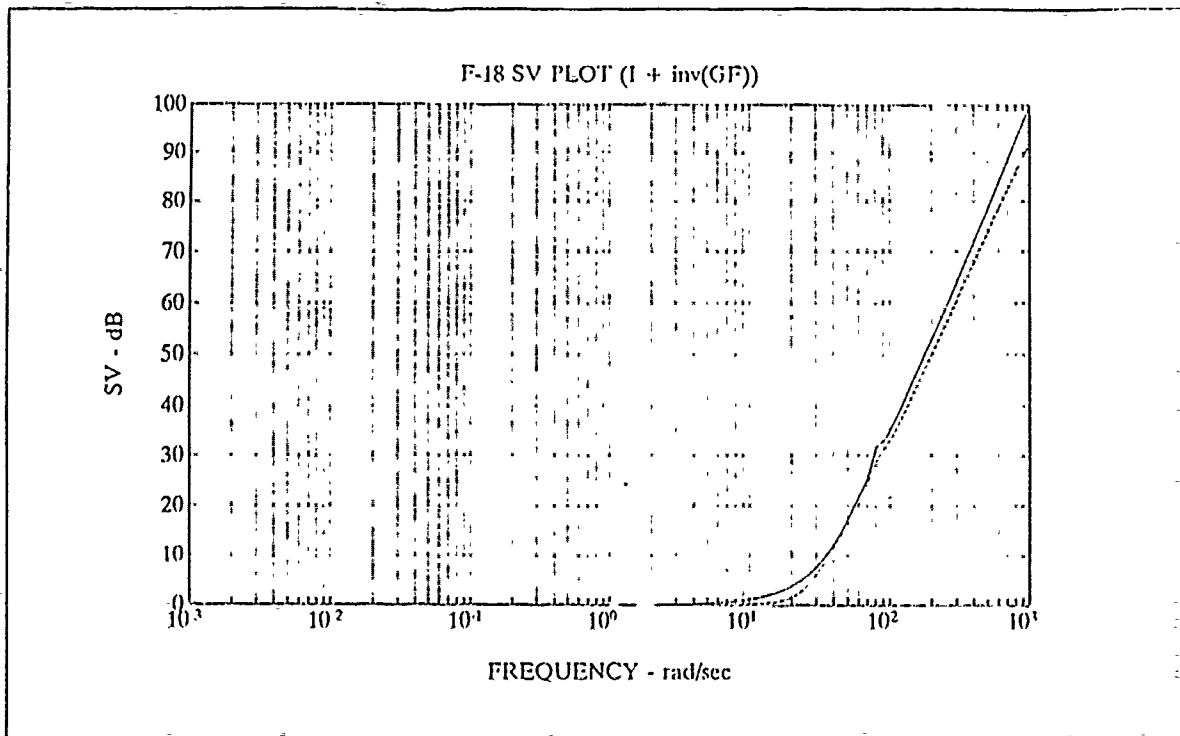


Figure 4-16 SV Plot of  $I+(G(s)F(s))^{-1}$ ,  $H_\infty$  Design F-18

### 1. $H_\infty$ Input Return Difference Analysis

The input additive and input multiplicative return difference matrices are plotted in figures 4-17 and 4-18, respectively. The input additive return difference matrix has poor disturbance attenuation with the minimum singular value (dashed curve) below -3 db in the range of frequency of 1 to 60 rad/sec. A  $\sigma_{\min}[I+(F(j\omega)G(j\omega))^{-1}]$  of -20 db (figure 4-18) translates to a gain margin of -2 to +2 db and a phase margin of  $5^\circ$ . In figure 4-18, the minimum value of the input multiplicative return difference matrix  $I+(F(s)G(s))^{-1}$  violates the  $W_3$  boundary. The conclusion is that the  $H_\infty$  design does not guarantee stability at the inputs to the plant  $G(s)$  since the design is based on the plant output.

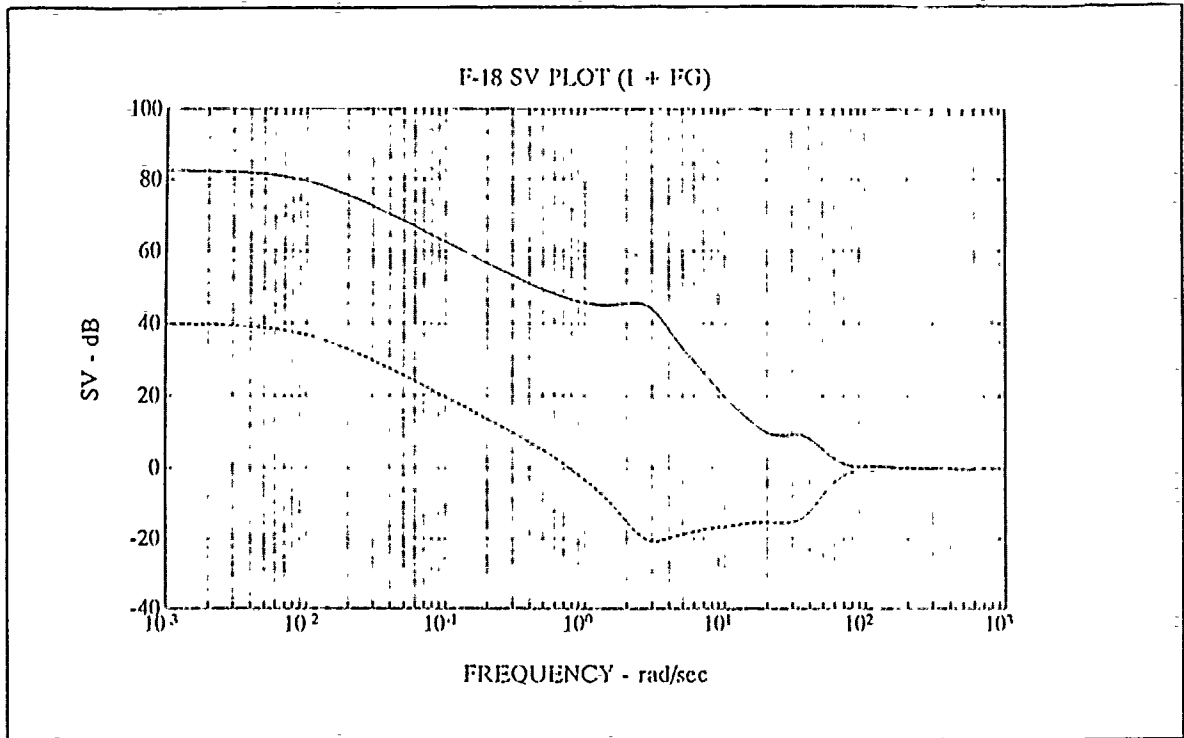


Figure 4-17 SV Plot of  $I+FG$ ,  $H_\infty$  Design for the F-18

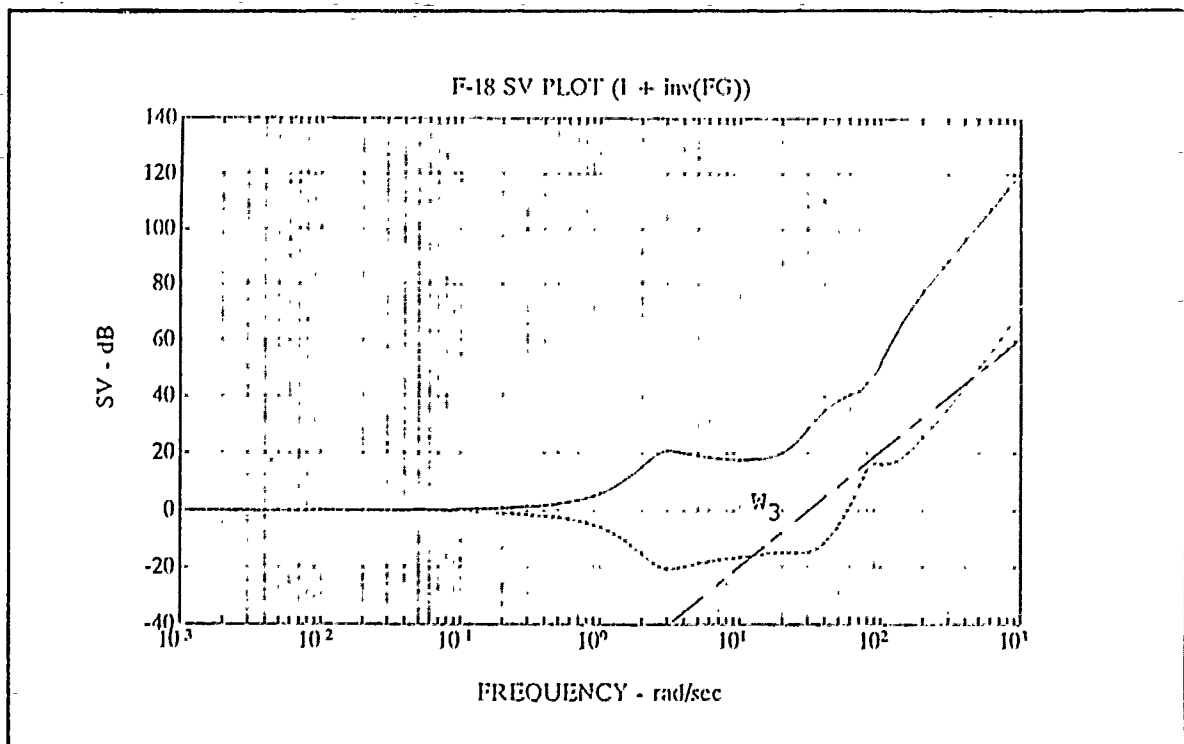


Figure 4-18 F-18 SV Plot of  $I+(FG)^{-1}$ ,  $H_\infty$  Design for the F-18

## 2. Precision Longitudinal Control Modes

The  $H_\infty$  solution in the two-input, two-output case ideally will result in control of output 1 by input 1 and output 2 by input 2. This feature allows for multiple, independently controlled surface deflections. Safonov [Ref. 10] listed the three precision longitudinal modes of control observed with the  $H_\infty$  derived designs:

1. Varying the vehicle vertical velocity by varying angle of attack while holding the pitch angle constant or keeping  $q$  equal to 0.
2. Direct lift control by varying  $\theta$  while keeping  $\alpha$  constant so that the velocity vector remains fixed along the aircraft stability axis  $x_s$  as  $x_s$  rotates.
3. Pitch pointing by controlling  $\theta$  at a constant flight path angle so that the flight path angle or velocity vector remains fixed while  $x_s$  rotates ( $\theta=\alpha$ ).

Closed loop Bode Plots of  $\alpha$  and  $q$  responses to inputs 1 and 2 are shown in figures 4-19 through 4-22. The response of  $\alpha$  to input 1, figure 4-19 shows a gain of 1 or 0 db for frequencies of up to 6 rad/sec which is above the short period frequency of the F-18. However the  $q$  response to input 1 in figure 4-20 never gets above -32 db which occurs at a frequency of 20 rad/sec, well beyond the short period frequency of the F-18. Figure 4-21 shows the  $q$  response to input 2 to have a gain of 1 or 0 db to a frequency of 10 rad/sec while the transfer function  $\alpha/u_2$  in figure 4-22 is suppressed with a maximum of -36 db at 22 rad/sec. These Bode plots show the great separation with very little cross-coupling which allows input 1 to be used to control only  $\alpha$  and input 2 to control only  $q$ .

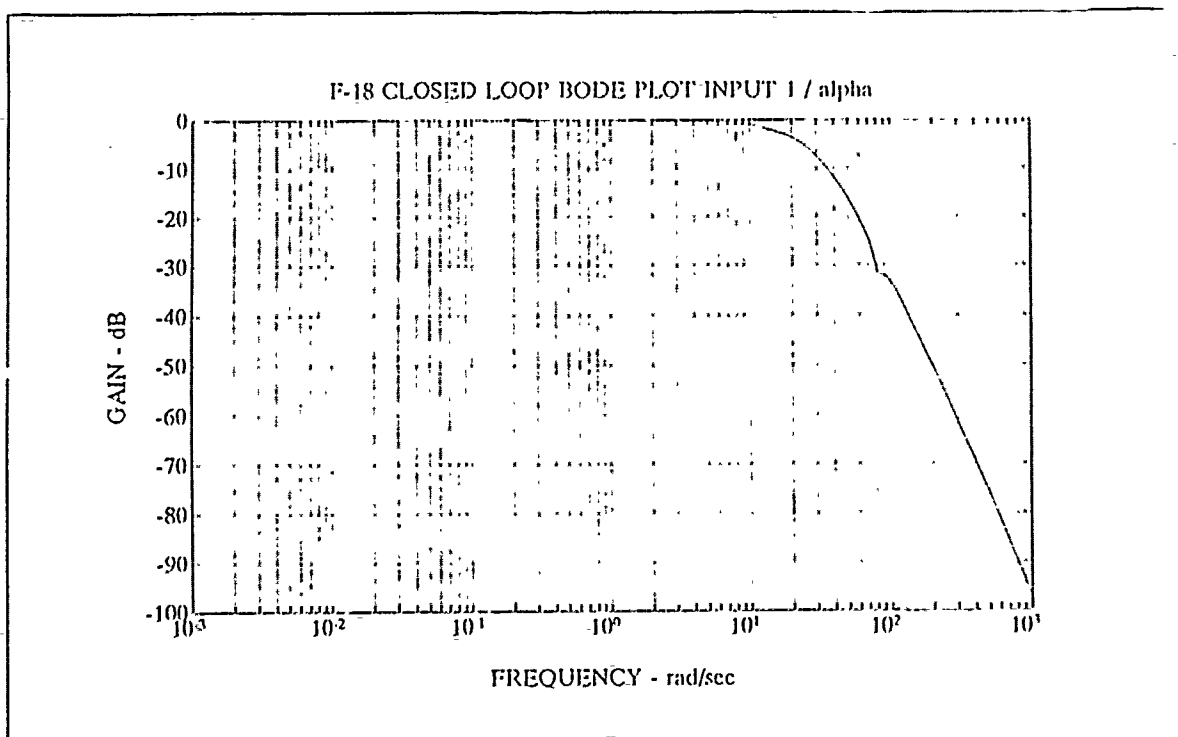


Figure 4-19 Bode Plot of F-18  $\alpha/u_1$  T.F.,  $H_\infty$  Design

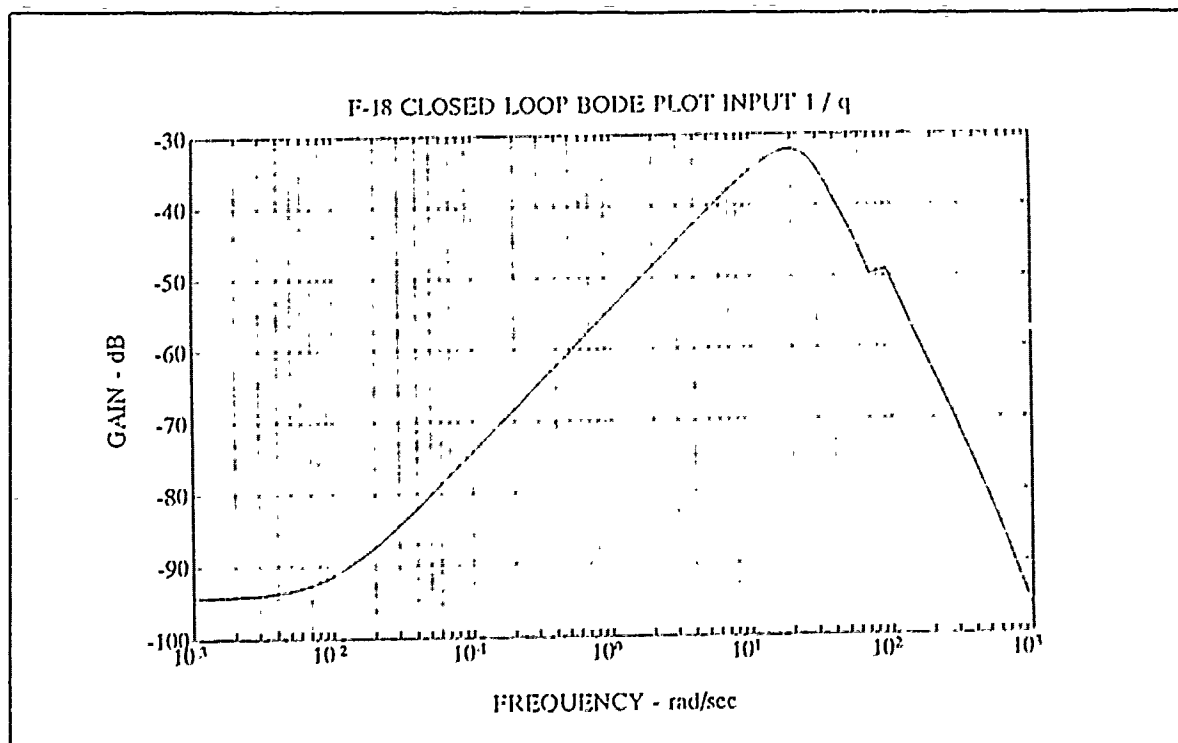


Figure 4-20 Bode Plot of F-18  $q/u_1$  T.F.,  $H_\infty$  Design



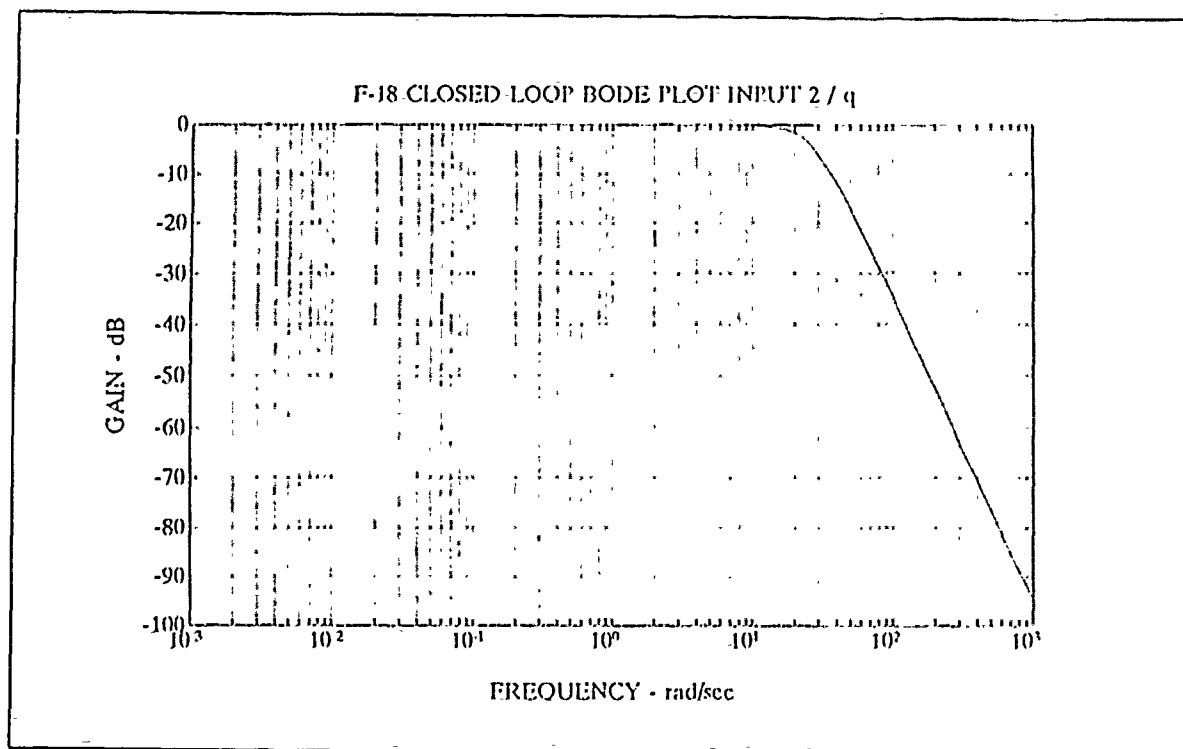


Figure 4-21 F-18 Bode Plot of  $q/u_2$  T.F.  $H_\infty$  Design

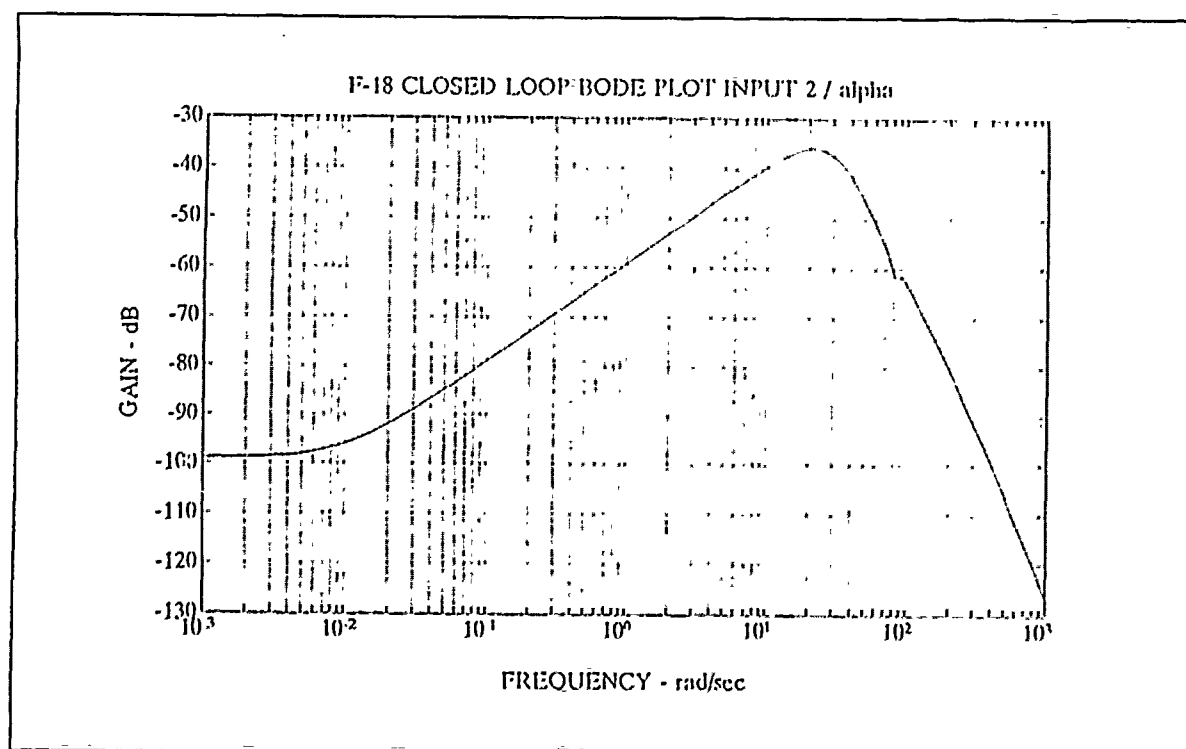


Figure 4-22 F-18 Bode Plot of  $\alpha/u_2$  T.F.  $H_\infty$  Design

The time responses of  $\alpha$  and  $q$  to a  $1^\circ$  pulse of 1 second duration in input 1 is shown in figure 4-23 and to a  $1^\circ/\text{sec}$  pulse of 1 second duration in input 2 is shown in figure 4-24. Figure 4-23 shows a fast rise time in the alpha response to  $u_1$  of .2 sec to reach the commanded input but the  $q$  response barely makes a ripple along the  $0^\circ/\text{sec}$  line when plotted on the same scale. Figure 4-24 shows that the pitch rate response  $q$  slightly overshoots the commanded  $u_2$  before settling out to the commanded value but here again the other output  $\alpha$  is essentially zero due to the second input  $u_2$ . The rise time of  $\alpha$  to  $u_1$  is .1 sec and the rise time of  $q$  to  $u_2$  is .088 sec.

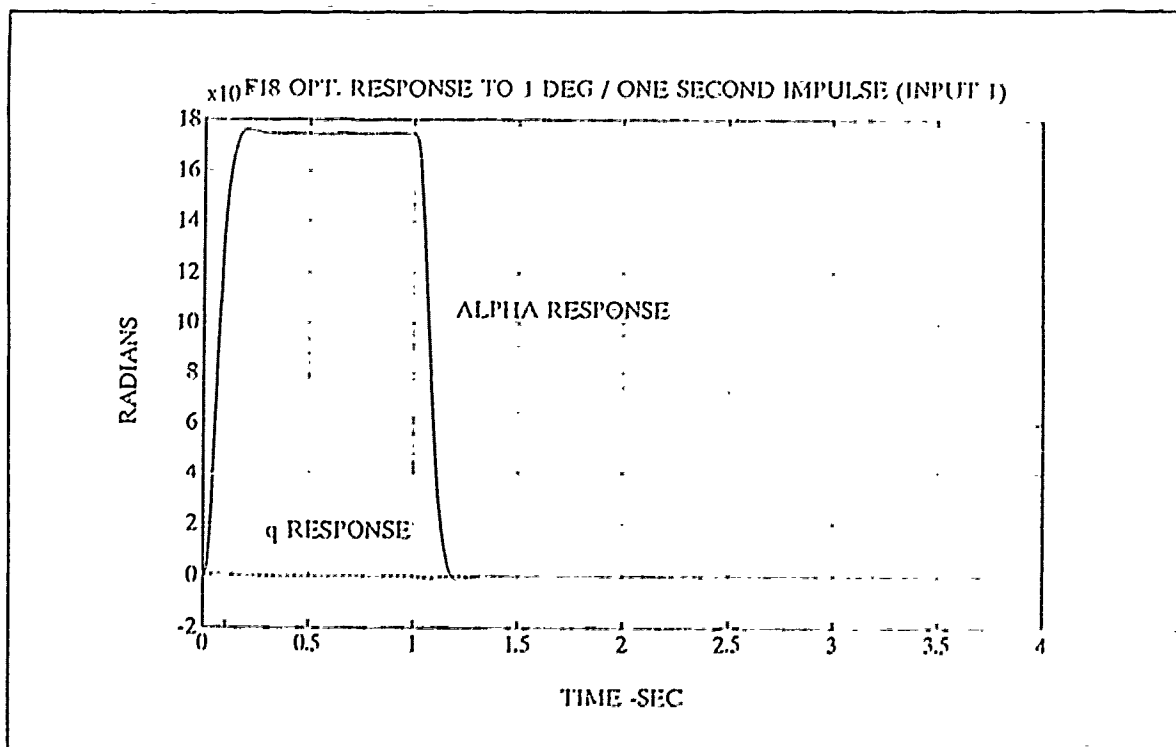


Figure 4-23  $\alpha$  and  $q$  Responses to  $1^\circ/\text{sec}$  1-sec Pulse in  $u_1$ ,  $H_\infty$

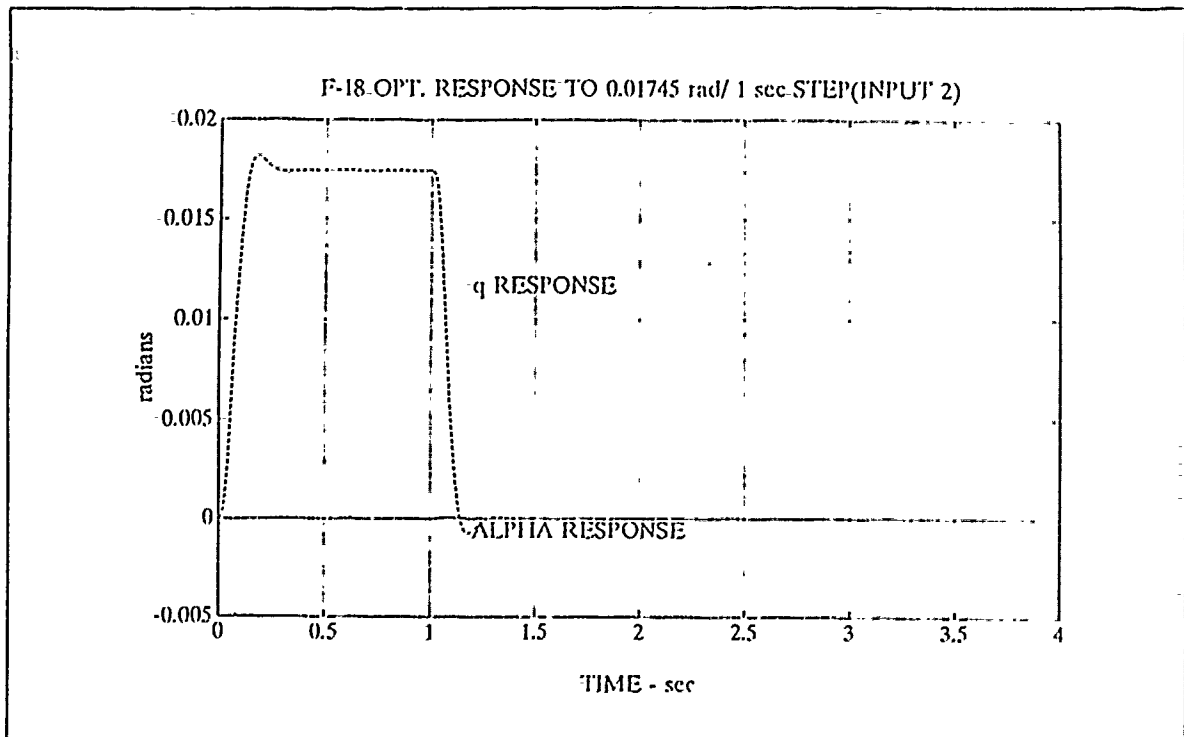


Figure 4-24  $\alpha$  and  $q$  Responses to  $1^\circ/\text{sec}$  1-sec Pulse in  $u_2$ ,  $H_\infty$

The deflections of the stabilator, leading flap and trailing flap due to a  $1^\circ$  1-second pulse at input 1 are plotted as a function of time in figures 4-25, 4-26, and 4-27, respectively. Since a negative deflection is required to produce a positive  $\alpha$  response and the only control surface with a negative deflection during the 1-second pulse in input 1 is the stabilator then it is concluded that it is the stabilator that controls  $\alpha$ . This result would be expected from the open loop state space representation which is in the feedforward loop of the closed loop system in which input 1 is fed through the stabilator.

The time response of the stabilator, leading flap, and trailing flap due to a  $1^\circ/\text{sec}$  1-second pulse in input 2 is shown in figures 4-28, 4-29, and 4-30. The negative rectangular pulses

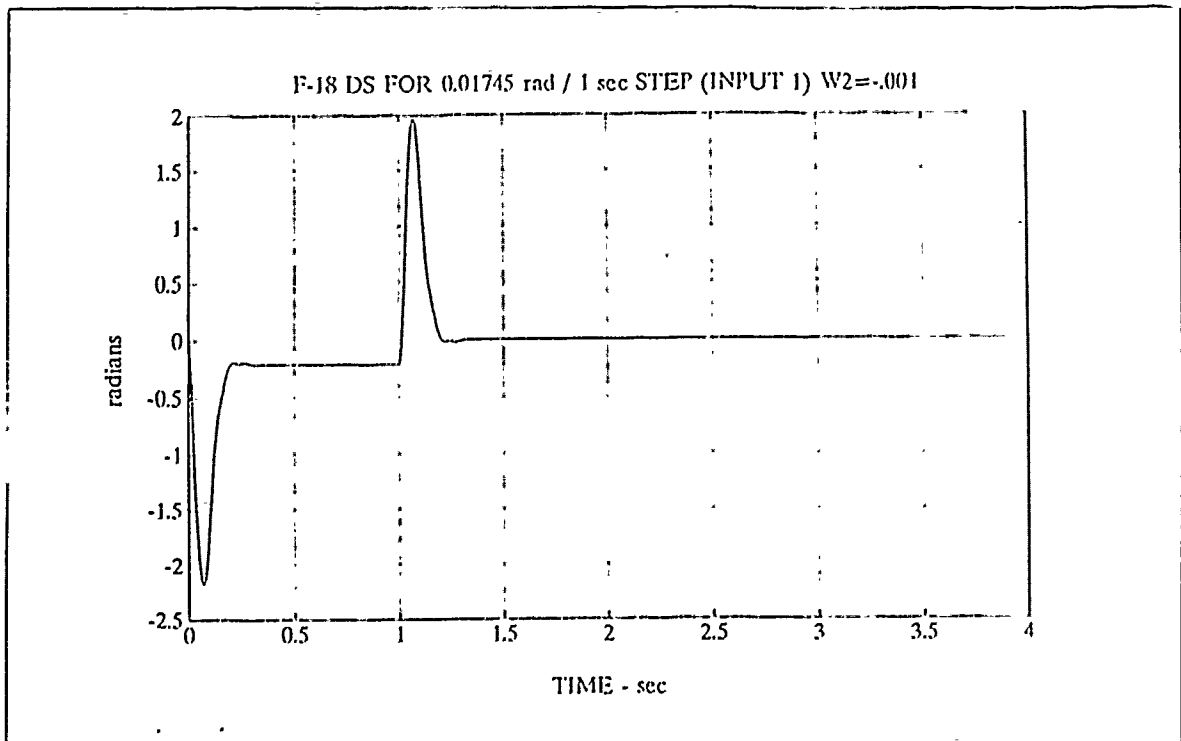


Figure 4-25 Stabilator Response to  $1^\circ/\text{sec}$  1-sec Pulse in  $u_1$

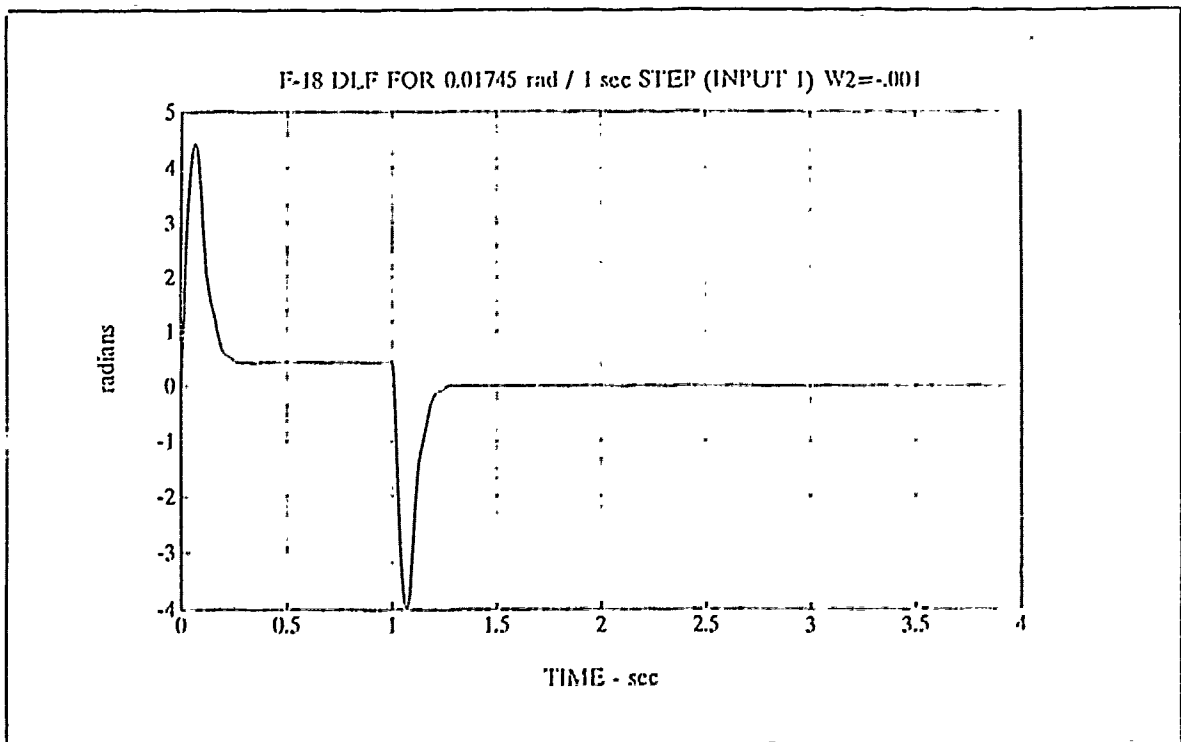


Figure 4-26 Leading Flap Response to  $1^\circ$  1-sec Pulse in  $u_1$

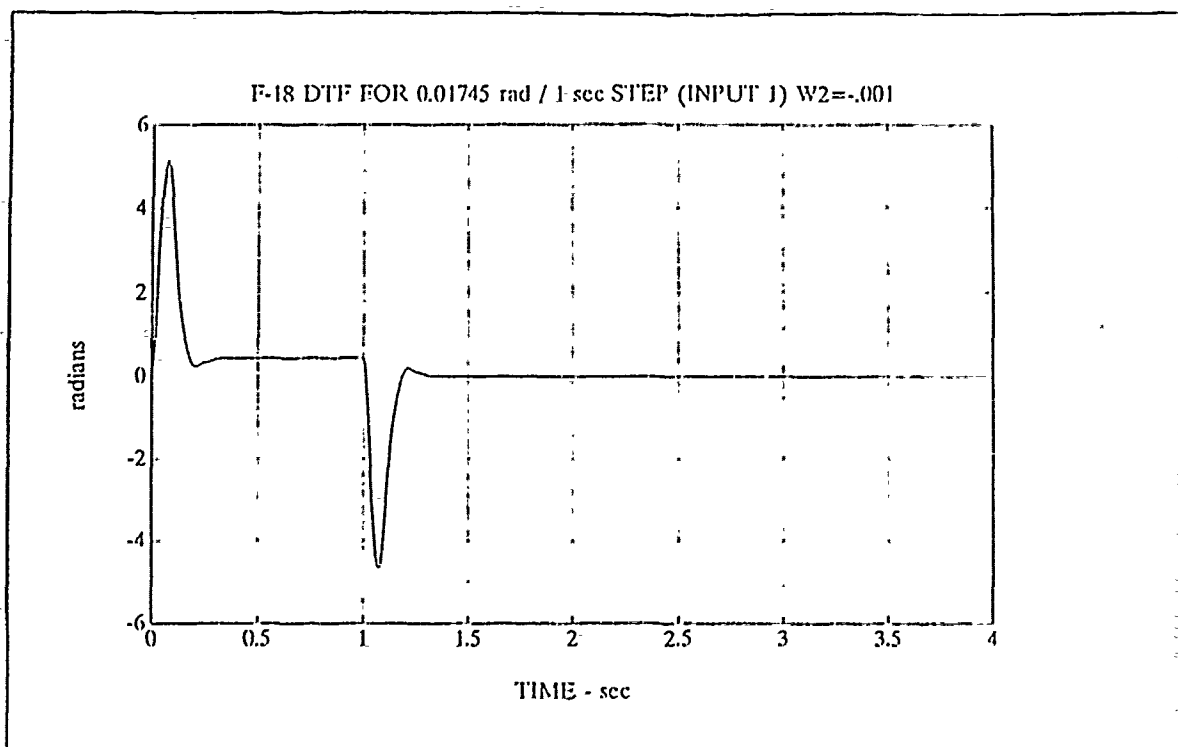


Figure 4-27 Trailing Flap Response to  $1^\circ$  1-sec Pulse in  $u_1$ ,  $H_\infty$

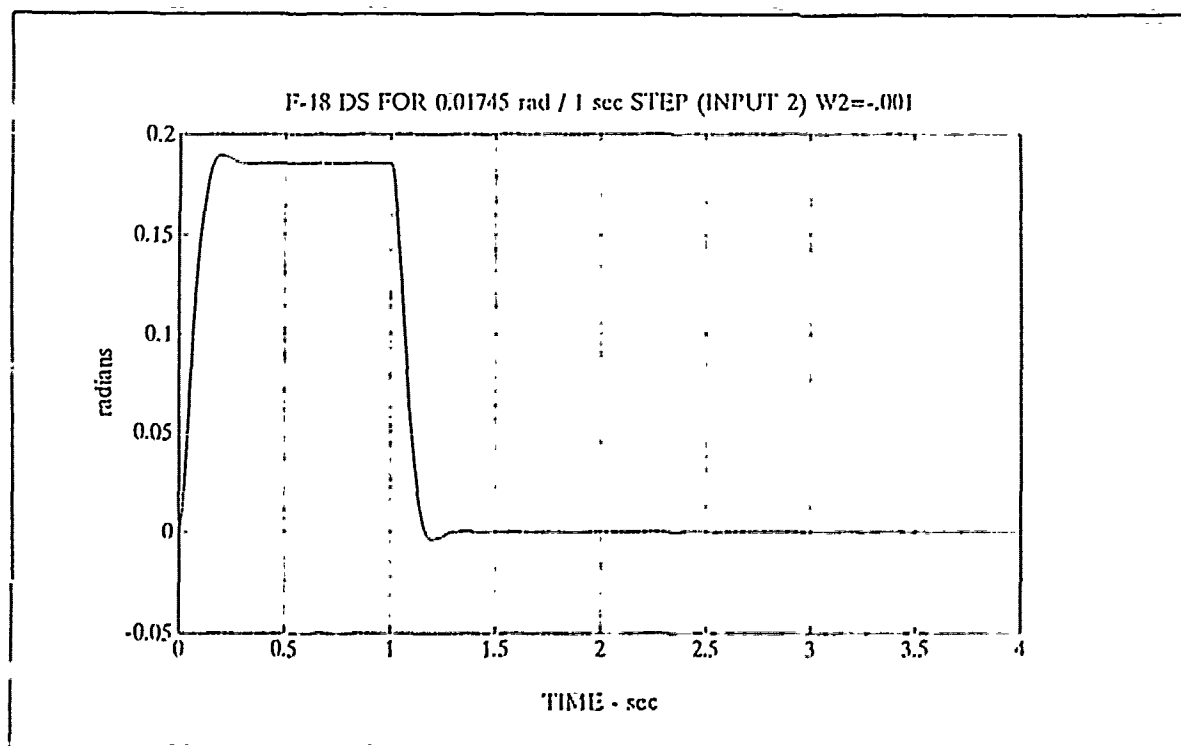


Figure 4-28 Stabilator Response to  $1^\circ/\text{sec}$  1-sec Pulse in  $u_2$ ,  $H_\infty$

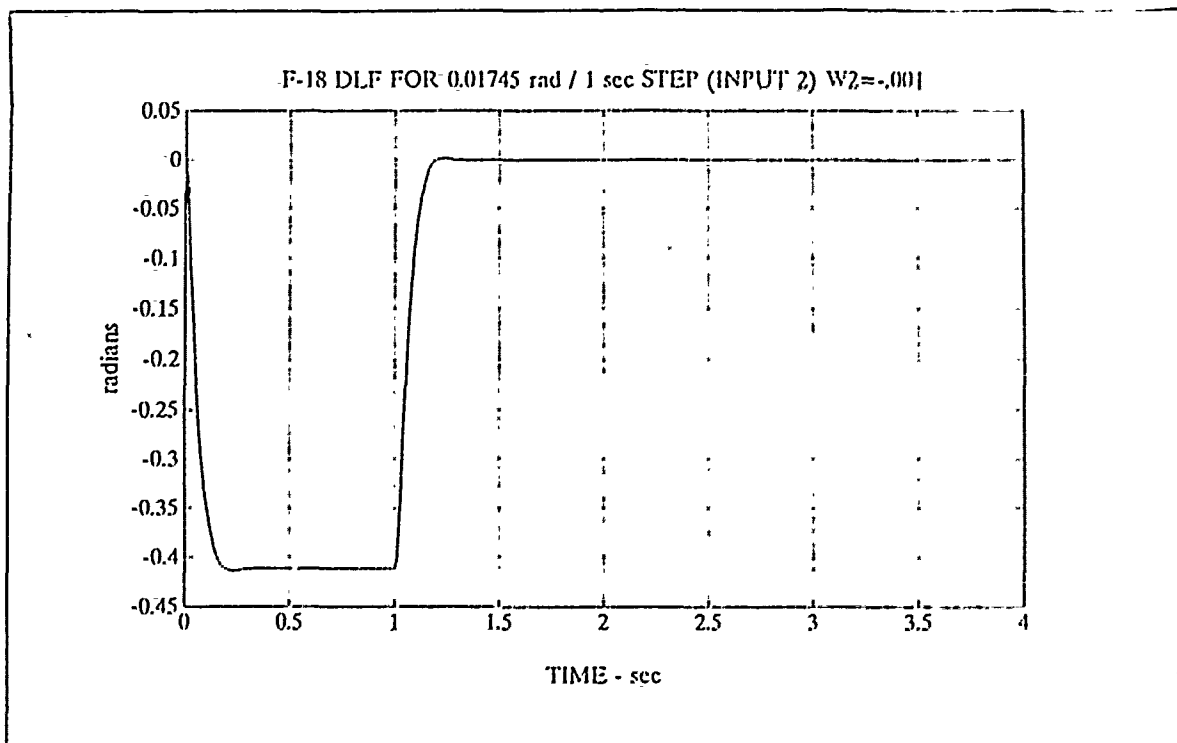


Figure 4-29 Leading Flap Response to  $1^\circ/\text{sec}$  1-sec Pulse in  $u_2$

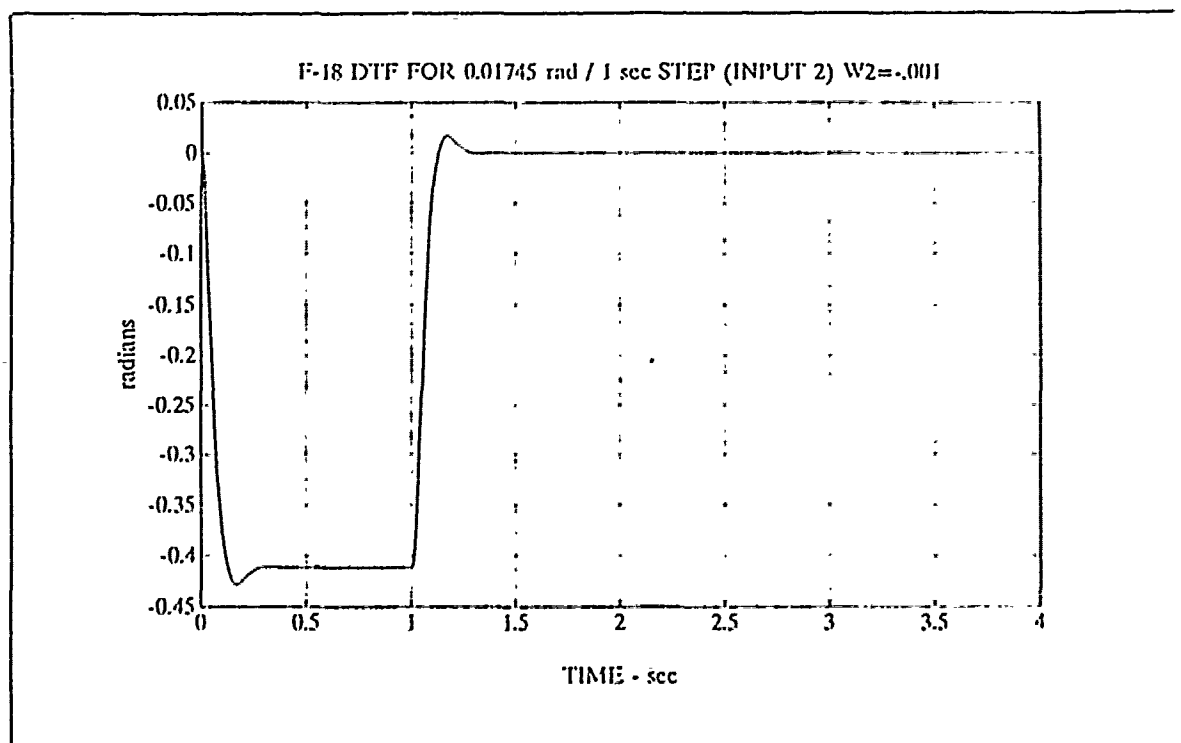


Figure 4-30 Trailing Flap Response to  $1^\circ/\text{sec}$  1-sec Pulse in  $u_2$

in  $\delta_{1f}$  and  $\delta_{tf}$  show that they are controlling the response to a positive pitch rate command  $u_2$  and  $\delta_s$  is not controlling  $q$ .

The maximum actuator deflection limits and the actuator no load rate limits are given in Table 4-4:

---

Table 4-4 F-18 Actuator Deflection and Rate Limits

Actuator	Deflection Limits	No Load Rate Limits
Stabilator	+10.5° -24	40°/sec
Leading Flap	+34 - 3	15
Trailing Flap	+45 - 8	18

---

The maximum deflections observed occurred for input 1 with 2.2 rad for  $\delta_s$ , 4.4 rad for  $\delta_{1f}$ , and 5 rad for  $\delta_{tf}$ . The maximum deflections for input 2 were smaller with 1.38 rad for  $\delta_s$ , 2.8 rad for  $\delta_{1f}$  and 3.1 rad for  $\delta_{tf}$ . The actuator limits in table 4-4 were greatly exceeded for both actuator angular limits and rate limits. The  $H_\infty$  solution developed here did not penalize the controls enough in the cost function and unrealistic actuator performance resulted. The  $H_\infty$  limited performance design is presented next with a higher  $W_2$  to insure that the cost function places a greater weight on the controls in order to get a more realistic  $H_\infty$  design.

#### D. DESIGN RESULTS OF THE LIMITED PERFORMANCE $H_\infty$ CONTROLLER

The  $H_\infty$  design was reworked to bring it within practical limits by increasing the  $W_2$   $\epsilon$  term to .018 and decreasing the corner frequency from 100 to 2.5 rad/sec in the  $W_1^{-1}(s)$  weighting function. The weighting function assignments are:

$$(\gamma W_1(s))^{-1} = \frac{.01(100s+)}{\gamma(.4s+1)} * I_{2 \times 2} \quad (4-3)$$

$$W_2(s) = -.018 * I_{2 \times 2} \quad (4-4)$$

$$W_3^{-1}(s) = \frac{1000}{s^2} * I_{2 \times 2} \quad (4-5)$$

A plot of  $W_1^{-1}(s)$  and  $W_3^{-1}(s)$  weighting functions are shown in figure 4-31.

The maximum  $\gamma$  achievable with the above  $W_2 = .018I$  was found to be 1.58 which only pushed the singular value of the cost function  $\|T_{y1u1}\|_\infty$  to within 2 db of the all-pass 0 db line in figure 4-32. The optimum  $H_\infty$  design with  $\gamma=1.58$  in figure 4-33 shows much less disturbance rejection and more sensitivity to plant and modeling errors than the optimum  $H_\infty$  design. The complementary sensitivity function for  $\gamma=1.58$  in figure 4-34 shows a greatly reduced bandwidth of 2 rad/sec as against 20 rad/sec in the  $H_\infty$  optimum design. The closed loop poles are listed in Table 4-5.



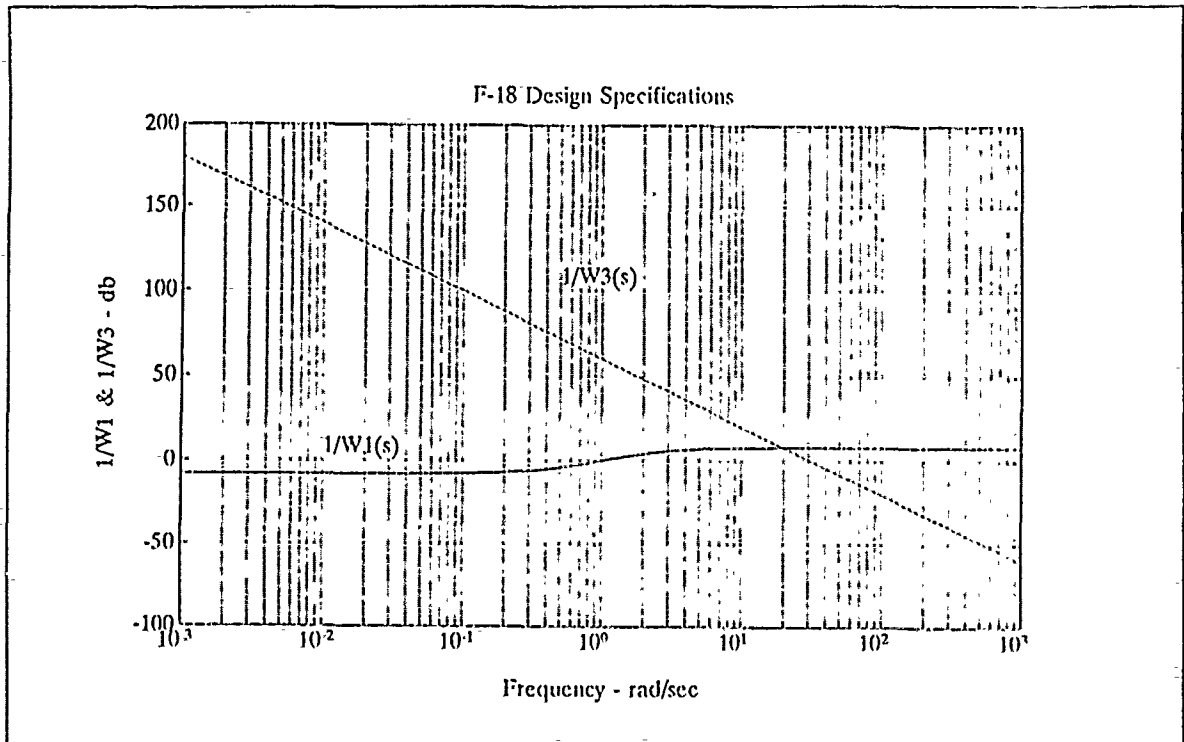


Figure 4-31 F-18 Limited Performance Design Specifications

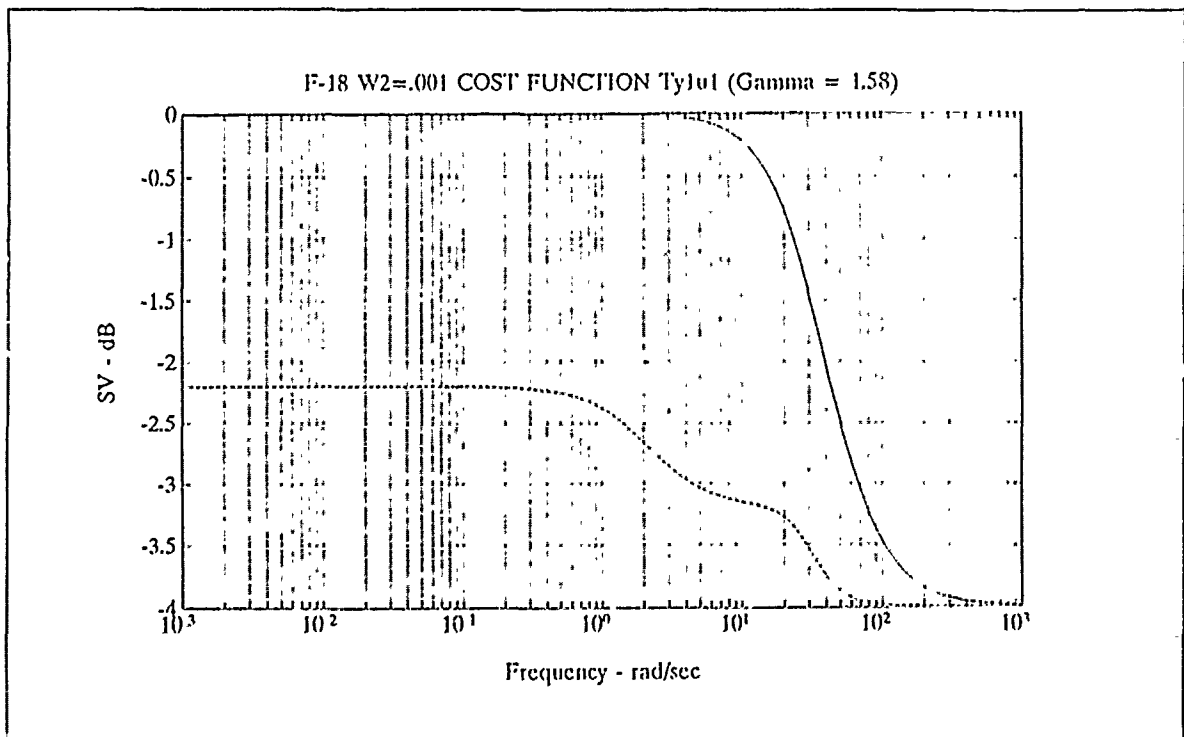


Figure 4-32 Limited Perf. Cost Function  $\|T_{y1u1}\|_\infty$  for  $\gamma=1.58$

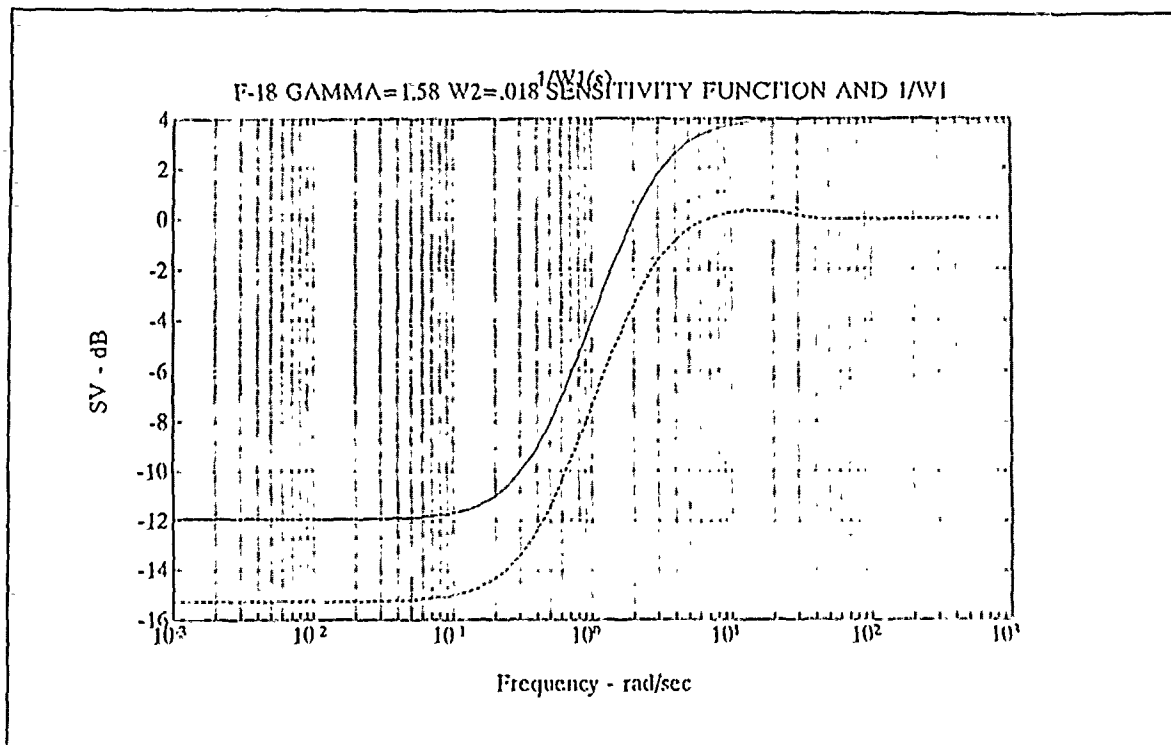


Figure 4-33 Limited Perf. Sensitivity Function with  $\gamma=1.58$

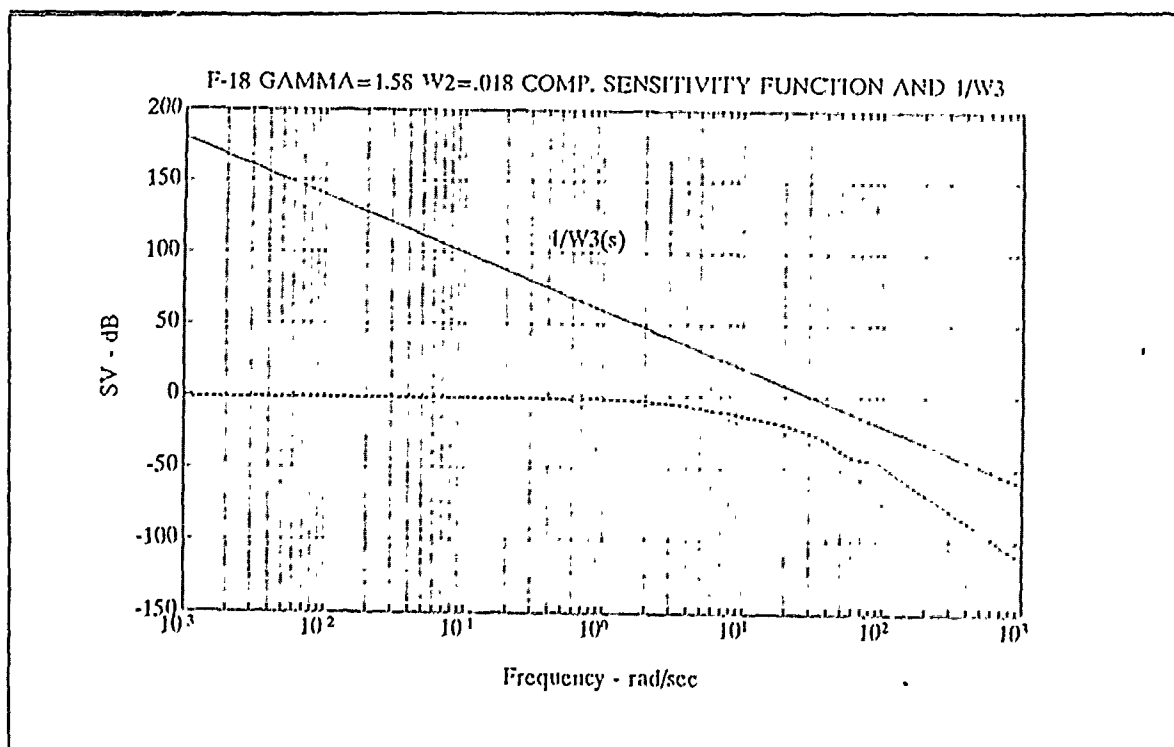


Figure 4-34 Limited Perf. Compl. Sensitivity Function,  $\gamma=1.58$

---

Table 4-5

F-18 Limited Performance Closed Loop Poles

-1.0017e+03  
-6.2126e+01 ± j8.5022e+01  
-1.7711e+01 ± j8.1027e+01  
-8.2898e+01  
-7.6597e+01  
-1.4924e+01 ± j3.3199e+01  
-2.4200e+01 ± j2.5758e+01  
-2.4850e+01 ± j2.4647e+01  
-2.0234e+01 ± j2.0813e+01  
-2.6902e+01  
-2.5668e+01 ± j7.8886e-01  
-9.7451e-01 ± j2.6269e+00  
-2.5001e+00  
-1.9977e+00  
-1.8000e-02  
-1.8000e-02

---

Investigation of the output return difference matrices show how much the performance has degraded. The singular value  $\sigma_{\min}[\mathbf{I}+\mathbf{G}(j\omega)\mathbf{F}(j\omega)]$  in figure 4-35 shows how much the performance has degraded. The singular value plot of  $[\mathbf{I}+(\mathbf{G}(j\omega)\mathbf{F}(j\omega))^{-1}]$  in figure 4-36 shows a steady state gain of 2 db or -7 to +3 db and a  $\pm 78^\circ$  gain and phase margin, respectively. A typical modern fighter aircraft has a gain margin of -8 to +4 db and a phase margin of  $\pm 35^\circ$ .

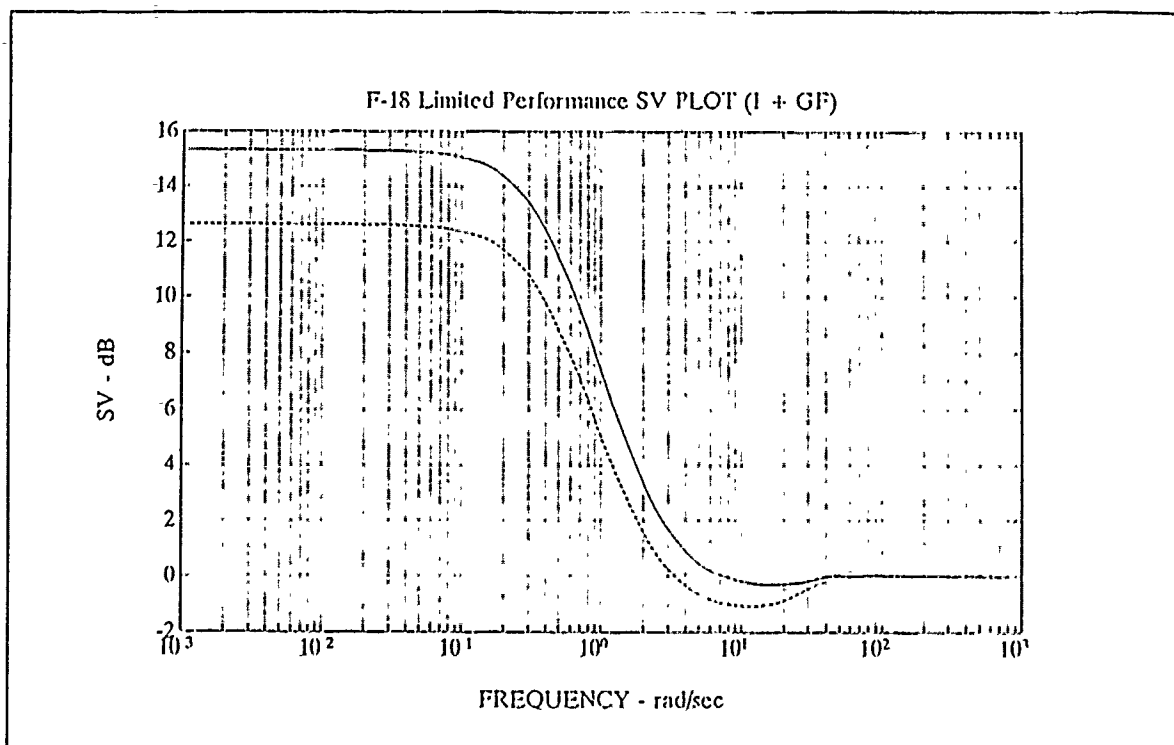


Figure 4-35 Limited Perf. SV Plot of  $(I+GF)$ ,  $\gamma=1.58$

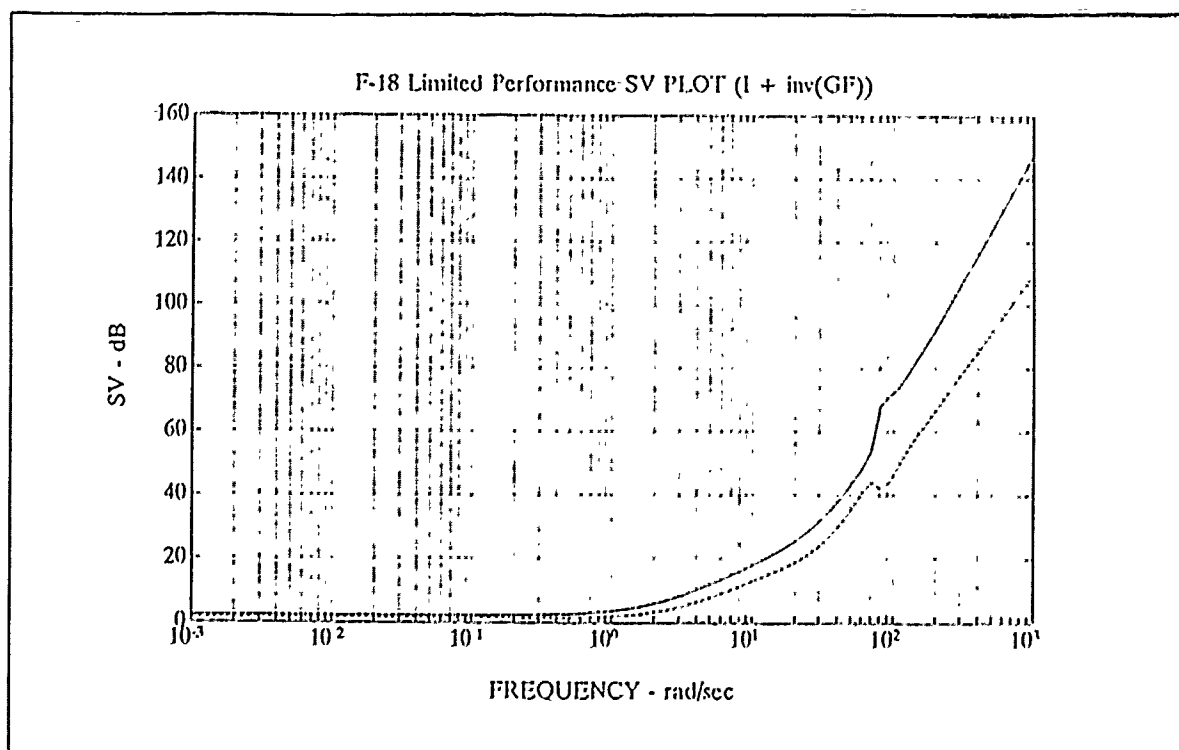


Figure 4-36 Limited Perf. SV plot of  $[I+(GF)^{-1}]$ ,  $\gamma=1.58$

### 1. Limited Performance $H_\infty$ Plant input Problem

The singular value plot of the input additive return difference matrix in figure 4-37 shows that the stability of the limited performance F-18 at the plant inputs is further degraded over that of the optimum  $H_\infty$  design. The plot of the input multiplicative return difference matrix  $I+(FG)^{-1}$  in figure 4-38 shows that  $\sigma_{\min}$  violates the  $W_3$  boundary as did the optimum  $H_\infty$  design. Stability robustness is not guaranteed at the plant inputs as in the optimum  $H_\infty$  design.

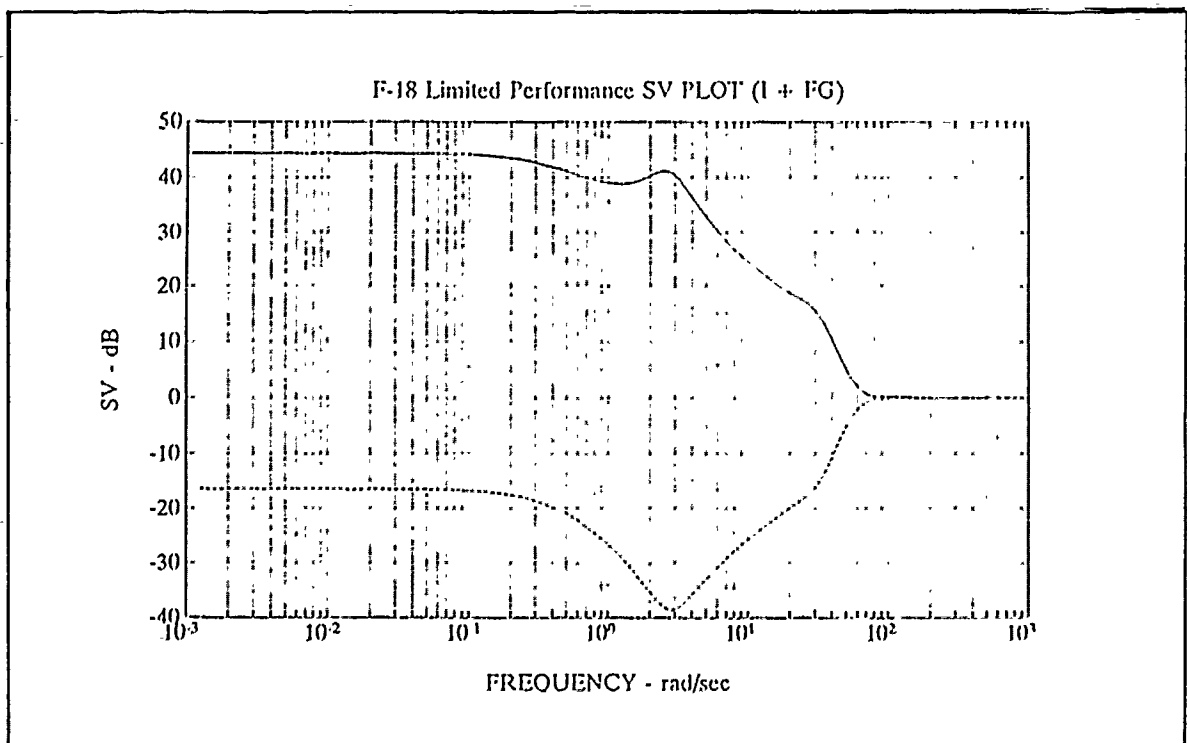


Figure 4-37 F-18 Limited Performance SV Plot of  $I+FG$ ,  $\gamma=1.58$

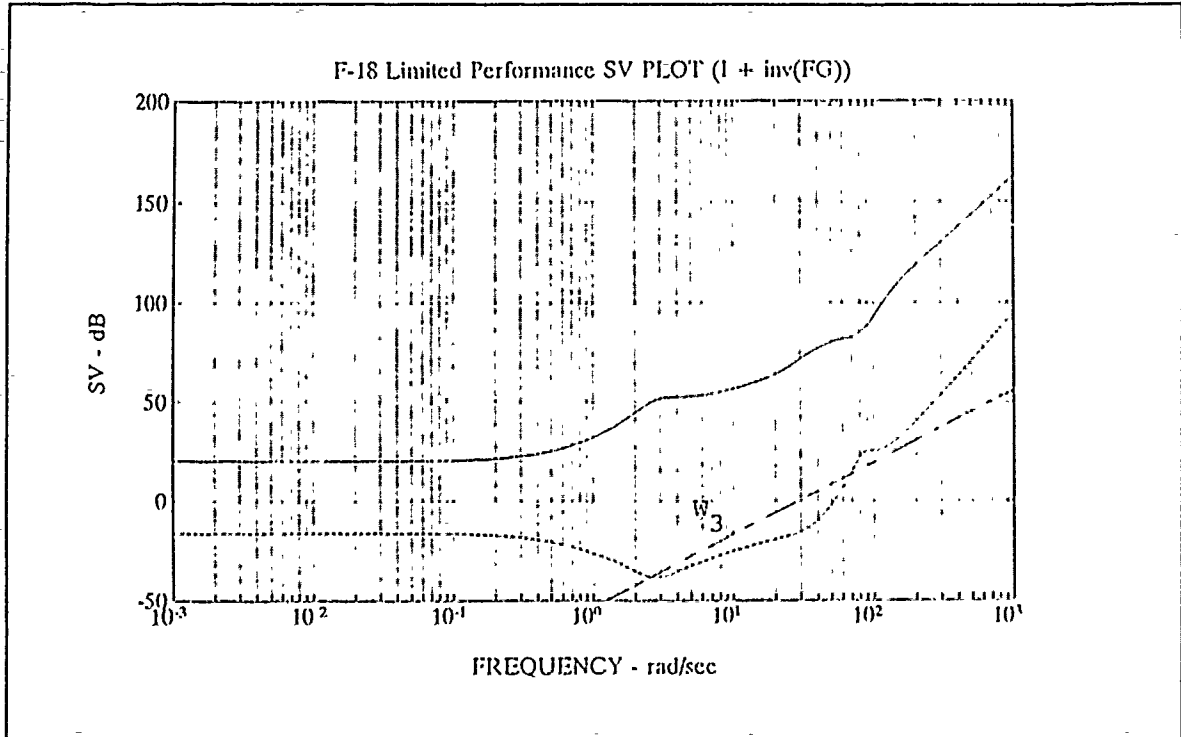


Figure 4-38 F-18 Limited Perf. SV Plot of  $I + (FG)^{-1}$ ,  $\gamma = 1.58$

## 2. Limited Performance Precision Longitudinal Modes

Examination of the closed loop bode plots of the four transfer functions  $\alpha/u_1$ ,  $q/u_1$ ,  $q/u_2$ , and  $\alpha/u_2$  in figures 4-39 through 4-42 shows that the cross coupling between  $u_1$  and  $q$ , and between  $u_2$  and  $\alpha$  is now not negligible with the limited performance design. The optimum  $H_\infty$  had for all practical purposes no cross coupling. Figure 4-39 shows a steady state gain of -2 db for the  $\alpha$ /input 1 transfer function which translates to an absolute gain of .794 instead of the 0 db gain noted for the optimum  $H_\infty$  gain. The  $q$ /input 2 transfer function in figure 4-40 had a peak of -22 db instead of the -32 db of the optimum design showing an increased cross coupling. The results with input 2 are similar with the  $q/u_2$

transfer function having a steady state gain slightly greater than -2 db in figure 4-41. Figure 4-42 shows the peak of the  $\alpha/u_2$  bode plot to be -20 db at 2 rad/sec so not only is the peak higher than for the optimum  $H_\infty$  case. Actually the cross coupling is a little stronger because the frequency at which both cross transfer functions peak is close to the short period frequency of 2.8 rad/sec. The vertical scales in figures 4-40 and 4-42 are suppressed.

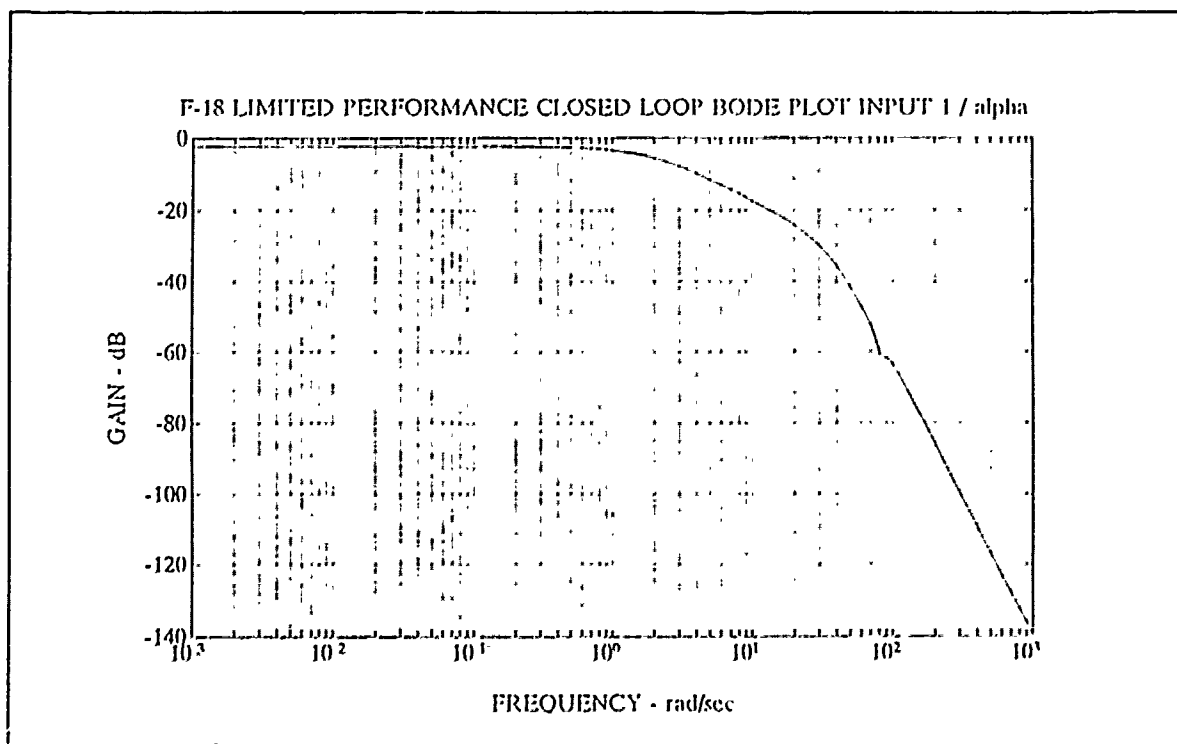


Figure 4-39 F-18 Limited Perf. Closed Loop Bode of  $\alpha/u_1$

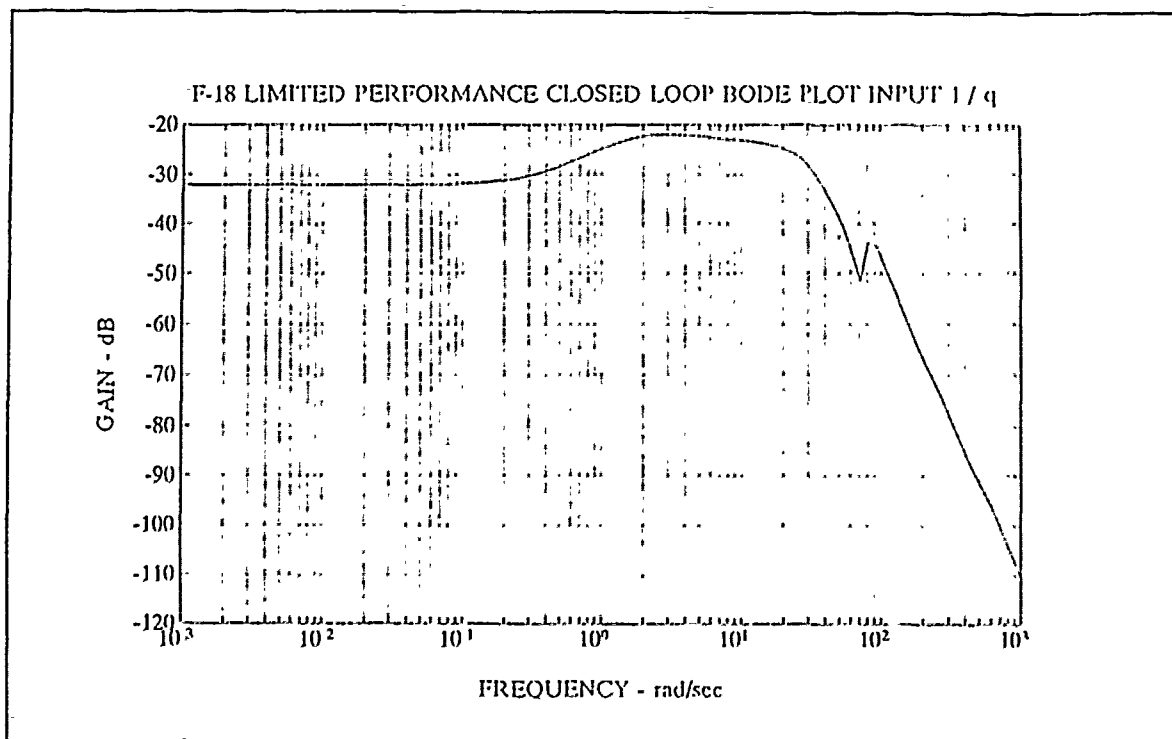


Figure 4-40 F-18 Lim. Perf. Closed Loop Bode Plot of  $q/u_1$

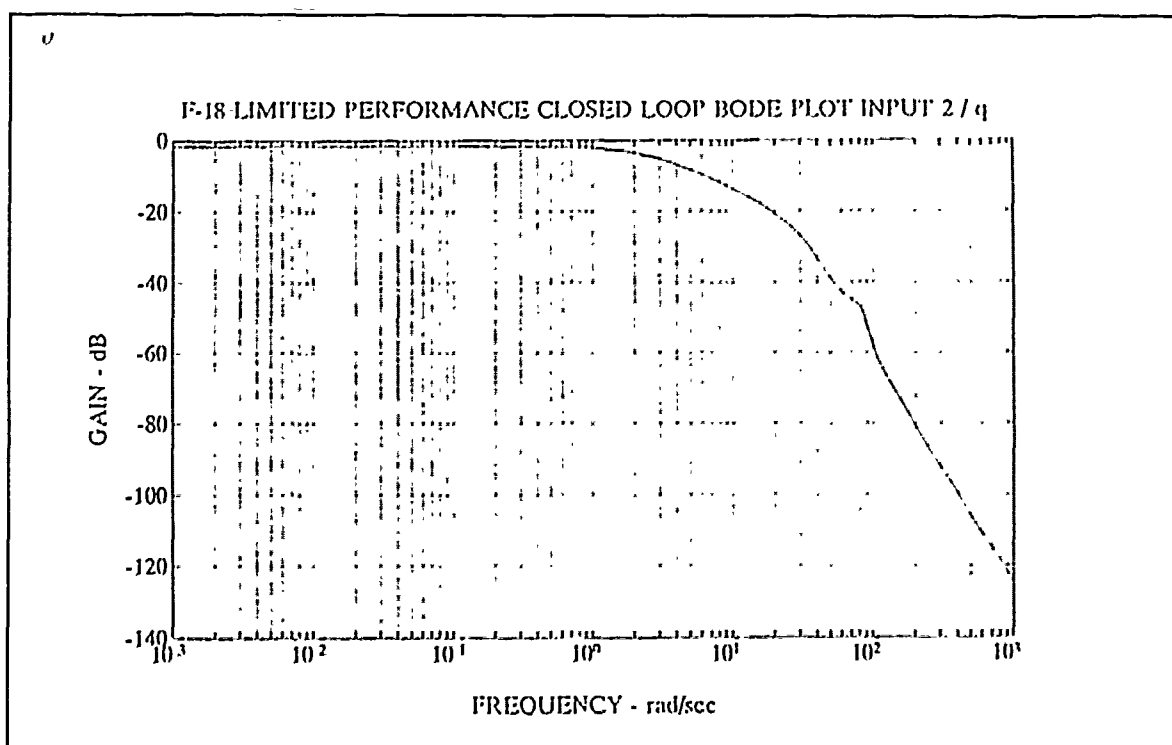


Figure 4-41 F-18 Lim. Perf. Closed Loop Bode Plot of  $q/u_2$



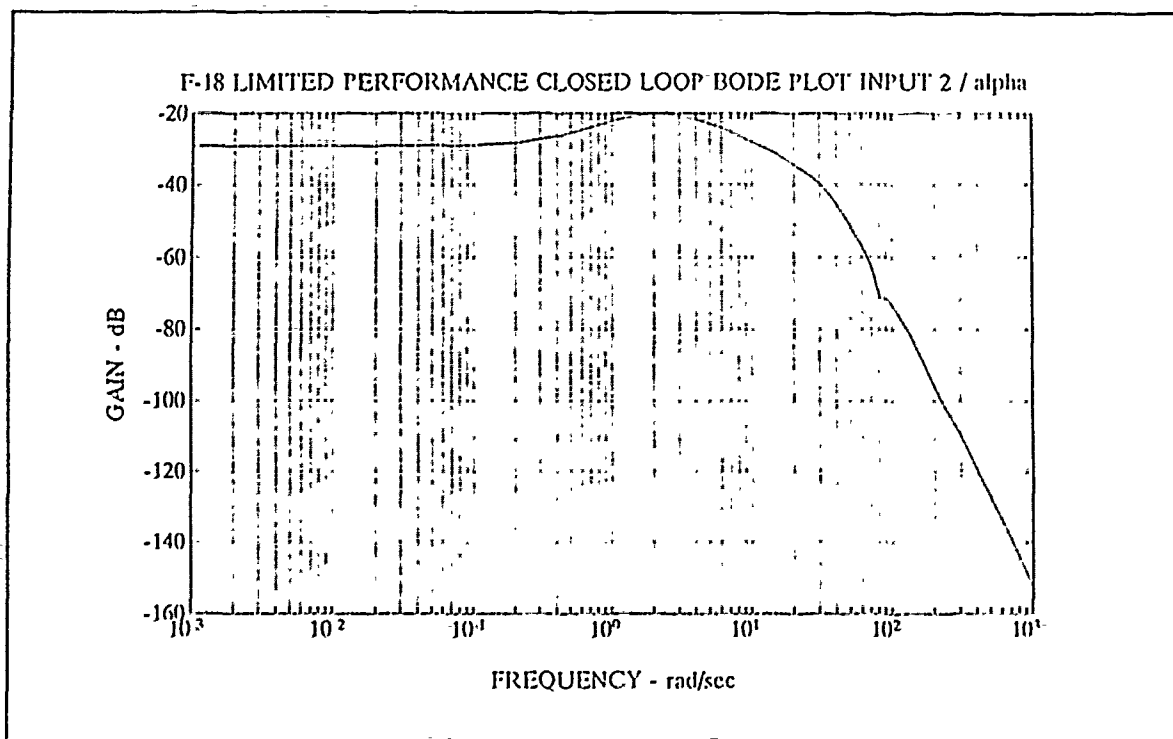


Figure 4-42 F-18 Lim. Perf. Closed Loop Bode Plot of  $\alpha/u_2$

A  $1^\circ$  pulse of 1-sec duration was applied at input 1 and then at input 2 with the limited performance  $H_\infty$  design as was done with the optimum  $H_\infty$  design. A plot of the  $\alpha$  and  $q$  time responses in figure 4-43 still show that input 1 still dominates in the control of angle of attack but the pitch rate response is not negligible. Similarly input 2 still dominates the pitch rate response but the angle of attack response is noticeable as seen in figure 4-44. The rise times are much longer as expected since the controls are being limited by a larger weighting value for  $\bar{W}_2$ . After 1 sec the angle of attack reaches .0113 radians of the .01745 radians commanded by input 1. The .01745 rad/sec commanded by input 2 caused the pitch rate to reach .0134 rad/sec after 1 sec. The rise time of the optimum performance  $H_\infty$  design again took .2 sec in both cases.

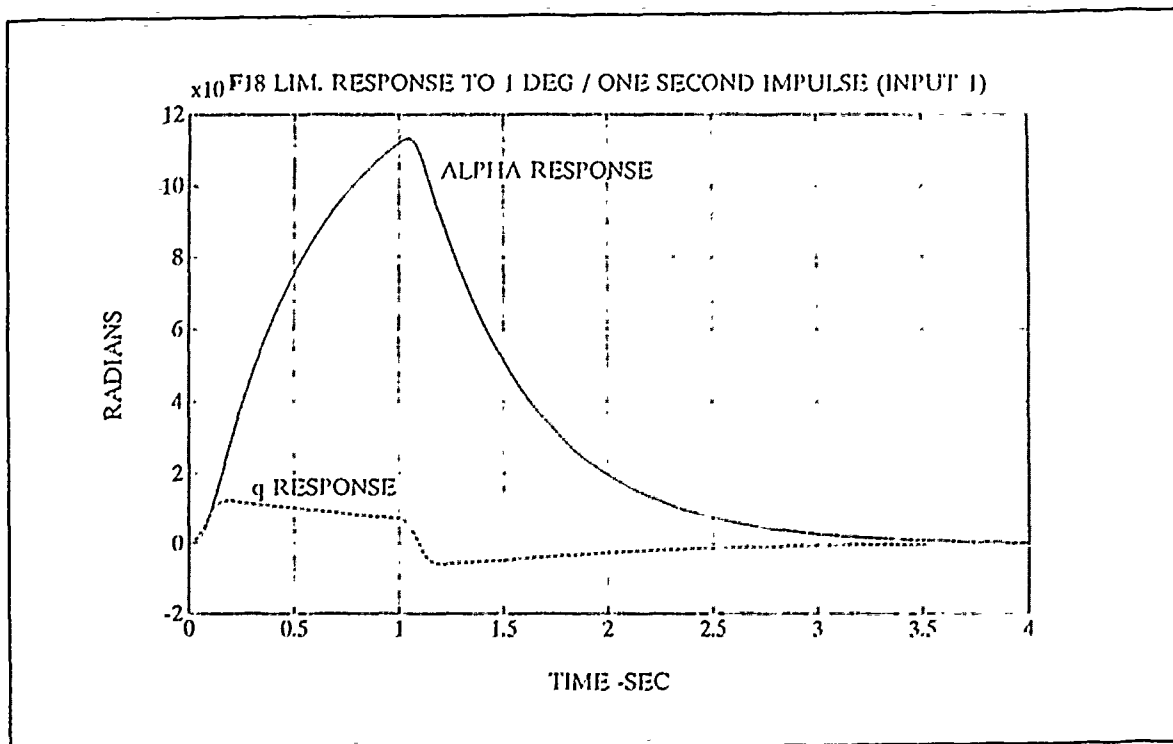


Figure 4-43 Lim. Perf.  $\alpha$  and  $q$  Resp. to  $1^\circ/\text{s}$  1-s Pulse at  $u_1$

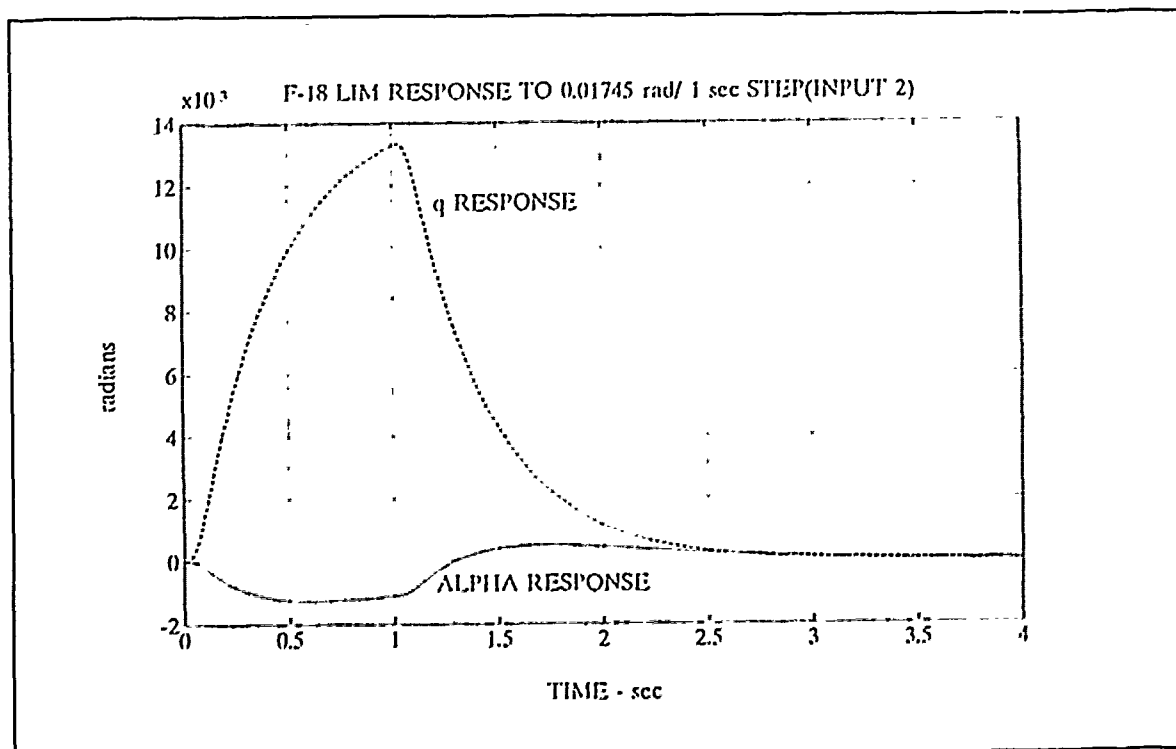


Figure 4-44 Lim. Perf.  $H_\infty$   $\alpha$  &  $q$  Resp. to  $1^\circ/\text{s}$  1-sec Pulse at  $u_2$

The control deflections  $\delta_s$ ,  $\delta_{lf}$ , and  $\delta_{tf}$  for the limited performance F-18 are much smaller than for the optimum performance F-18  $H_\infty$  design as seen in figures 4-45 through 4-47 for input 1 and figures 4-48 through 4-50 for input 2. The control deflections for input 1 were all within the acceptable limits for the F-18. The leading flap and trailing flap both exceeded the maximum negative deflections allowed for the F-18 of  $-.052$  rad for the leading flap and  $-.14$  rad for the trailing flap for input 2. The stabilator deflection was completely within its limits for either input. The main problem in utilization of the three control surfaces in the F-18 is that the leading and trailing flaps have most of their travel in the downward positive direction which from figure 4-1 can be seen to cause a negative pitching moment. The leading flap has a deflection range of  $-3$  to  $+34$  degrees and the trailing flap has a deflection range of  $-8$  to  $+45$  degrees. The X-29 had a good range of positive and negative travel on the canards and strakes making it a little more ideal for the  $H_\infty$  approach [Ref. 6]. NASA Dryden has been testing a more maneuverable F-18 modified to use canards which would make it a more ideal candidate for the  $H_\infty$  approach.

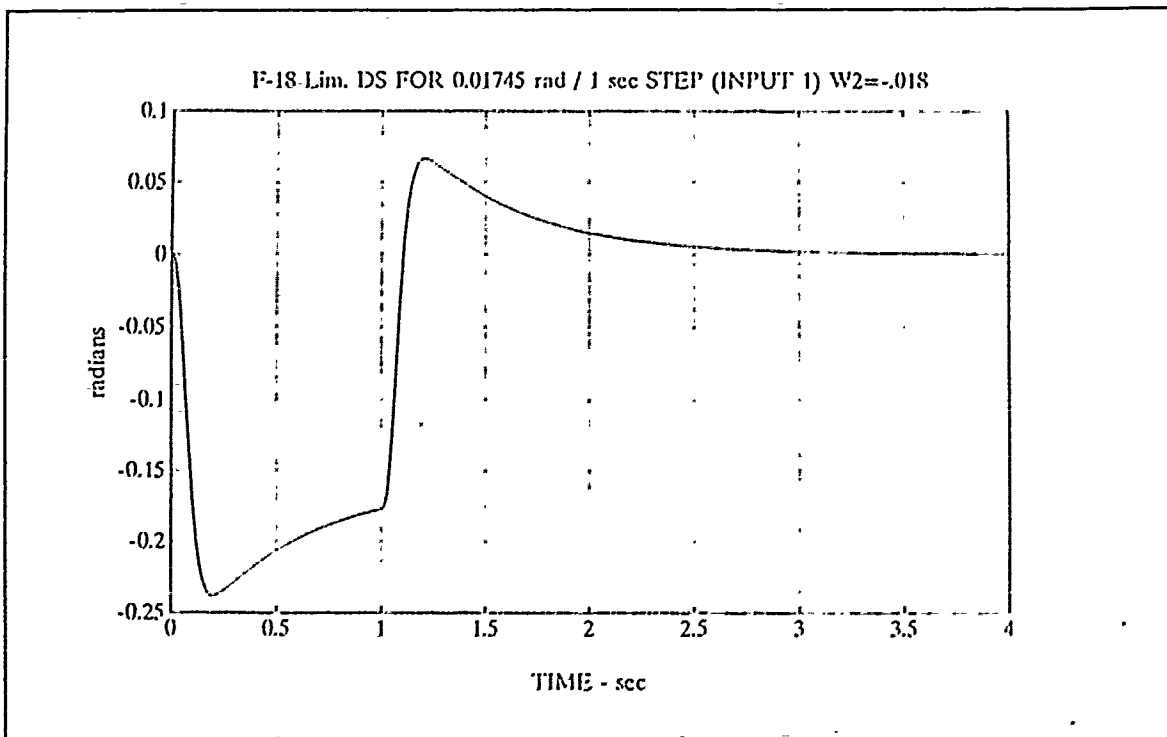


Figure 4-45 F-18 Lim. Perf. Stabilator  $\delta_s$  to  $1^\circ$  1-s Pulse at  $u_1$

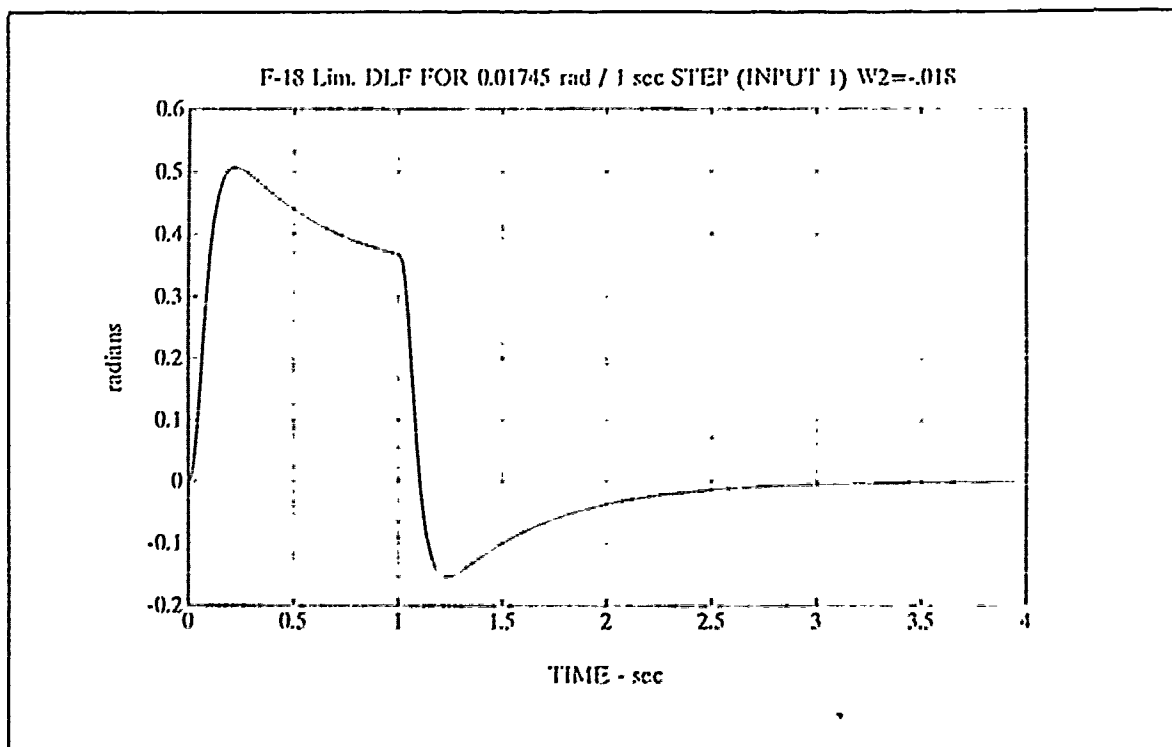


Figure 4-46 Lim. Perf. Leading Flap  $\delta_{lf}$  to  $1^\circ$  1-s Pulse in  $u_1$

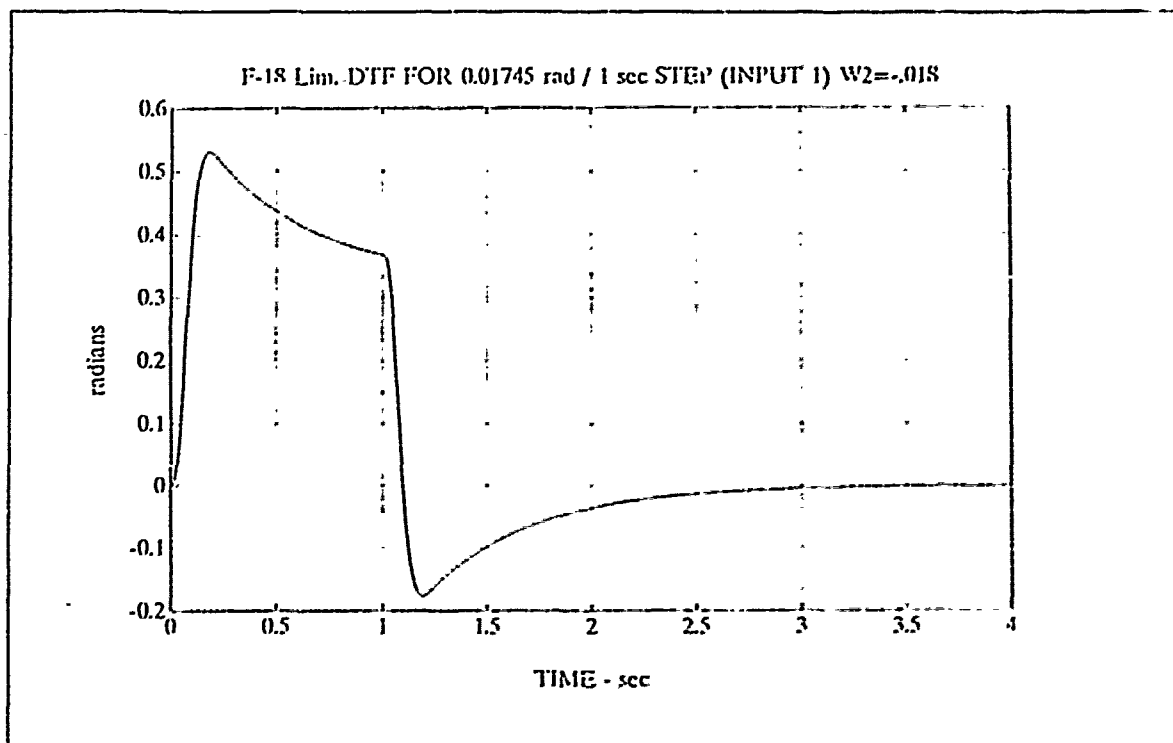


Figure 4-47 Lim. Perf. Trailing Flap  $\delta_{tf}$  to  $1^\circ$  1-s Pulse at  $u_1$

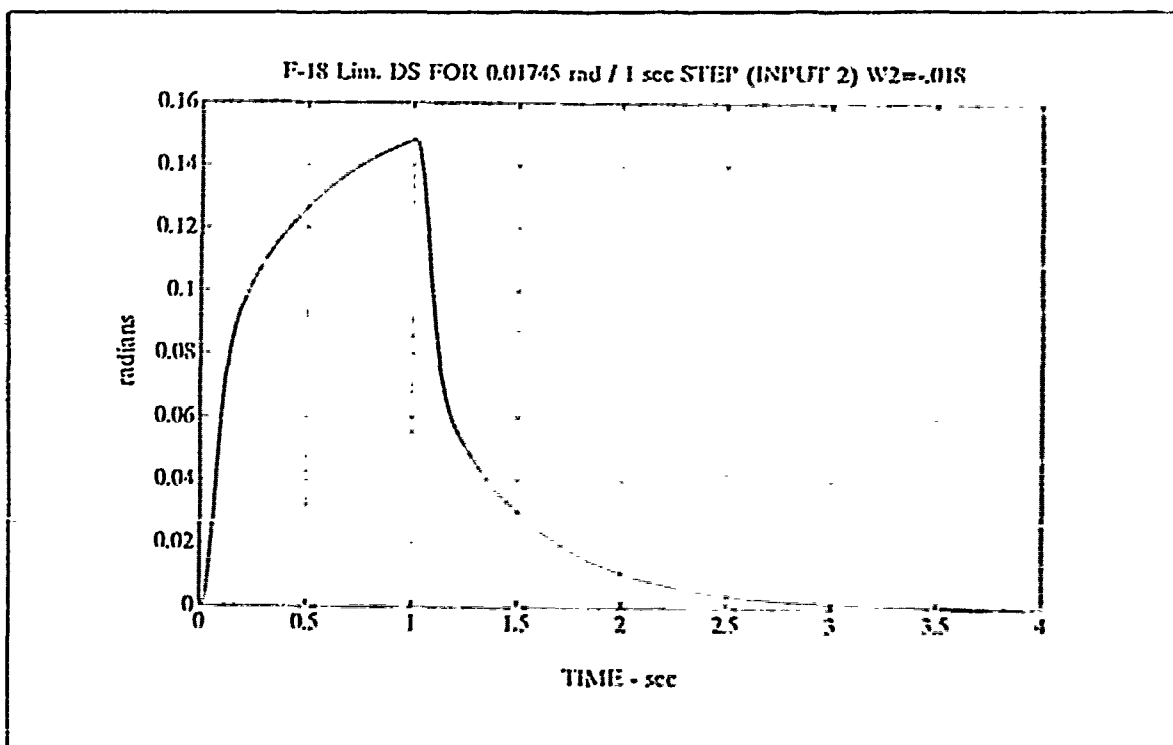


Figure 4-48 Lim. Perf. Stabilator  $\delta_s$  to  $1^\circ/s$  1s Pulse at  $u_2$

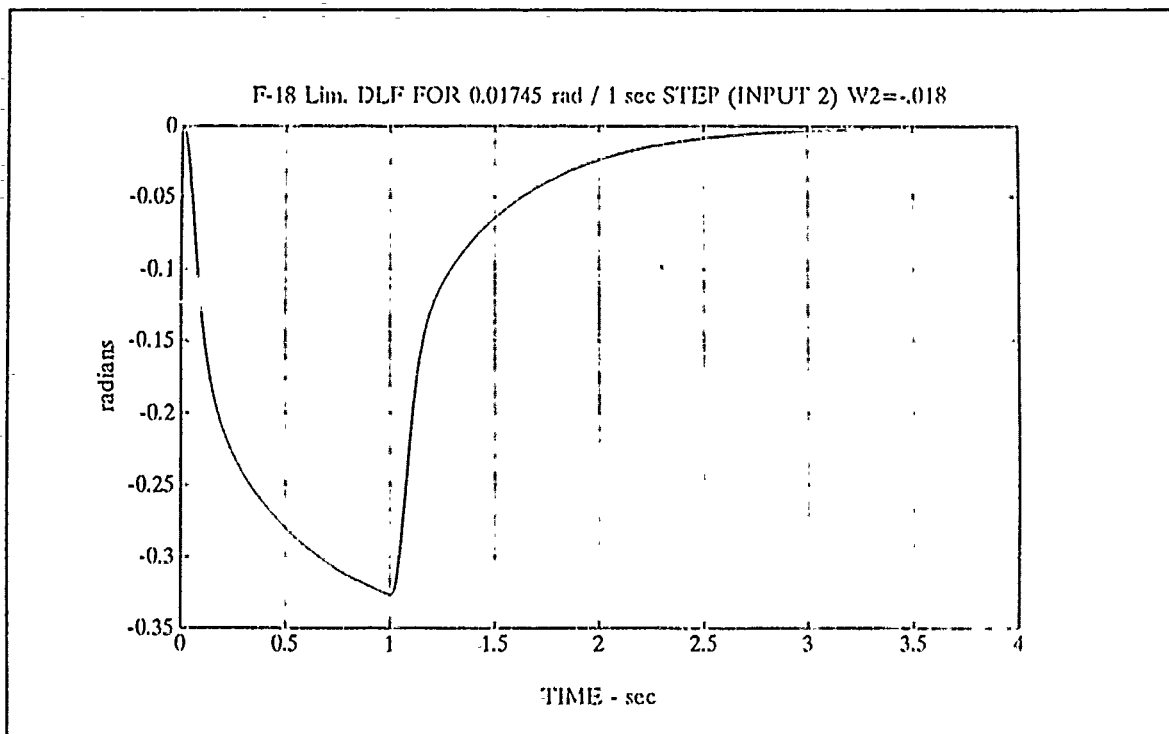


Figure 4-49 Lim. Perf. Leading Flap  $\delta_{lf}$  to  $1^\circ/s$  1s Pulse at  $u_2$

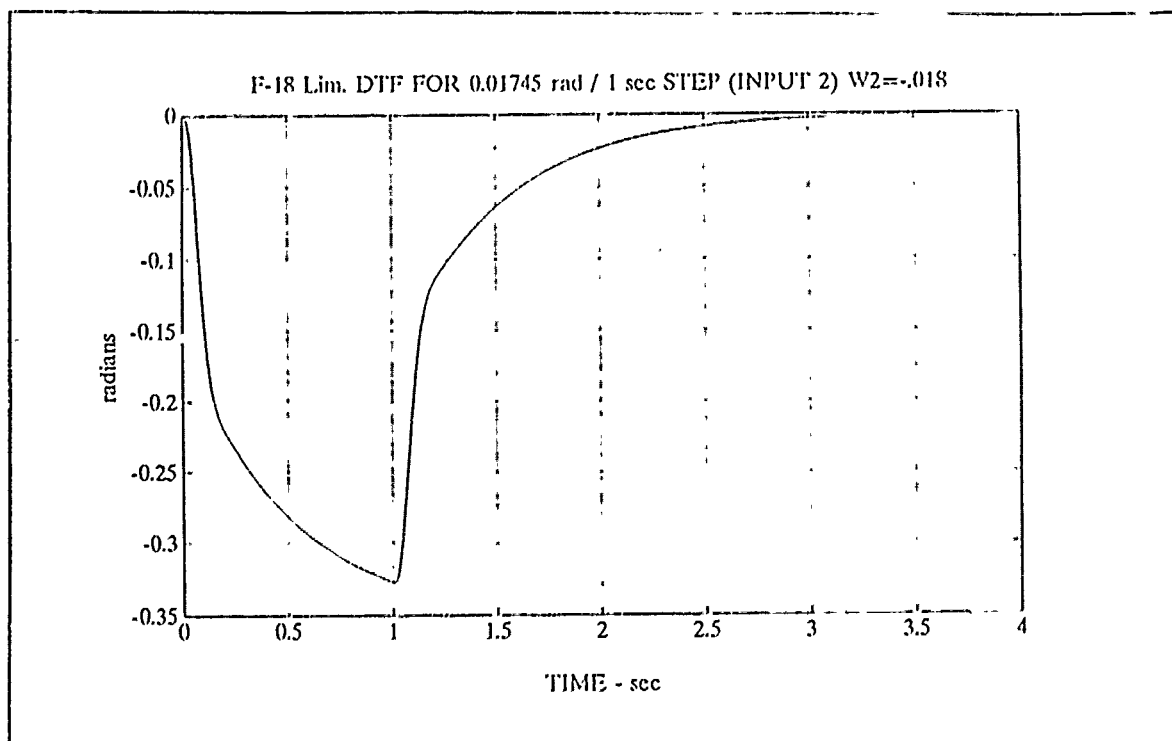


Figure 4-50 Lim. Perf. trailing Flap  $\delta_{tf}$  to  $1^\circ/s$  1s Pulse at  $u_2$

The actuator no load rate limits shown in table 4-4 were exceeded in both input 1 and input 2. The control rates of the actuators are shown in figures 4-51 through 4-53 for the pulse from input 1 and figures 4-54 through 4-56 for the pulse from input 2. The peak rates range from .8 to 6 rad/sec which exceed the capabilities of the actuators.

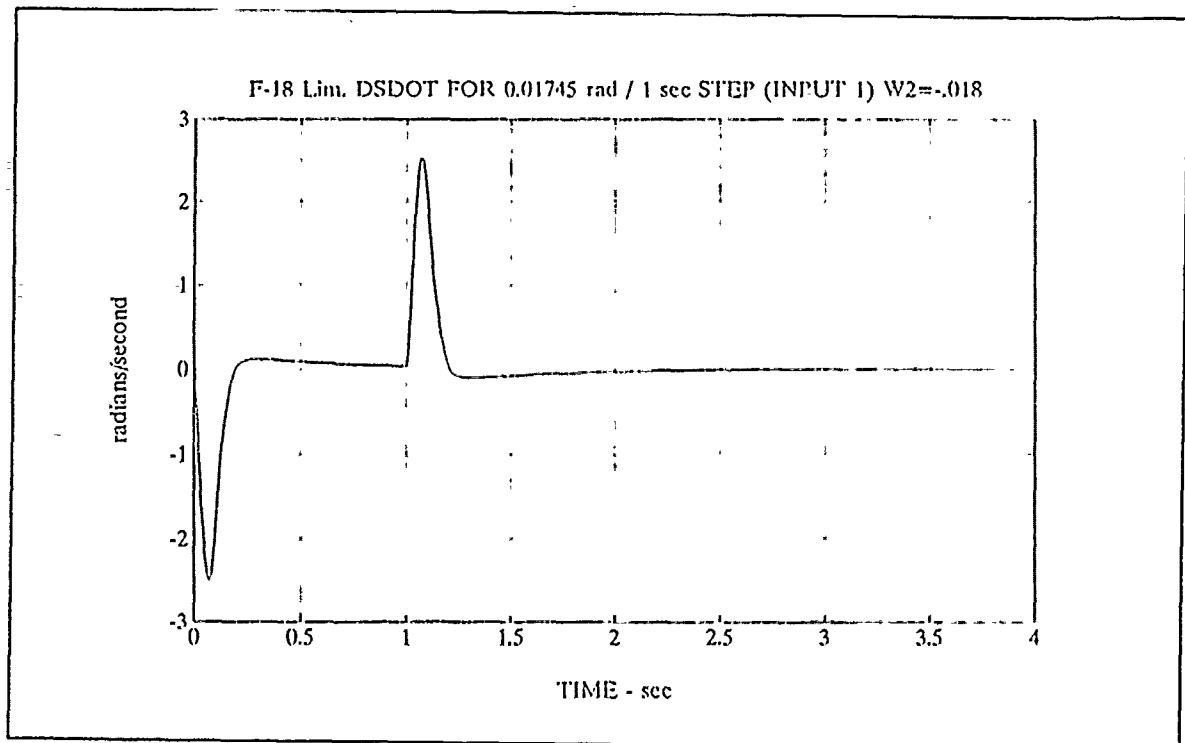


Figure 4-51 Lim. Perf.  $d\delta_s/dt$  due to  $1^\circ/s$  1s Pulse in  $u_1$

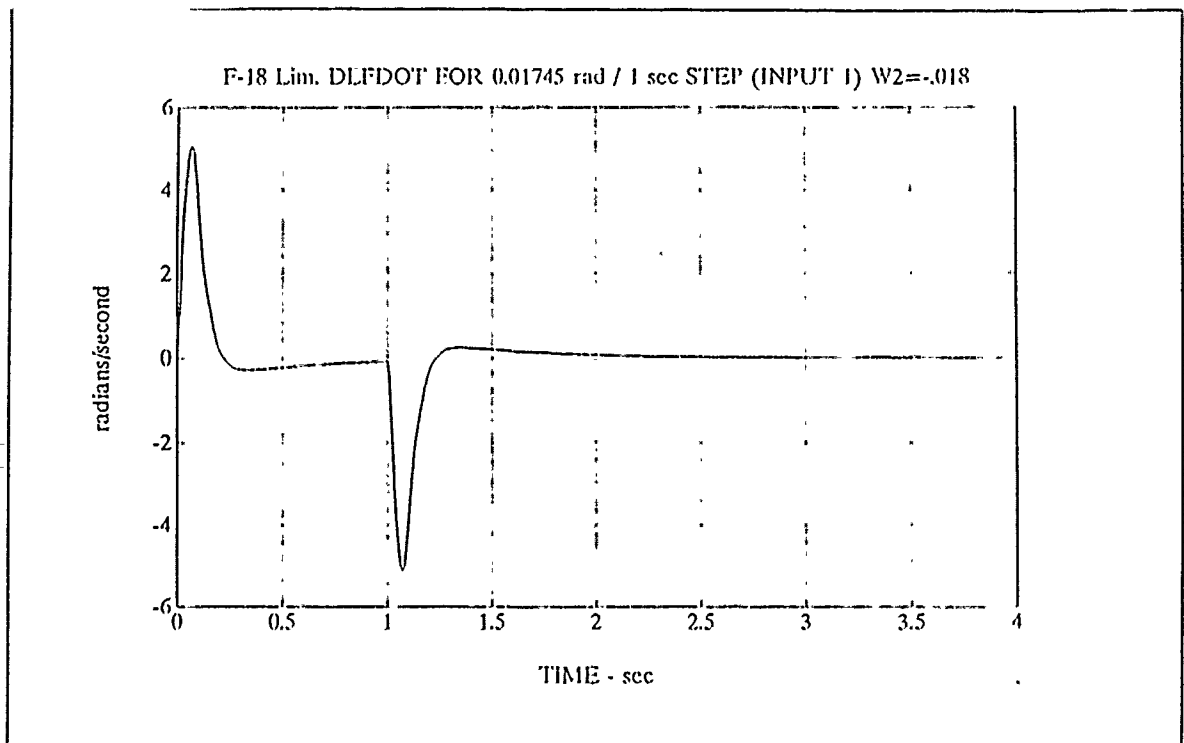


Figure 4-52 Lim. Perf.  $d\delta_{1f}/dt$  due to  $1^\circ$  1s Pulse in  $u_1$

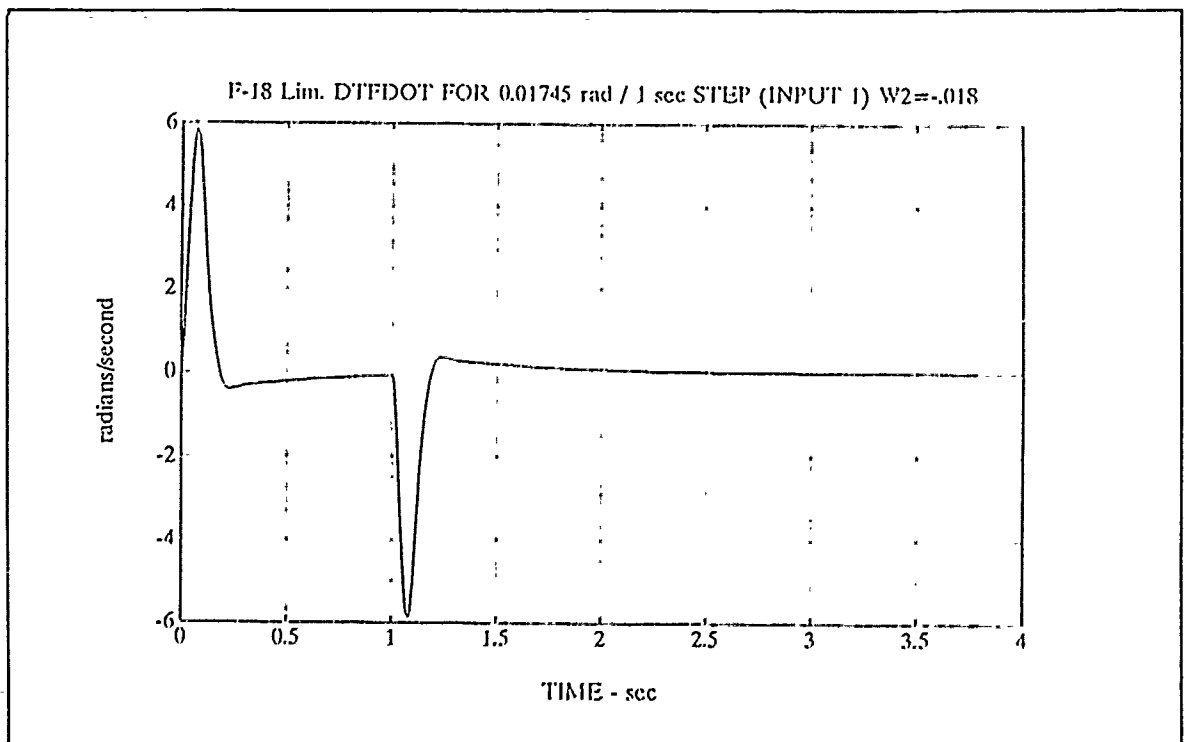


Figure 4-53 Lim. Perf.  $d\delta_{tf}/dt$  for  $1^\circ$  1s Pulse in  $u_1$



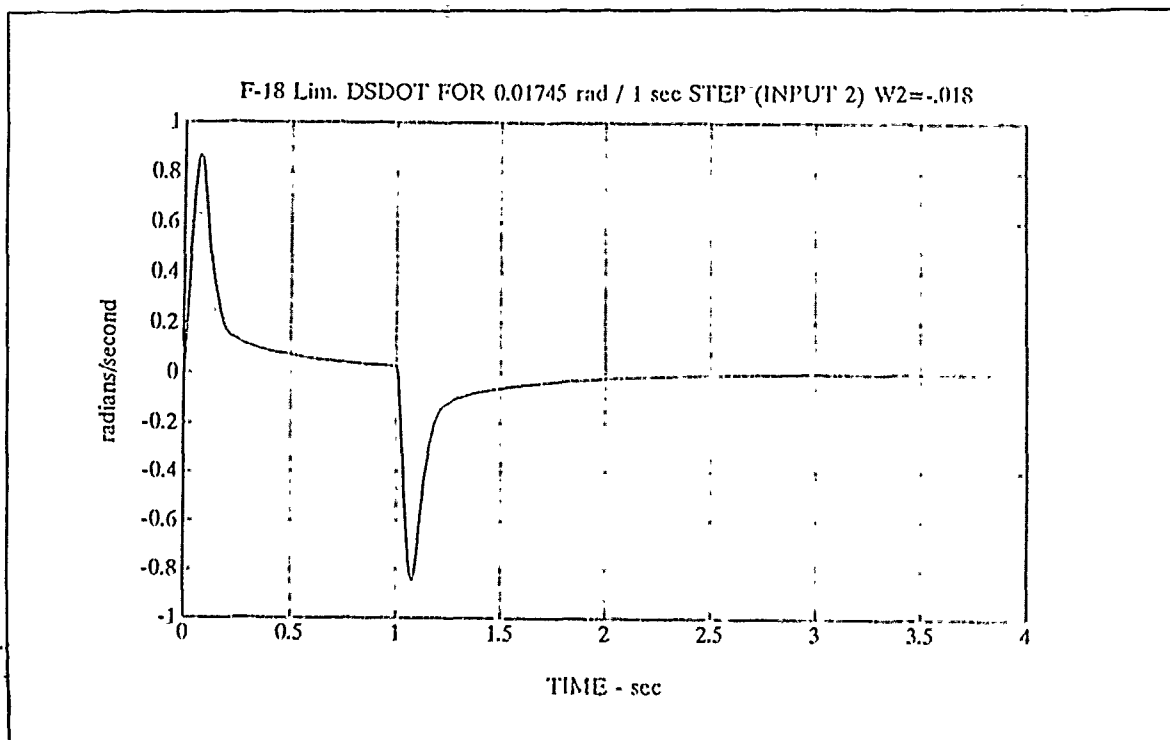


Figure 4-54 Lim. Perf.  $d\delta_B/dt$  for  $1^\circ/s$  1s Pulse at  $u_2$

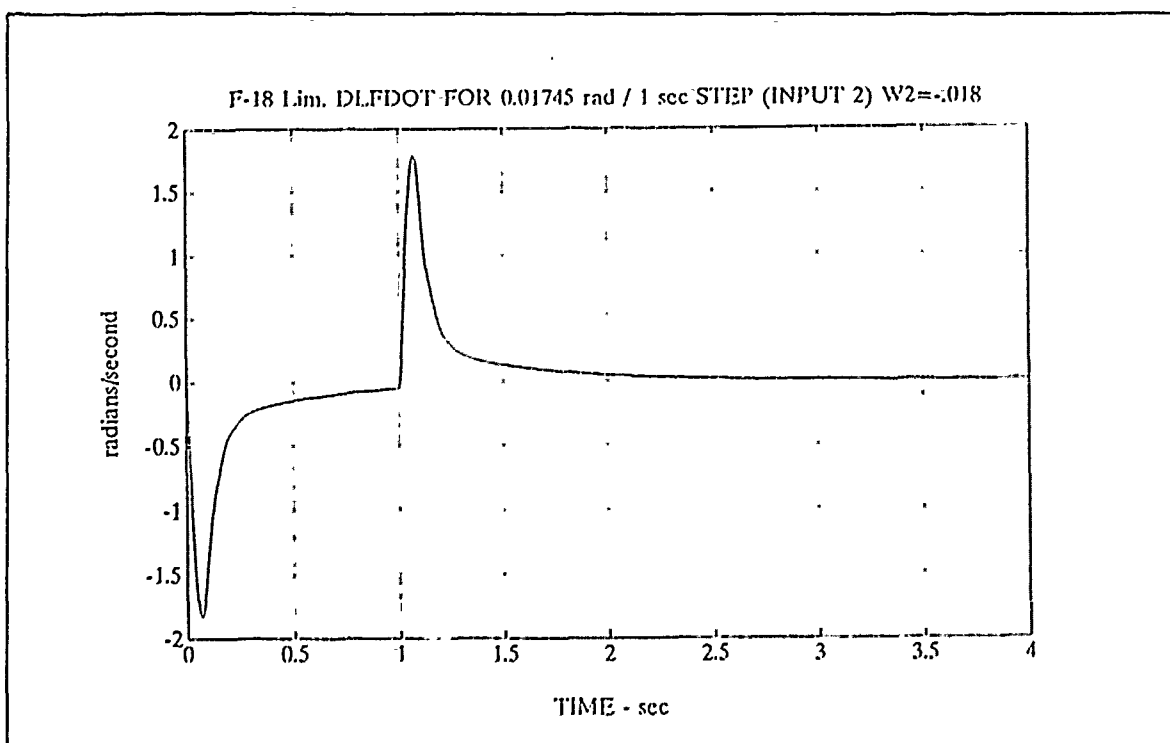


Figure 4-55 Lim. Perf.  $d\delta_{1f}/dt$  due to  $1^\circ/s$  1s Pulse in  $u_2$

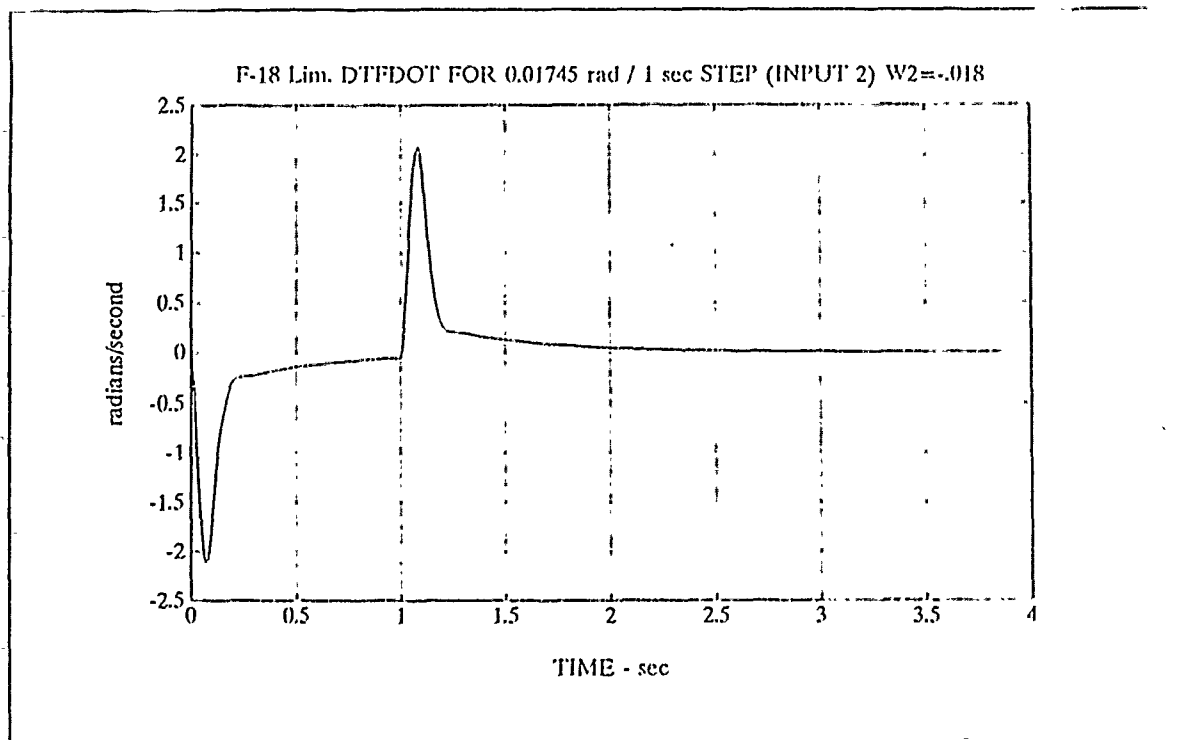


Figure 4-56 Lim. Perf.  $d\delta_{tf}/dt$  due to  $1^\circ/s$  1s Pulse at  $u_2$

The approach to a limited control design did show a reduction in control deflections and rates by increasing the control weight in the cost function but at the cost of system performance and robustness. In addition to the higher control weighting the F-18  $W_1^{-1}$  weighting performance specification had to be relaxed. The small control weightings in the optimum  $H_\infty$  design required unacceptably high energy influx into the system beyond the capability of the actuators to provide. The limited performance design still demonstrated predominantly separate control of  $\alpha$  by input 1 and  $q$  by input 2 but not near the separation demonstrated by the optimum  $H_\infty$  design.

## V. CONCLUSIONS AND RECOMMENDATIONS

$H_\infty$  control theory implemented with the Matlab Robust Controls Toolbox was shown to be a systematic and straightforward method to shape the frequency response of a multi-output, multi-output system of the F-18 to achieve both robustness and system performance. The decoupling of the pitch rate and angle of attack states demonstrates the potential for precision flying modes in which different independent control surfaces control different outputs. The stabilator was controlled by input 1 and was able to control angle of attack separately from input 2 which controlled the pitch rate by commanding the leading and trailing flaps which were ganged together. It was shown that the performance level of the optimum performance  $H_\infty$  design placed too great of an energy demand on the actuators. A limited performance  $H_\infty$  design was demonstrated which placed a greater weight on the control energy in the  $H_\infty$  cost function. The sensitivity weighting function specification had to be relaxed to arrive at the final design. The control deflection rates are still too high and the design will have to be limited still further.

The  $H_\infty$  theory was shown to be superior to the  $H_2$  frequency weighted linear quadratic regulator theory by achieving higher levels of plant disturbance attenuation, better suppression of plant variations and modeling errors, and wider system control bandwidth. Stability of the plant outputs was demonstrated although it was found that the plant inputs did not meet the design

specifications. The inputs failed the design specifications because the specifications are in terms of the sensitivity and complementary sensitivity functions which are formulated in terms of the plant outputs.

Actuator performance has been found to be the most severely limiting factor in the  $H_\infty$  design and has to be more directly accounted for. Including the control deflections and/or rates in the output vector as Rogers [Ref. 6] suggested would be a way to make the design process more practical.

The promise of  $H_\infty$  design theory may make it more practical to include higher performance actuators in future aircraft design. Faster actuators mean cost penalties and more weight. Improving the speed of the actuators must be shown to improve the capabilities and performance of the aircraft sufficiently to pay for the cost and weight penalties. A concern of using faster actuators in the past has been the excitation of flexible structural modes. An  $H_\infty$  design which can suppress the flexible structural modes, provide independently controlled outputs, suppress disturbances and plant variations and achieve respectable control bandwidths might provide the incentive to use improved actuators.

Applying  $H_\infty$  design to the highly maneuverable modified F-18 being tested at NASA Dryden with canards and flow deflectors would seem to be a worthwhile project for future investigation. The  $H_\infty$  design analysis should be applied to other F-18 flight conditions.

## APPENDIX A

### MATLAB SCRIPT FILES

```

f18h2.m
diary f18h2.dat
format short e
disp(' ')
disp(' ')
disp(' This script file is designed to solve the H2 optimal
control ')
disp(' problem for the F-18. The 10th order FDLTI model, in
state ')
disp(' space form, is that of the F-18 aircraft and actuator
dynamics.')
disp(' Four states are those of the aircraft dynamics, i.e.,
alpha & q')
disp(' The remaining 8 states are the dynamics of a fourth ')
disp(' order and two 2nd order actuators, i.e., the stabilator,
leading ')
disp(' flap and trailing flap actuators. The order of the
unbalanced ')
disp(' states is as follows:')
disp(' ')
disp(' alpha, q, ds, dsdot, dsdbldot, dstrpldot, dlf,
dlfdot,')
disp(' dtf, dtfdot ')
disp(' ')
disp(' Given the open loop transfer function  $G(s)=Cinv(Is-A)+D$ ,
a ')
disp(' stabilizing controller  $F(s)$  will be found such that the
H2 norm')
disp(' of  $Ty_{l1}$  is minimized. ')
disp(' ')
disp(' H2 optimal control synthesis is performed to determine
attainable')
disp(' performance levels. Once completed, an Hinf optimal
control ')
disp(' synthesis is performed.')
disp(' ')
disp(' ')
%pause
clc
disp(' The scaled F-18 aircraft and actuator state space
representation')
disp(' ')
disp(' ')
ag=[-.114d+01 9.7938d-01 -9.9461d-02 0.0 0.0 0.0 ...
5.6206d-04 0.0 -3.9669d-03 0.0;-7.0738d+00 -.80902d+00 ...
-7.9063d-00 0.0 0.0 0.0 -3.008d-02 0.0 -1.8786d-00 0.0;
0.0 0.0 0.0 1.0 0.0 0.0 0.0 0.0 0.0 0.0;
0.0 0.0 0.0 0.0 1.0 0.0 0.0 0.0 0.0 0.0;
0.0 0.0 0.0 0.0 0.0 1d+04 0.0 0.0 0.0 0.0;
0.0 0.0 -.14691d+04 -.49559d+02 -.16122d+01 -.1541d+03 0.0 0.0
...
0.0 0.0; 0.0 0.0 0.0 0.0 0.0 0.0 0.0 0.0 1.0 0.0 0.0;

```

```

0.0 0.0 0.0 0.0 0.0 0.0 0.0 0.0 -.1225d+04 -.497d+02]
bg=[0.0 0.0;
    0.0 0.0;
    0.0 0.0;
    .21377d+04 0.0;
    -.30532d+06 0.0;
    .27277d+04 0.0;
    0.0 0.0;
    0.0 .22301d+04;
    0.0 0.0;
    0.0 .1225d+04]
cg=[1.0 0.0 0.0 0.0 0.0 0.0 0.0 0.0 0.0 0.0;
    0.0 1.0 0.0 0.0 0.0 0.0 0.0 0.0 0.0 0.0]
dg=zeros(2)
%pause
disp(' ')

disp(' ')
disp(' Calculate the poles and transmission zeros of the open
loop plant')
disp(' ')
poleg=eig(ag), tzerog=tzero(ag,bg,cg,dg)
disp(' ')
disp(' ')
disp(' Determine the condition number of ag')
disp(' ')
disp(' ')
condag=cond(ag), rcondag=rcond(ag)
disp(' ')
disp(' ')
%pause
disp(' ')
disp(' << Design Specifications >> ')
disp(' ')
disp(' 1). Robustness Spec. : -40 dB roll-off, -20 db @ 100
Rad/Sec.')
disp(' Associated Weighting:')
disp(' ')
disp(' -1 1000 ')
disp(' W3(s) = ----- * I (fixd)')
disp(' 2 ')
disp(' s 2x2')
disp(' ')
disp(' ')
disp(' 2). Performance Spec.: minimizing the sensitivity
function')
disp(' as much as possible.')
disp(' Associated Weighting:')
disp(' ')
disp(' ')
disp(' -1 -1 (100s + 1) ')

```

```

disp('
                                W1(s) = Gam * ----- * I')
disp('
                                100                2x2')
disp(' ')
disp('          where "Gam" in this design is iteratively updated
          from 1')
w=logspace(-3,3,100);
k=1000; mn=[2 2]; tau=0.0;
nuw3i = [0.0 k]; dnw3i = [1.0 0 0];
svw3i = bode(nuw3i,dnw3i,w); svw3i = 20*log10(svw3i);
nuw1i = [100.0 1.0]; dnw1i =[0 100.0];
svw1i = bode(nuw1i,dnw1i,w); svw1i = 20*log10(svw1i);
aw2=-.001*eye(2); bw2=zeros(2); cw2=zeros(2); dw2=-.001*eye(2);
disp(' ')
disp(' ')
disp('          (strike a key to see the plot of the
          weightings ...)' )
%pause
semilogx(w,svw1i,w,svw3i)
grid
title('F-18 Design Specifications')
xlabel('Frequency - Rad/Sec')
ylabel('1/W1 & 1/W3 - dB')
text(.01,0,'1/W1(s)')
text(.5,100,'1/W3(s)')
meta f18specs
%pause
clc
disp('          << Problem Formulation >>')
disp(' ')
disp('          Form an augmented plant P(s) with these two weighting
          functions:')
disp(' ')
disp('          1). Gam*W1 penalizing error signal "e"')
disp(' ')
disp('          2). W3 penalizing plant output "y"')
disp(' ')
disp('          and find a stabilizing controller F(s) such that the H2
          norm')
disp('          of TF Ty1u1 is minimized, i.e.')
disp(' ')
disp('          min |Ty1u1| < 1,')
disp('          F(s)      2')
disp(' ')
disp('          where ')
disp('          |          -1|')

disp('          Ty1u1 = | Gam*W1*(I + GF) | = | Gam * W1 * S
|')
disp('          |          -1|          | W3 * (I - S)
|')
disp('          | W3*GF*(I + GF) |')
disp(' ')

```



```

disp(' ')
disp(' ')
disp('                                     (strike a key to continue
...')
%pause
clc
disp(' ')
disp(' ')
disp('                                     << DESIGN PROCEDURE >>')
disp(' ')
disp(' * * * * *')
disp(' * * * * *')
disp(' * [Step 1]. Do plant augmentation (run
AUGMENT.M or *')
disp(' * AUGF18.M)
*')
disp(' *')
disp(' *')
disp(' * [Step 2]. Do H2 synthesis (run H2LQG.M)
*')
disp(' *')
disp(' *')
disp(' * [Step 3]. Redo the plant augmentation for a
*')
disp(' * new "Gam" and rerun H2LQG.M
*')
disp(' *')
disp(' * [Step 4]. Redo the plant augmentation for a
*')
disp(' * higher "Gam" then run HINF.M
*')
disp(' * * * * *')
disp(' * * * * *')
disp(' ')
disp(' ')
disp('                                     (strike a key to continue
...')
%pause
clc
disp(' ')
disp(' ')
disp(' ')
disp(' Assign the cost coefficients "Gam" with Gam=1 ')
disp(' ')
disp(' serving as the baseline design ....')
pack
gama=[6.7];
ngama=length(gama);
for i=1:ngama
Gam=gama(1,i)
k=1000

```

```

disp(' ')
disp('-----')
disp('          augment      % Plant augmentation of the F-18
      dynamics')
disp('-----')
disp(' ')
disp(' ')
augf18
disp(' ')
disp(' ')
disp('          (strike a key to continue
      ...)' )
[ac,bc,cc,t,k1]=ctrbf(A,[B1 B2],[C1;C2]);
sum(k1)
pause
clc
%disp(' ')
%disp(' ')
%disp('          Do state space balancing on the augmented plant if
      needed')
%disp(' ')
%disp(' ')
%[augA,augB,augC,augD]=minreal(A,[B1 B2],[C1;C2],[D11 D12;D21 D22])
%[abal,bbal,cbal,g,t]=obalreal(augA,augB,augC)
%[abal,bbal,cbal,g,t]=obalreal(A,[B1 B2],[C1;C2])
%A=abal,      B1=bbal(:,1:2),      B2=bbal(:,3:4),      C1=cbal(1:6,:),
C2=cbal(7:8,:)
disp(' ')
disp(' ')
disp('          The transmission zeros, poles and condition number of the
      augmented')
disp('          plant follow.  In addition, determine if (A,B1) & (A,B2)
      are ')
disp('          stabilizable and if (C1,A) & (C2,A) are detectable.')
disp(' ')
disp(' ')
%tzeroaug=tzero(abal,bbal,cbal,dbal)
tzeroaug=tzero(A,[B1 B2],[C1;C2],[D11 D12;D21 D22])
poleaugA=eig(A)
%poleaugA=eig(abal)
condaugA=cond(A)
rcondaugA=rcond(A)
%condaugA=cond(abal)
%rcondaugA=rcond(abal)
eps=eps
toldef=10*max(size(A))*norm(A,1)*eps
%toldef=10*max(size(abal))*norm(abal,1)*eps
tol=100*eps*norm([A B1])
[A1c,B1c,C1c,t,k]=ctrbf(A,B1,C1,tol)
tol=100*eps*norm([A B2])

```

```

[A2c,B2c,C2c,t,k]=ctrbf(A,B2,C2,tol)
tol=100*eps*norm([A;C1])
[A1o,B1o,C1o,t,k]=obsvf(A,B1,C1,tol)
tol=100*eps*norm([A;C2])
[A2o,B2o,C2o,t,k]=obsvf(A,B2,C2,tol)
clear condag rcondag poleg tzerog svw3i svw1i
clear condaugA rcondaugA
clear functions
%pause
disp(' ')
disp(' ')
d          i          s          p          (          '
-----')
disp('          h2lqg          % Running script file H2LQG.M for H2
optimization')
d          i          s          p          (          '
-----')
aretype='Schur'
h2lqg
disp(' ')
disp(' ')
disp('                                     (strike a key to continue
...))')
clear functions
%pause
%pltopmod          % Preparing singular values for plotting
%end
disp(' ')
disp(' ')
disp('                                     (strike a key to continue
...))')
%pause
disp(' ')
disp(' ')
disp(' State space representation of controller (acp, bcp, ccp,
dcp) ')
disp(' and CLTF Tylul (acl, bcl, ccl, dcl) and poles,
controllability, ')
disp(' observability, and condition number of the controller. ')
disp(' ')
disp(' ')

pltopmod          %preparing singular values for plotting
end
acp,bcp,ccp,dcp
polec=eig(acp)
tol=100*eps*norm([acp bcp])
[acpc,bcpc,ccpc,t,k]=ctrbf(acp,bcp,ccp,tol)
lc=sum(k)
pause
tol=100*eps*norm([acp;ccp])
[acpo,bcpo,ccpo,t,k]=obsvf(acp,bcp,ccp,tol)

```

```

lo=sum(k)
pause
condacp=cond(acp), rcondacp=rcond(acp)
acl,bcl,ccl,dcl
polet=eig(acl)
disp(' ')
disp(' ')
disp(' (strike a key to continue
...))')
%pause
disp(' ')
disp(' ')
disp(' Open loop state space representation of controller/plant
series')
disp(' ')
[algf,blgf,clgf,dlgf]=series(acp,bcp,ccp,dcg,ag,bg,cg,dg)
polol=eig(algf)
disp(' ')
disp(' ')
disp(' (strike a key to continue
...))')
%pause
disp(' ')
disp(' ')
disp(' Closed loop state space representation of
controller/plant series,')
disp(' controllability, observability, and condition number of
the closed')
disp(' loop acgf matrix. ')
disp(' ')
disp(' ')
[acgf,bcgf,ccgf,dcgf]=feedback(algf,blgf,clgf,dlgf,2)
tol=100*eps*norm([acgf bcgf])
[acgfc,bcgfc,ccgfc,t,k]=ctrbf(acgf,bcgf,ccgf,tol)
tol=100*eps*norm([acgf;ccgf])
[acgfo,bcgfo,ccgfo,t,k]=obsvf(acgf,bcgf,ccgf,tol)
condacgf=cond(acgf)
disp(' ')
disp(' ')
disp(' (strike a key to continue
...))')
%pause
disp(' ')
disp(' Poles of the closed loop system')
disp(' ')
polcl=eig(acgf)
end

```

```

%fl8hinf.m
diary fl8hinf.dat
format short e
disp('      f18hinf.m')
disp('      ')
disp('      This script file is designed to solve the Hinf optimal
      control ')
disp('      problem for the f-18.  The 10th order FDLTI model, in
      state ')
disp('      space form, is that of the f-18 aircraft and actuator
      dynamics.')
disp('      Two states are those of the aircraft dynamics, i.e.,
      alpha & q ')
disp('      The remaining 8 states are the dynamics of the fourth
      order')
disp('      stabilator, the 2nd order leading flap, and the 2nd
      order trailing')
disp('      flap actuators.  The order of the unbalanced states is
      as ')
disp('      follows:')
disp('      ')
disp('      alpha, q, ds, dsdot, dsdbldot, dstrpldot, dlf, dlfdot,')
disp('      dtf, dtfdot')
disp('      ')
disp('      Given the open loop transfer function  $G(s)=Cinv(Is-A)+D$ ,
      a ')
disp('      stabilizing controller  $F(s)$  will be found such that the
      Hinf norm')
disp('      of  $T_{y1u1}$  is less than or equal to one.  ')
disp('      ')
disp('      ')
pause
clc
disp('      F-18 aircraft and actuator state space representation')
disp('      ')
ag=[-.114d+01 9.7938d-01 -9.9461d-02 0.0 0.0 0.0 ...
5.6206d-04 0.0 -3.9669d-03 0.0;-7.0738d+00 -.80902d+00 ...
-7.9063d-00 0.0 0.0 0.0 -3.008d-02 0.0 -1.8786d-00 0.0;
0.0 0.0 0.0 1.0 0.0 0.0 0.0 0.0 0.0 0.0;
0.0 0.0 0.0 0.0 1.0 0.0 0.0 0.0 0.0 0.0;
0.0 0.0 0.0 0.0 0.0 1d+04 0.0 0.0 0.0 0.0;
0.0 0.0 -.14691d+04 -.49559d+02 -.16122d+01 -.1541d+03 0.0 0.0
...
0.0 0.0; 0.0 0.0 0.0 0.0 0.0 0.0 0.0 0.0 1.0 0.0 0.0;
0.0 0.0 0.0 0.0 0.0 0.0 -.22301d+04 -.1098d+03 0.0 0.0;
0.0 0.0 0.0 0.0 0.0 0.0 0.0 0.0 0.0 1.0;
0.0 0.0 0.0 0.0 0.0 0.0 0.0 0.0 -.1225d+04 -.497d+02];

ag(2,7)=ag(2,7)*57.296
bg=[0.0 0.0;
0.0 0.0;
0.0 0.0;

```

```

.21377d+04  0.0;
-.30532d+06  0.0;
.27277d+04  0.0;
    0.0  0.0;
    0.0  .22302d+04;
    0.0  0.0;
    0.0  .1225d+04]
cg=[1.0  0.0  0.0  0.0  0.0  0.0  0.0  0.0  0.0  0.0;
    0.0  1.0  0.0  0.0  0.0  0.0  0.0  0.0  0.0  0.0]
dg=zeros(2)
%pause
disp(' ')
poleg=eig(ag),  tzerog=tzero(ag,bg,cg,dg)
disp(' ')
disp(' ')
disp(' Determine determine the condition number of ag')
disp(' ')
disp(' ')
condag=cond(ag),  rcondag=rcond(ag), rank(ag),
pause
disp(' ')
disp(' ')

%pause
disp(' ')
disp(' << Design Specifications >> ')
disp(' ')
disp(' 1). Robustness Spec. : -40 dB roll-off, -20 db @ 100
Rad/Sec.')
disp(' Associated Weighting:')
disp(' ')
disp('          -1      1000 ')
disp(' W3(s) =  ----- * I      (fixd)')
disp('              2      2x2')
disp('              s      ')
disp(' ')
disp(' ')
disp(' 2). Performance Spec.: minimizing the sensitivity
function')
disp(' as much as possible.')
disp(' Associated Weighting:')
disp(' ')
disp(' ')
disp('          -1      -1 .01(100s + 1) ')
disp(' W1(s) = Gam * ----- * I')
disp('              (.01s + 1)      2x2')
disp(' ')
disp(' ')
disp(' note gamma 13.5 .01s + 1 and limited gamma 1.58 .4s +
1 ')
disp(' where "Gam" in this design is iteratively updated
from 1')

```

```

w=logspace(-3,3,100);
k=1000.; mn=[2 2]; tau=0.0;
nuw3i = [0.0 k]; dnw3i = [1.0 0.0 0.0];
svw3i = bode(nuw3i,dnw3i,w); svw3i = 20*log10(svw3i);
nuw1i = [1 .01]; dnw1i = [.01 1.];
svw1i = bode(nuw1i,dnw1i,w); svw1i = 20*log10(svw1i);

disp(' w2 weigning matrix 13.5 =-.001    1.55 = -.018')
aw2=-0.001*eye(2); bw2=zeros(2); cw2=zeros(2); dw2=-0.001*eye(2);

disp(' ')
disp(' ')
disp('                                (strike a key to see the plot of the
    weightings ...)' )
%pause

semilogx(w,svw1i,w,svw3i)
grid
title('F-18 Design Specifications')
xlabel('Frequency - rad/sec')
ylabel('1/W1 & 1/W3 - db')
text(.01,0,'1/W1(s)')
text(.5,100,'1/W3(s)')
%meta f18specs
%pause

clc
disp('                                << Problem Formulation >>')
disp(' ')
disp('    Form an augmented plant P(s) with these two weighting
    functions:')
disp(' ')
disp('                1). Gam*W1 penalizing error signal "e"')
disp(' ')
disp('                2). W3 penalizing plant output "y"')
disp(' ')
disp('    and find a stabilizing controller F(s) such that the Hinf
    norm')
disp('    of TF Tylu1 is less than or equal to one, i.e.')
disp(' ')
disp('                |Tylu1|    < or = 1,')
disp('                F(s)    inf')
disp(' ')
disp('    where ')
disp('                |                -1|')

disp('                Tylu1 = | Gam*W1*(I + GF) | = | Gam * W1 * S
disp('                |                -1|    | W3 * (I - S)
disp('                | W3*GF*(I + GF) |')
disp(' ')

```

```

disp(' ')
disp(' ')
disp('                                     (strike a key to continue
    ...))')
%pause
clc
disp(' ')
disp(' ')
disp('                                     << DESIGN PROCEDURE >>')
disp('                                     * * * * *')
disp(' * * * * *')
disp(' * [Step 1]. Do plant augmentation (run
    AUGMENT.M or *')
disp(' * AUGX29.M)
    *')
disp(' *')
disp(' *')
disp(' * [Step 2]. Balance the augmented plant for
    better *')
disp(' * numerical condition if necessary
    *')
disp(' *')
disp(' * [Step 3]. Do Hinf synthesis with "Gam" = 1
    *')
disp(' *')
disp(' * [Step 4]. Redo the plant augmentation for a
    *')
disp(' * higher "Gam" and rerun HINF.M
    *')
disp(' * * * * *')
disp(' * * * * *')
disp(' ')
disp(' ')
disp('                                     (strike a key to continue
    ...))')
%pause
clc
disp(' ')
disp(' ')
disp(' ')
disp(' Assign the cost coefficients "Gam" with Gam=1 ')
disp(' ')
disp(' serving as the baseline design ....')
gama=[10.5];
ngama=length(gama);
for i=1:ngama
    Gam=gama(1,i)
    k=1000
    disp(' ')

```



```

d i s p ( '
-----')
disp('          augment    % Plant augmentation of the F-18
dynamics')
d i s p ( '
-----')
disp(' ')
disp(' ')
augf18;
disp(' ')
disp(' ')
disp('          (strike a key to continue
...))')
%pause
clc
disp(' ')
disp(' ')
%disp('      Do state space balancing on the augmented plant if
needed')
%disp(' ')
%disp(' ')
%[abal,bbal,cbal,g,t]=obalreal(A,[B1 B2],[C1;C2])
%A=abal,      B1=bbal(:,1:2),      B2=bbal(:,3:4),      C1=cbal(1:4,:),
C2=cbal(5:6,:))
disp(' ')
disp(' ')
disp('      The transmission zeros, poles and condition number of the
augmented')
disp('      plant follow. In addition, determine if (A,B1) & (A,B2)
are ')
disp('      stabilizable and if (C1,A) & (C2,A) are detectable.')
disp(' ')
disp(' ')
tzeroaug=tzero(A,[B1      B2],[C1;C2],[D11      D12;D21      D22]),
poleaugA=eig(A)
condaugA=cond(A), rcondaugA=rcond(A)

eps=eps
toldef=10*max(size(A))*norm(A,1)*eps
tol=100*eps*norm([A B1])
[A1c,B1c,C1c,t,k]=ctrbf(A,B1,C1,tol)
tol=100*eps*norm([A B2])
[A2c,B2c,C2c,t,k]=ctrbf(A,B2,C2,tol)
tol=100*eps*norm([A;C1])
[A1o,B1o,C1o,t,k]=obsvf(A,B1,C1,tol)
tol=100*eps*norm([A;C2])
[A2o,B2o,C2o,t,k]=obsvf(A,B2,C2,tol)
clear condag rcondag poleg tzerog svw3i svw1i
clear condaugA rcondaugA
clear functions
%pause

```

```

disp(' ')
disp(' ')
disp('-----')
disp('      hinf      % Running script file HINF.M for Hinf
      optimization')
disp('-----')
aretype='Schur'
hinf
disp(' ')
disp(' ')
disp('                                (strike a key to continue
      ...))')
clear functions
%pause
disp(' ')
disp(' ')
disp('      State space representation of the full order controller')
disp('      (acp, bcp, ccp, dcp) with its poles and condition
      number')
disp(' ')
acp,bcp,ccp,dcp
polec=eig(acp)
condacp=cond(acp)
rank(acp)
pause
toldef=10*max(size(acp))*norm(acp,1)*eps
tol=100*eps*norm([acp bcp;ccp dcp])
disp('      Poles, controllability, observability, and condition of
      the ')
disp('      controller')
disp(' ')

polet=eig(acl)
%pause
disp(' ')
disp(' ')
pltopmod      % Preparing singular values for plotting
end
disp(' ')
disp(' ')
disp('                                (strike a key to continue
      ...))')
%pause
disp(' ')
disp(' ')
disp('      Open loop state space representation of controller/plant
      series')
disp(' ')
[algf,blgf,clgf,dlgf]=series(acp,bcp,ccp,dcp,ag,bg,cg,dg)

```

```

polol=eig(algf)
disp('  ')
disp('  ')
disp('                                (strike a key to continue
    ...))')
%pause
disp('  ')
disp('  ')
disp('          Closed loop state space representation of
    controller/plant series,')
disp('    controllability, observability, and condition number of
    the closed')
disp('    loop acgf matrix. ')
disp('  ')
disp('  ')
[acgf,bcgf,ccgf,dcgf]=feedback(algf,blgf,clgf,dlgf,2)
tol=100*eps*norm([acgf bcgf])
[acgfc,bcgfc,ccgfc,t,k]=ctrbf(acgf,bcgf,ccgf,tol)
tol=100*eps*norm([acgf;ccgf])
[acgfo,bcgfo,ccgfo,t,k]=obsvf(acgf,bcgf,ccgf,tol)
condacgf=cond(acgf)
disp('  ')
disp('  ')
disp('                                (strike a key to continue
    ...))')
%pause
disp('  ')
disp('    Poles of the closed loop system')
disp('  ')
polcl=eig(acgf)
end

```

```

%augf18.m
% Plant Augmentation for the F-18 H2 and Hinf problem as W3 is not
a
% proper transfer function. Includes contingency for adding W2 to
% ensure d12 is full column rank. This script file is designed for
% the F-18 system without theta as a state, ie, 2 inputs & 2
  outputs.
disp(' ')
disp(' ')
disp('          << Plant Augmentation >>')
%Gam=gama(1,i)
Gam = input('          Input the cost coefficient "Gam" = ');
cgb = 1/k*[cg(1,:)*ag*ag;cg(2,:)*ag*ag*ag*tau+cg(2,:)*ag*ag]
dgb = 1/k*[cg(1,:)*ag*bg;cg(2,:)*ag*ag*bg*tau]
nw1 = Gam*[dnw1i;0 0;0 0;dnw1i]
dw1 = nuw1i
sysw2=[aw2 bw2;cw2 dw2]; xw2=2;
%sysw2=[]; xw2=0;
%[A,B1,B2,C1,C2,D11,D12,D21,D22]=augmod(ag,bg,cg,cgb,dg,dgb,nw1,d
w1,mn)
[A,B1,B2,C1,C2,D11,D12,D21,D22]=augf18pl(ag,bg,cg,cgb,dg,dgb,nw1,
dw1,sysw2,xw2,mn)

disp(' ')
disp('          - - - State-Space (A,B1,B2,C1,C2,D11,D12,D21,D22) is
ready for')
disp('          the Small-Gain problem - - -')
%
% ----- End of AUGF18.M ----- %

```

```

f      u      n      c      t      i      o      n
[a,b1,b2,c1,c2,d11,d12,d21,d22]=augf18pl(ag,bg,cga,cgb,dga,dgb,num,den,sys,x,mn)

```

```

%
%
[A,B1,B2,C1,C2,D11,D12,D21,D22]=AUGF18PL(AG,BG,CG,CGB,DG,DGB,NUM,DEN,SYS,X,MN)

```

```

% augf18pl produces the augmented plant for the F-18 h2 and hinf
problem for
% an improper W3 weighting and W2 added to make d12 full
column rank.

```

```

%
% Weighted Plant :

```

$$\dot{X}_g = A_g X_g + B_g U_g$$

$$\begin{bmatrix} Y_{ga} \\ Y_{gb} \end{bmatrix} = \begin{bmatrix} C_{ga} \\ C_{gb} \end{bmatrix} X_g + \begin{bmatrix} D_{ga} \\ D_{gb} \end{bmatrix} U_g$$

```

%
% Weighting W1 :

```

$$\dot{X}_{w1} = A_{w1} X_{w1} + B_{w1} U_{w1}$$

$$Y_{w1} = C_{w1} X_{w1} + D_{w1} U_{w1}$$

```

%
% Weighting W2 :

```

$$\dot{X}_{w2} = A_{w2} X_{w2} + B_{w2} U_{w2}$$

$$Y_{w2} = C_{w2} X_{w2} + D_{w2} U_{w2}$$

```

%
% Over all augmented plant :

```

$$\begin{bmatrix} \dot{X}_g \\ \dot{X}_{w1} \\ \dot{X}_{w2} \end{bmatrix} = \begin{bmatrix} A_g & 0 & 0 \\ -B_{w1}C_{ga} & A_{w1} & 0 \\ 0 & 0 & A_{w2} \end{bmatrix} \begin{bmatrix} X_g \\ X_{w1} \\ X_{w2} \end{bmatrix} + \begin{bmatrix} 0 & B_g \\ B_{w1} & -B_{w1}D_{ga} \\ 0 & B_{w2} \end{bmatrix} \begin{bmatrix} U_1 \\ U_2 \end{bmatrix}$$

$$\begin{bmatrix} Y_{1a} \\ Y_{1b} \\ Y_{1c} \\ Y_2 \end{bmatrix} = \begin{bmatrix} -D_{w1}C_{ga} & C_{w1} & 0 \\ 0 & 0 & C_{w2} \\ C_{gb} & 0 & 0 \\ -C_{ga} & 0 & 0 \end{bmatrix} \begin{bmatrix} X_g \\ X_{w1} \\ X_{w2} \end{bmatrix} + \begin{bmatrix} D_{w1} & -D_{w1}D_{ga} \\ 0 & D_{w2} \\ 0 & D_{gb} \\ I & -D_{ga} \end{bmatrix} \begin{bmatrix} U_1 \\ U_2 \end{bmatrix}$$

```

% State Space of Weighting W1 & W2:

```

```

%
[aw1,bw1,cw1,dw1] = tfm2ss(num,den,mn(1),mn(2))
[aw2,bw2,cw2,dw2] = sys2ss(sys,x)

```

```

% State Space of Augmented Plant :

```

```

% ----- A matrix :

```

```

[rag,cag] = size(ag);
[raw1,caw1] = size(aw1);
[raw2,caw2] = size(aw2);
a = [ag zeros(rag,caw1) zeros(rag,caw2);-bw1*cga aw1

```

```

        zeros(raw1,caw2);
        zeros(raw2,cag) zeros(raw2,caw1) aw2];
%
% ----- B matrix :
%
[rbg,cbg] = size(bg);
[rbw1,cbw1] = size(bw1);
[rbw2,cbw2] = size(bw2);
b1 = [zeros(rbg,cbw1);bw1;zeros(rbw2,cbw1)];
b2 = [bg;-bw1*dga;bw2];
%
% ----- C matrix :
%
[rcgb,ccgb] = size(cgb);
[rcw1,ccw1] = size(cw1);
[rcw2,ccw2] = size(cw2);
c1 = [-dw1*cga    cw1    zeros(rcw1,ccw2);zeros(rcw2,ccgb)
zeros(rcw2,ccw1) cw2;
      cgb zeros(rcgb,ccw1) zeros(rcgb,ccw2)];
[rcga,ccga] = size(cga);
c2 = [-cga zeros(rcga,ccw1) zeros(rcga,ccw2)];
%
% ----- D matrix :
%
[rdgb,cdgb] = size(dgb);
[rdw1,cdw1] = size(dw1);
[rdw2,cdw2] = size(dw2);
d11 = [dw1;zeros(rdw2,cdw1);zeros(rdgb,cdw1)];
d12 = [-dw1*dga;dw2;dgb];
[rdga,cdga] = size(dga);
d21 = eye(rdga);
d22 = -dga;
%
% ----- End of AUGPL.M ----- %

```

```

%fl8analy.m
diary fl8analy.dat
format short e
disp(' ')
disp(' ')
disp(' This script file analyzes the results of Hinf synthesis
      of the')
disp(' F-18 MIMO model by plotting resultant system return
difference')
disp(' singular values, calculating the poles/zeros, and making
      Bode and')
disp(' Nyquist plots.')
disp(' ')
disp(' ')
disp(' The unaugmented state space plant representation')
disp(' ')
disp(' ')
ag,bg,cg,dg
disp(' ')
disp(' ')
%pause
disp(' State space representation of the controller')
disp(' ')
disp(' ')
acp,bcp,ccp,dcp
disp(' ')
disp(' ')
%pause
disp(' Open loop state space representation of controller')
disp(' plant series')
disp(' ')
disp(' ')
algf,blgf,clgf,dlgf
[alfg,blfg,clfg,dlfg]=series(ag,bg,cg,dg,acp,bcp,ccp,dcp)
disp(' ')
disp(' ')
disp(' Compute singular value plot of return difference
      matrices')
disp(' ')
disp(' ')
w=logspace(-3,3,100);
svg=sigma(ag,bg,cg,dg,3,w); svg=20*log10(svg);
semilogx(w,svg)
title('F-18 Limited Performance SV PLOT (I + G)')
xlabel('FREQUENCY - rad/sec')
ylabel('SV - dB')
grid
meta f18sv1L
pause
svgf=sigma(algf,blgf,clgf,dlgf,3,w); svgf=20*log10(svgf);
semilogx(w,svgf)
title('F-18 Limited Performance SV PLOT (I + GF)')

```

```

xlabel('FREQUENCY - rad/sec')
ylabel('SV - dB')
grid
meta f18sv2L
pause
svfg=sigma(alfg,blfg,clfg,dlfg,3,w); svfg=20*log10(svfg);
semilogx(w,svfg)
title('F-18 Limited Performance SV PLOT (I + FG)')
xlabel('FREQUENCY - rad/sec')
ylabel('SV - dB')
grid
meta f18sv3L
pause
svgf=sigma(algf,blgf,clgf,dlgf,4,w); svgf=20*log10(svgf);
semilogx(w,svgf)
title('F-18 Limited Performance SV PLOT (I + inv(GF))')
xlabel('FREQUENCY - rad/sec')
ylabel('SV - dB')
grid
meta f18sv4L
pause
svfg=sigma(alfg,blfg,clfg,dlfg,4,w); svfg=20*log10(svfg);
semilogx(w,svfg)
title('F-18 Limited Performance SV PLOT (I + inv(FG))')
xlabel('FREQUENCY - rad/sec')
ylabel('SV - dB')
grid
meta f18sv5L
pause
svloop=sigma(algf,blgf,clgf,dlgf,1,w); svloop=20*log10(svloop);
semilogx(w,svloop)
title('F-18 Limited Performance SV PLOT (GF)')
xlabel('FREQUENCY - rad/sec')
ylabel('SV - dB')
grid
meta f18sv6L
pause
disp(' ')
disp(' ')
disp('          Closed loop state space representation of
      controller/plant series')
disp(' ')
disp(' ')
acgf,bcgf,ccgf,dcgf
tzerocgf=tzero(acgf,bcgf,ccgf,dcgf)
disp(' ')
disp(' ')
%pause
disp('          Poles and zeros of the closed loop controller/plant
      system ')
disp('          (acgf, bcgf, ccgf, dcgf) ')
disp(' ')

```



```

disp(' ')
disp(' output alpha/q vs input 1 ')
disp(' ')
[z,p,k]=ss2zp(acgf,bcgf,ccgf,dcgf,1)
%pause
disp(' ')
disp(' output alpha/q vs input 2 ')
disp(' ')
[z,p,k]=ss2zp(acgf,bcgf,ccgf,dcgf,2)
pause
disp(' ')
disp(' ')
disp(' Open loop Bode plots of outputs vs inputs')
disp(' ')
disp(' ')
[mag1,phase1]=bode(algf,blgf,clgf,dlgf,1,w); mag1=20*log10(mag1);
[mag2,phase2]=bode(algf,blgf,clgf,dlgf,2,w); mag2=20*log10(mag2);
semilogx(w,mag1(:,1))
title('F-18 LIMITED PERFORMANCE OPEN LOOP BODE PLOT INPUT 1 / alpha
      (GF)')
xlabel('FREQUENCY - rad/sec')
ylabel('GAIN - dB')
grid
meta f18bode1L
pause
semilogx(w,mag1(:,2))
title('F-18 LIMITED PERFORMANCE OPEN LOOP BODE PLOT INPUT 1 / q
      (GF)')
xlabel('FREQUENCY - rad/sec')
ylabel('GAIN - dB')
grid
meta f18bode2L
pause
semilogx(w,mag2(:,1))
title('F-18 LIMITED PERFORMANCE OPEN LOOP BODE PLOT INPUT 2 / alpha
      (GF)')
xlabel('FREQUENCY - rad/sec')
ylabel('GAIN - dB')
grid
meta f18bode3L
pause
semilogx(w,mag2(:,2))
title('F-18 LIMITED PERFORMANCE OPEN LOOP BODE PLOT INPUT 2 / q
      (GF)')
xlabel('FREQUENCY - rad/sec')
ylabel('GAIN - dB')
grid
meta f18bode4L
disp(' ')
disp(' ')
disp(' Closed loop Bode plots of outputs vs inputs')
disp(' ')

```

```

disp(' ')
[mag1,phase1]=bode(acgf,bcgf,ccgf,dcgf,1,w); mag1=20*log10(mag1);
[mag2,phase2]=bode(acgf,bcgf,ccgf,dcgf,2,w); mag2=20*log10(mag2);
semilogx(w,mag1(:,1))
title('F-18 LIMITED PERFORMANCE CLOSED LOOP BODE PLOT INPUT 1 /
      alpha ')
xlabel('FREQUENCY - rad/sec')
ylabel('GAIN - dB')
grid
meta f18bode5L
pause
semilogx(w,mag1(:,2))
title('F-18 LIMITED PERFORMANCE CLOSED LOOP BODE PLOT INPUT 1 / q
      ')
xlabel('FREQUENCY - rad/sec')
ylabel('GAIN - dB')
grid
meta f18bode6L
pause
semilogx(w,mag2(:,1))
title('F-18 LIMITED PERFORMANCE CLOSED LOOP BODE PLOT INPUT 2 /
      alpha ')
xlabel('FREQUENCY - rad/sec')
ylabel('GAIN - dB')
grid
meta f18bode7L
pause
semilogx(w,mag2(:,2))
title('F-18 LIMITED PERFORMANCE CLOSED LOOP BODE PLOT INPUT 2 / q
      ')
xlabel('FREQUENCY - rad/sec')
ylabel('GAIN - dB')
grid
meta f18bode8L
%pause
disp(' ')
%disp(' ')
%disp(' Open loop nyquist plots of outputs vs inputs')
%disp(' ')
%disp(' ')
%w=logspace(-4,5,200);
%[re1,im1]=nyquist(algf,blgf,clgf,dlgf,1,w);
%[re2,im2]=nyquist(algf,blgf,clgf,dlgf,2,w);
%re1=[re1;re1]; im1=[im1;-im1];
%re2=[re2;re2]; im2=[im2;-im2];
%plot(re1(:,1),im1(:,1))
%title('NYQUIST PLOT INPUT 1 / alpha (GF)')
%xlabel('real (GF)')
%ylabel('imag (GF)')
%grid
%meta x29nyqu
%pause

```

```

%plot(re1(:,2),im1(:,2))
%title('NYQUIST PLOT INPUT 1 / q (GF)')
%xlabel('real (GF)')
%ylabel('imag (GF)')
%grid
%meta
%pause
%plot(re2(:,1),im2(:,1))
%title('NYQUIST PLOT INPUT 2 / alpha (GF)')
%xlabel('real (GF)')
%ylabel('imag (GF)')
%grid
%meta
%pause
%plot(re2(:,2),im2(:,2))
%title('NYQUIST PLOT INPUT 2 / q (GF)')
%xlabel('real (GF)')
%ylabel('imag (GF)')
%grid
%meta
%pause
end

```

```

%fl8resp.m
diary fl8resp.dat
format short e
disp(' ')
disp(' ')
disp(' This script file is designed to calculate and plot the
time')
disp(' response of the augmented F-18 (controller/plant closed
loop series)')
disp(' to 1 degree / 1 second step input from each of')
disp(' the two inputs separately.')
disp(' ')
disp(' ')
disp(' Setting up the time vectors')
disp(' ')
time=[0:0.01:4];
%stas=[1 0 0 0 0;0 1 0 0 0;0 0 1 0 0;0 0 0 1 0;0 0 0 0 1]
%ccgfwc=[zeros(5,18) stas zeros(5,6)]
%dcgfwc=zeros(5,2)
%stas=[1 0 0 0 0 0 0 0;0 1 0 0 0 0 0 0;0 0 1 0 0 0 0 0;0 0 0 1 0 0
0 0;...
%0 0 0 0 1 0 0 0;0 0 0 0 0 1 0 0;0 0 0 0 0 0 1 0;0 0 0 0 0 0 0 1]
%ccgfwc=[zeros(8,15) stas zeros(8,6)]
%dcgfwc=zeros(8,2)
disp(' ')
disp(' Plotting alpha, q, ds, dlf, and dtf responses to a
0.01745 rad / 1 ')
disp(' second step from input one')
disp(' ')
u=[0.01745*ones(1,101) zeros(1,300);zeros(1,401)]';
%[y]=lsim(acgf,bcgf,ccgfwc,dcgfwc,u,time)
[y,x]=lsim(acgf,bcgf,ccgf,dcgf,u,time);
%plot(time,y(:,1))
%title('F-18 alpha RESPONSE TO 0.01745 rad / 1 sec STEP (INPUT 1)
W2=-.001')
%xlabel('TIME - sec')
%ylabel('radians')
%grid
%meta fl8rsp11U
%pause
%plot(time,y(:,2))
%title('F-18 q RESPONSE TO 0.01745 rad / 1 sec STEP (INPUT 1)
W2=-.001')
%xlabel('TIME - sec')
%ylabel('radians/second')
%grid
%meta fl8rsp12U
%pause
plot(time,x(:,17))
title('F-18 DS FOR 0.01745 rad / 1 sec STEP (INPUT 1) W2=-.001')
xlabel('TIME - sec')
ylabel('radians')

```

```

grid
%meta f18rsp13L
pause
plot(time,y(:,1),time,y(:,2))
title('F18 OPT. RESPONSE TO 1 DEG / ONE SECOND IMPULSE (INPUT 1)')
xlabel('TIME -SEC')
ylabel('RADIANS')
text(1.2,.0102,'ALPHA RESPONSE')
text(0.3,.0012,'q RESPONSE')
grid
meta alphaq112U
pause
plot(time,x(:,21))
title('F-18 DLF FOR 0.01745 rad / 1 sec STEP (INPUT 1) W2=-.001')
xlabel('TIME - sec')
ylabel('radians')
grid
%meta f18rsp17L
pause
plot(time,x(:,23))
title('F-18 DTF FOR 0.01745 rad / 1 sec STEP (INPUT 1) W2=-.001')
xlabel('TIME - sec')
ylabel('radians')
grid
%meta f18rsp19L
pause
plot(time,x(:,18))
title('F-18 DSDOT FOR 0.01745 rad / 1 sec STEP (INPUT 1) W2=-.001')
xlabel('TIME - sec')
ylabel('radians/second')
grid
%meta f18rsp14L
pause
plot(time,x(:,22))
title('F-18 Lim. DLFDOT FOR 0.01745 rad / 1 sec STEP (INPUT 1)
      W2=-.001')
xlabel('TIME - sec')
ylabel('radians/second')
grid
%meta f18rsp18L
pause
plot(time,x(:,24))
title('F-18 Lim. DTFDOT FOR 0.01745 rad / 1 sec STEP (INPUT 1)
      W2=-.001')
xlabel('TIME - sec')
ylabel('radians/second')
grid
%meta f18rsp110L
pause
disp('      ')
disp('      Plotting alpha, q, dc, df, and ds responses to a 0.01745
      rad / 1')

```

```

disp('    second step input from input two')
disp('    ')
u=[zeros(1,401);0.01745*ones(1,101) zeros(1,300)]];
%[y]=lsim(acgf,bcgf,ccgfwc,dcgfwc,u,time)
[y,x]=lsim(acgf,bcgf,ccgf,dcgf,u,time);
plot(time,y(:,1),time,y(:,2))
title('F-18 OPT. RESPONSE TO 0.01745 rad/ 1 sec STEP(INPUT 2)')
xlabel('TIME - sec')
ylabel('radians')
text(1.2,.011,'q RESPONSE')
text(1.2,-.001,'ALPHA RESPONSE')
grid
meta alphaq212U
pause
%plot(time,y(:,2))
%title('F-18 q RESPONSE TO 0.01745 rad / 1 sec STEP (INPUT 2)
%      W2=-.001')
%xlabel('TIME - sec')
%ylabel('radians/second')
%grid
%meta f18rsp22U
%pause
plot(time,x(:,17))
title('F-18 DS FOR 0.01745 rad / 1 sec STEP (INPUT 2) W2=-.001')
xlabel('TIME - sec')
ylabel('radians')
grid
%meta f18rsp23L
%pause
plot(time,x(:,21))
title('F-18 DLF FOR 0.01745 rad / 1 sec STEP (INPUT 2) W2=-.001')
xlabel('TIME - sec')
ylabel('radians')
grid
%meta f18rsp27L
%pause
plot(time,x(:,23))
title('F-18 DTF FOR 0.01745 rad / 1 sec STEP (INPUT 2) W2=-.001')
xlabel('TIME - sec')
ylabel('radians')
grid
%meta f18rsp29L
%pause
plot(time,x(:,18))
title('F-18 DSDOT FOR 0.01745 rad / 1 sec STEP (INPUT 2) W2=-.001')
xlabel('TIME - sec')
ylabel('radians/second')
grid
%meta f18rsp26L
%pause
plot(time,x(:,22))
title('F-18 DLFDOT FOR 0.01745 rad / 1 sec STEP (INPUT 2)

```

```

W2=-.001')
xlabel('TIME - sec')
ylabel('radians/second')
grid
%meta f18rsp27L
pause
plot(time,x(:,24))
title('F-18 DTFDOT FOR 0.01745 rad / 1 sec STEP (INPUT 2)
W2=-.001')
xlabel('TIME - sec')
ylabel('radians/second')
grid
%meta f18rsp210L
end

```

## APPENDIX B

### F-18 STATE SPACE MODELS

- 1) Open Loop F-18 Plant
- 2) Optimum  $H^\infty$  Closed Loop Controller
- 3) Limited Performance  $H^\infty$  Closed Loop Controller



```
% Open Loop Plant of the F-18
```

```
>> ag
```

```
ag =
```

```
Columns 1 through 5
```

-1.1400e+00	9.7938e-01	-9.9461e-02	0	0
-7.0738e+00	-8.0902e-01	-7.9063e+00	0	0
0	0	0	1.0000e+00	0
0	0	0	0	1.0000e+00
0	0	0	0	0
0	0	-1.4691e+03	-4.9559e+01	-1.6122e+00
0	0	0	0	0
0	0	0	0	0
0	0	0	0	0
0	0	0	0	0

```
Columns 6 through 10
```

0	5.6206e-04	0	-3.9669e-03	0
0	-1.7235e+00	0	-1.8786e+00	0
0	0	0	0	0
0	0	0	0	0
1.0000e+04	0	0	0	0
-1.5410e+02	0	0	0	0
0	0	1.0000e+00	0	0
0	-2.2301e+03	-1.0980e+02	0	0
0	0	0	0	1.0000e+00
0	0	0	-1.2250e+03	-4.9700e+01

```
>> bg
```

bg =

```
      0      0
      0      0
      0      0
2.1377e+03      0
-3.0532e+05      0
2.7277e+03      0
      0      0
      0 2.2301e+03
      0      0
      0 1.2250e+03
```

>> cg

cg =

```
      1      0      0      0      0      0      0      0      0      0
      0      1      0      0      0      0      0      0      0      0
```

>> dg

dg =

```
      0      0
      0      0
```

>> % Poles of the F-18 Open Loop Plant

>> eig(ag)

ans =

```
-9.7451e-01 + 2.6269e+00i
-9.7451e-01 - 2.6269e+00i
-6.2126e+01 + 8.5022e+01i
-6.2126e+01 - 8.5022e+01i
-1.4924e+01 + 3.3199e+01i
-1.4924e+01 - 3.3199e+01i
-2.6902e+01
-8.2898e+01
-2.4850e+01 + 2.4647e+01i
-2.4850e+01 - 2.4647e+01i
```

>> diary off

```
>> % Optimal Closed Loop State Space F-18 H-Infinity Controller
>> acgf
```

```
acgf =
```

```
Columns 1 through 6
```

-8.5374e+04	-1.0132e+04	-3.1614e+03	1.4349e+04	-6.2351e+00
3.6195e+03				
-1.0476e+05	-1.2541e+04	-3.8866e+03	1.7514e+04	-7.5004e+00
4.2957e+03				
2.2082e+06	2.6104e+05	8.1683e+04	-3.7082e+05	1.6204e+02
-9.5204e+04				
2.0282e+02	-8.9659e+02	-3.0481e+01	-2.0145e+02	2.4393e-01
3.6679e+02				
-1.1859e-01	-6.6984e-01	-4.0737e-02	-1.9136e-01	-6.0713e-04
-2.6865e-01				
-5.9038e+04	-7.7319e+03	-2.2235e+03	9.7030e+03	-4.0591e+00
2.3185e+03				
2.2799e+02	1.3562e+03	8.0283e+01	3.7452e+02	-7.9406e-01
4.2695e+02				
-1.1229e+00	-6.9592e+00	-4.0987e-01	-1.9229e+00	4.0321e-03
-2.1645e+00				
-1.6276e+04	-2.5326e+03	-6.3355e+02	2.5765e+03	-9.5432e-01
5.6803e+02				
4.5355e-02	3.8317e-03	1.5852e-03	-8.4079e-03	2.2515e-05
-3.2101e-03				
-2.6327e-03	2.0579e-03	4.8972e-05	1.5237e-03	-8.1576e-06
2.1350e-03				
5.1076e-03	4.2810e-03	4.1494e-04	7.3066e-04	8.0206e-06
2.8272e-03				
1.0102e-04	2.2190e-04	1.7064e-05	9.3235e-05	-1.7261e-06
1.9550e-04				
-5.3128e-03	-1.3122e-02	-9.8395e-04	-5.1009e-03	-3.3955e-06
-1.1396e-02				
0	0	0	0	0
0				
0	0	0	0	0
0				
0	0	0	0	0
0				
-1.5489e+04	-1.8299e+03	-5.7521e+02	2.6270e+03	-1.1398e+00
6.1035e+02				
2.2122e+06	2.6135e+05	8.2156e+04	-3.7521e+05	1.6280e+02
-8.7174e+04				
-1.9764e+04	-2.3349e+03	-7.3397e+02	3.3521e+03	-1.4544e+00
7.7880e+02				
0	0	0	0	0
0				
-5.9035e+03	-5.8679e+02	-2.1394e+02	1.0604e+03	4.1411e-02
2.6132e+02				

0	0	0	0	0
0				
-3.2428e+03	-3.2233e+02	-1.1752e+02	5.8248e+02	2.2747e-02
1.4355e+02				

Columns 7 through 12

1.6525e+04	-8.1213e+01	-2.3231e+04	-8.5392e+05	6.9207e+06
-7.4498e+05				
2.0288e+04	-9.9700e+01	-2.8096e+04	-1.0350e+06	8.3615e+06
-1.4361e+06				
-4.2803e+05	2.1036e+03	6.0049e+05	2.2132e+07	-1.7950e+08
1.7108e+07				
-3.1957e+02	1.7342e+00	-7.6547e+02	-5.8752e+03	5.6301e+04
2.3416e+05				
-1.2503e-01	6.8286e-04	3.7589e-01	2.0966e+01	-2.1836e+02
-9.4379e+02				
1.1240e+04	-5.5179e+01	-1.5821e+04	-5.8270e+05	4.7162e+06
-8.0642e+05				
2.5915e+02	-1.4309e+00	-5.7113e+02	-4.0438e+04	4.2610e+05
1.8520e+06				
-1.3490e+00	6.4342e-03	2.8740e+00	2.0374e+02	-2.1444e+03
-9.3152e+03				
2.9882e+03	-1.4625e+01	-4.3413e+03	-1.5528e+05	1.2459e+06
-4.5709e+05				
-9.5054e-03	3.9627e-05	1.4779e-02	-1.0894e+01	6.4179e+01
-1.9358e+01				
1.1639e-03	-3.2869e-06	-4.4338e-03	-3.7177e+00	-2.5802e+01
-2.6626e+00				
-7.7386e-06	8.6395e-07	-4.0636e-03	1.1824e+00	2.4380e+00
-2.1952e+01				
4.3551e-05	-4.5444e-08	-3.5537e-04	-1.7868e+00	-3.3436e+00
8.4419e-02				
-2.3656e-03	9.6950e-06	2.0069e-02	-7.2702e-01	2.8198e+00
1.8088e+01				
0	0	0	0	0
0				
0	0	0	0	0
0				
0	0	0	0	0
0				
2.9858e+03	-1.4683e+01	-4.2382e+03	-1.5529e+05	1.2595e+06
-1.2031e+05				
-4.2645e+05	2.0971e+03	6.0533e+05	2.2180e+07	-1.7989e+08
1.7184e+07				
3.8099e+03	-1.8735e+01	-5.4079e+03	-1.9815e+05	1.6071e+06
-1.5352e+05				
0	0	0	0	0
0				
1.1873e+03	-5.7597e+00	-1.7001e+03	-1.9306e+04	6.8154e+04
-1.8230e+06				
0	0	0	0	0

0	6.5219e+02	-3.1638e+00	-9.3384e+02	-1.0605e+04	3.7437e+04
-1.0014e+06					

Columns 13 through 18

7.0693e+07	-8.8082e+07	6.3851e-06	5.6121e-07	0
0				
8.6707e+07	-9.2874e+07	1.7489e-05	1.2253e-06	0
0				
-1.8283e+09	2.3406e+09	1.2740e-06	9.4237e-08	0
0				
-7.1948e+03	-6.7861e+06	6.4987e-06	5.0962e-07	0
0				
1.0692e+02	2.7226e+04	2.1491e-08	-2.8717e-09	0
0				
4.8902e+07	-5.2479e+07	1.4223e-05	1.0717e-06	0
0				
-2.3186e+05	-5.3390e+07	3.2873e-06	2.4095e-07	0
0				
1.1552e+03	2.6856e+05	1.7794e-08	-7.8433e-09	0
0				
1.3509e+07	-7.6963e+06	-2.4679e-05	-1.9379e-06	0
0				
6.7517e+02	-5.6786e+02	1.5331e-03	-1.0727e-02	0
0				
-2.7816e+02	3.0149e+02	-1.4656e-02	-4.8733e-02	0
0				
7.1802e+01	5.2404e+02	-6.8026e-02	1.8007e-02	0
0				
-4.1241e+01	2.8042e-02	1.3820e-01	5.5572e+00	0
0				
5.9266e-02	-4.6653e+02	-2.1299e+01	5.1950e-01	0
0				
0	0	-1.1400e+00	9.7938e-01	-9.9461e-02
0				
0	0	-7.0738e+00	-8.0902e-01	-7.9063e+00
0				
0	0	0	0	0
1.0000e+00				
1.2829e+07	-1.6416e+07	0	0	0
0				
-1.8323e+09	2.3446e+09	0	0	0
0				
1.6369e+07	-2.0946e+07	0	0	-1.4691e+03
-4.9559e+01				
0	0	0	0	0
0				
5.0852e+06	4.5020e+07	0	0	0
0				
0	0	0	0	0
0				

Columns 19 through 24

101

-4.9700e+01

>> bcgf

bcgf =

-6.3851e-06	-5.6121e-07
-1.7489e-05	-1.2253e-06
-1.2740e-06	-9.4237e-08
-6.4987e-06	-5.0962e-07
-2.1491e-08	2.8717e-09
-1.4223e-05	-1.0717e-06
-3.2873e-06	-2.4095e-07
-1.7794e-08	7.8433e-09
2.4679e-05	1.9379e-06
-1.5331e-03	1.0727e-02
1.4656e-02	4.8733e-02
6.8026e-02	-1.8007e-02
-1.3820e-01	-5.5572e+00
2.1299e+01	-5.1950e-01
0	0
0	0
0	0
0	0
0	0
0	0
0	0
0	0
0	0
0	0

>> ccgf

ccgf =

Columns 1 through 12

0	0	0	0	0	0	0	0	0	0	0	0
0	0	0	0	0	0	0	0	0	0	0	0
0	0	0	0	0	0	0	0	0	0	0	0

Columns 13 through 24

0	0	1	0	0	0	0	0	0	0	0	0
0	0	0	0	0	0	0	0	0	0	0	0

```
0
0 0 0 0 1 0 0 0 0 0 0 0
0
```

```
>> dcgf
```

```
dcgf =
```

```
0 0
0 0
```

```
>> diary off
```



```
>> % Limited Performance F-18 H-Infinity Closed Loop Controller
>> acgf
```

```
acgf =
```

```
Columns 1 through 6
```

5.4853e+01	6.8308e+01	-2.4157e-03	-4.5556e+01	-1.3317e-03
2.7764e+00				
-8.2591e+02	-7.1443e+02	-1.2218e-01	4.5375e+02	3.9671e-02
-1.2620e+01				
5.1971e-01	3.5172e-01	-1.7881e-02	-2.4551e-01	-3.0125e-05
3.2926e-03				
-9.5636e+02	-6.4519e+02	-2.2369e-01	4.5000e+02	5.6299e-02
-5.8066e+00				
-2.3815e-01	-1.5991e-01	-5.5533e-05	1.1168e-01	-1.7986e-02
-1.4021e-03				
9.6310e+01	8.8451e+03	-3.9933e+00	-2.7804e+03	5.3889e-01
3.1452e+02				
9.9182e+01	1.0866e+02	-1.1930e-02	-6.1211e+01	5.3155e-04
2.3513e+00				
9.5922e+01	-2.0037e+01	7.2362e-02	-1.7863e+01	-1.4373e-02
-2.9221e+00				
-1.5046e+00	-3.3465e+00	1.3703e-03	2.3553e+00	-3.2388e-04
-1.6638e-01				
2.6692e-02	-1.7103e-01	1.9213e-04	1.1688e-01	-4.0487e-05
-9.7550e-03				
3.1661e-03	-1.2917e-03	-1.4128e-06	-1.1759e-03	2.4284e-07
-1.3737e-04				
-5.0138e-04	-2.2227e-04	-1.8603e-06	6.3267e-04	6.1350e-07
1.2726e-05				
-1.6750e-03	-9.6082e-04	-1.4759e-06	1.4166e-03	8.2410e-07
9.4405e-07				
-9.0621e-03	-4.9989e-03	-5.5652e-06	7.9886e-03	3.9378e-06
3.7032e-05				
0	0	0	0	0
0				
0	0	0	0	0
0				
0	0	0	0	0
0				
1.4537e+00	5.2614e+01	-3.4809e-02	-1.4738e+01	6.7451e-03
2.9299e+00				
-2.0763e+02	-7.5146e+03	4.9716e+00	2.1050e+03	-9.6337e-01
-4.1847e+02				
1.8550e+00	6.7135e+01	-4.4416e-02	-1.8805e+01	8.6067e-03
3.7386e+00				
0	0	0	0	0
0				
8.2662e+00	2.5557e+01	-5.3459e-03	-1.1852e+01	1.3675e-03
1.3263e+00				
0	0	0	0	0

0					
4.5406e+00	1.4039e+01	-2.9365e-03	-6.5102e+00	7.5116e-04	
7.2854e-01					

Columns 7 through 12

2.4278e+01	2.1970e+02	-7.4480e+02	3.4531e+02	-1.2883e+03	
-3.3764e+03					
1.1475e+02	-1.5275e+03	-7.4494e+02	-1.2081e+03	4.4261e+04	
-9.2265e+04					
-9.5175e-02	-1.7971e-01	5.6785e-01	-2.9031e-01	1.1063e+00	
2.0911e+00					
1.6948e+02	3.5540e+02	-1.2143e+03	4.9614e+02	-1.6824e+03	
-5.2722e+03					
4.4274e-02	9.2700e-02	-2.9961e-01	1.4758e-01	-5.4302e-01	
-1.1808e+00					
-1.9125e+03	1.1561e+05	6.2290e+04	7.5173e+04	-3.3642e+06	
7.1921e+06					
-5.8429e+01	5.4303e+02	-2.7287e+02	-3.3831e+02	-1.2467e+04	
2.7843e+04					
5.8473e+01	-1.2280e+03	-2.7012e+02	-9.3798e+02	3.3546e+04	
-6.8752e+04					
1.1817e+01	-3.5695e+01	-1.1411e+01	-9.2459e+01	1.0320e+03	
-1.7296e+03					
6.9902e-01	-2.7256e+00	2.7561e+00	-2.5003e+00	7.5173e+01	
-1.2975e+02					
-2.1093e-03	-5.0210e-02	-5.9644e-02	-5.4825e-02	-1.8913e+01	
4.2488e+01					
1.7545e-03	1.9797e-03	-2.0838e-02	1.5471e-01	-3.4565e+00	
-8.8331e+00					
3.3586e-03	2.9326e-03	-2.9569e-02	4.0374e-01	-1.1778e+00	
-4.0233e+00					
1.8870e-02	1.9025e-02	-1.7111e-01	2.1168e+00	1.1694e+00	
-5.7876e-02					
0	0	0	0	0	
0					
0	0	0	0	0	
0					
0	0	0	0	0	
0					
-8.2203e+01	8.0439e+02	4.3055e+02	5.2649e+02	-2.3556e+04	
5.0359e+04					
1.1741e+04	-1.1489e+05	-6.1494e+04	-7.5197e+04	3.3645e+06	
-7.1926e+06					
-1.0489e+02	1.0264e+03	5.4938e+02	6.7180e+02	-3.0058e+04	
6.4258e+04					
0	0	0	0	0	
0					
-5.8908e+01	3.1132e+02	4.2218e+02	6.3136e+02	-1.0651e+04	
1.3720e+04					
0	0	0	0	0	
0					

-3.2358e+01	1.7101e+02	2.3191e+02	3.4681e+02	-5.8509e+03
7.5365e+03				

Columns 13 through 18

1.5165e+04	3.6975e+05	9.1783e-04	-1.3066e-03	0
0				
-3.9813e+05	3.2931e+05	5.1616e-04	-7.3320e-04	0
0				
-1.1531e+01	-2.5544e+02	4.9055e-07	-6.5176e-07	0
0				
1.9814e+04	5.3119e+05	-7.9086e-04	1.1434e-03	0
0				
5.8190e+00	1.3581e+02	-3.6944e-07	5.4484e-07	0
0				
3.0288e+07	-3.4745e+07	-2.4893e-06	3.7570e-06	0
0				
1.2353e+05	-6.7487e+04	-1.8375e-03	2.7234e-03	0
0				
-3.0293e+05	1.7051e+05	-1.7620e-03	2.5693e-03	0
0				
-8.6093e+03	-8.2787e+03	1.6318e-02	-2.4067e-02	0
0				
-6.6522e+02	-6.4054e+02	-2.0863e-01	3.1158e-01	0
0				
1.8930e+02	-2.5011e+01	-1.5373e-01	2.4114e-01	0
0				
-2.6689e+01	1.4204e+01	-4.2717e-01	2.5781e-02	0
0				
-1.3793e+01	9.2262e-01	3.7563e-01	8.9772e-01	0
0				
-5.9566e-01	-2.1468e+01	-3.2120e+00	1.0946e+00	0
0				
0	0	-1.1400e+00	9.7938e-01	-9.9461e-02
0				
0	0	-7.0738e+00	-8.0902e-01	-7.9063e+00
0				
0	0	0	0	0
1.0000e+00				
2.1208e+05	-2.4328e+05	0	0	0
0				
-3.0290e+07	3.4747e+07	0	0	0
0				
2.7061e+05	-3.1042e+05	0	0	-1.4691e+03
-4.9559e+01				
0	0	0	0	0
0				
1.0552e+05	5.0492e+05	0	0	0
0				
0	0	0	0	0
0				
5.7960e+04	2.7735e+05	0	0	0

Columns 19 through 24

107

>> bcgf

bcgf =

-9.1783e-04	1.3066e-03
-5.1616e-04	7.3320e-04
-4.9055e-07	6.5176e-07
7.9086e-04	-1.1434e-03
3.6944e-07	-5.4484e-07
2.4893e-06	-3.7570e-06
1.8375e-03	-2.7234e-03
1.7620e-03	-2.5693e-03
-1.6318e-02	2.4067e-02
2.0863e-01	-3.1158e-01
1.5373e-01	-2.4114e-01
4.2717e-01	-2.5781e-02
-3.7563e-01	-8.9772e-01
3.2120e+00	-1.0946e+00
0	0
0	0
0	0
0	0
0	0
0	0
0	0
0	0
0	0
0	0

>> ccgf

ccgf =

Columns 1 through 12

0	0	0	0	0	0	0	0	0	0	0	0
0	0	0	0	0	0	0	0	0	0	0	0

Columns 13 through 24

0	0	1	0	0	0	0	0	0	0	0	0
0	0	0	1	0	0	0	0	0	0	0	0

```
>> dcgf
```

```
dcgf =
```

```
    0    0  
    0    0
```

```
>> % Poles of the F-18 Limited Performance Closed Loop Controller
```

```
>> eig(acgf)
```

```
ans =
```

```
-1.0017e+03  
-6.2126e+01 + 8.5022e+01i  
-6.2126e+01 - 8.5022e+01i  
-1.7711e+01 + 8.1027e+01i  
-1.7711e+01 - 8.1027e+01i  
-8.2898e+01  
-7.6597e+01  
-1.4924e+01 + 3.3199e+01i  
-1.4924e+01 - 3.3199e+01i  
-2.4200e+01 + 2.5758e+01i  
-2.4200e+01 - 2.5758e+01i  
-2.4850e+01 + 2.4647e+01i  
-2.4850e+01 - 2.4647e+01i  
-2.0234e+01 + 2.0813e+01i  
-2.0234e+01 - 2.0813e+01i  
-2.6902e+01  
-2.5668e+01 + 7.8886e-01i  
-2.5668e+01 - 7.8886e-01i  
-9.7451e-01 + 2.6269e+00i  
-9.7451e-01 - 2.6269e+00i  
-2.5001e+00  
-1.9977e+00  
-1.8000e-02  
-1.8000e-02
```

```
>> diary off
```

## REFERENCES

1. Doyle, J. C. and Stein, G., Multivariable Feedback Design: Concepts for a Classical/Modern Synthesis, IEEE Transactions on Automatic Control, Vol. AC-26, No. 1, pp. 4-16, February 1981.
2. Safonov, M. G., Stability and Robustness of Multivariable Feedback Systems, p. 68, The MIT Press, 1980.
3. Gordon, V. C., Utilization of Numerical Optimization Techniques in the Design of Robust Multi-Input Multi-Output Control Systems, Ph.D. Dissertation, Naval Postgraduate School, Monterey, California, September 1984.
4. Postlethwaite, I., and others, H $\infty$  Control System Design: A Critical Assessment, International Federation on Automatic Control, Vol. 8, pp. 328-333, 1987.
5. Chiang, R. Y., and Safonov, M. G., Robust-Control Toolbox, User's Guide, The Mathworks, Inc., June 1988.
6. Rogers, W. L., Applications of Modern Control Theory Synthesis to a Super-Augmented Aircraft, M.S. Thesis, Naval Postgraduate School, Monterey, California, June 1989.
7. Hsu, Ta-Chieh, Application of H $\infty$  Method to Modern Fighter Configuration, M.S. Thesis, Naval Postgraduate School, Monterey, California, December, 1989.
8. Rojek, F. W., Development of a Mathematical Model that Simulates the Longitudinal, and Lateral-Directional Response of the F-18 for the Study of Flight Control Reconfiguration, M. S. Thesis, Naval Postgraduate School, Monterey, California, September, 1986.
9. Kwaakernaak, H., and Sivan, R., Linear Optimal Control Systems, John Wiley and Sons, Inc., 1972.
10. Safonov, M. G., Laub, A. J., Hartman, G. L., Feedback Properties of Multivariable Systems: The Role and Use of the Return Difference Matrix, IEEE Transactions on Automatic Control, Vol. AC-26, No. 1, pp. 47-65, February, 1981.